PEOPLE'S DEMOCRATIC REPUBLIC OF ALGERIA
MINISTRY OF HIGHER EDUCATION AND SCIENTIFIC RESEARCH

UNIVERSITY ABOU-BEKR BELKAID – TLEMCEN

THESE LMD

Presented in :

FACULTY OF SCIENCES – DEPARTMENT OF PHYSIC

To obtained the diplôme of :

DOCTORAT

Field:*Renewables Energies*

by :

Mr SLAMI Abdelhadi

Intituled

Modeling and optimization of perovskite solar cell with different HTM and ETM layers for a solar installation

---

Publicly supported on…… in Tlemcen in front of the jury composed by :

Mr BENMOUSSA Nasr-Eddine	Professor	University of Tlemcen	President
Mr MERAD Laarej	Professor	University of Tlemcen	Supervisor
Mrs BOUCHAOUR Mama	Doctor	University of Tlemcen	Co-Thesis Director
Mr CHEKNANE Ali	Professor	University of Laghouat	Examiner
Mr BOUSAID Abdelhak	Professor	Université de Tlemcen	Examiner
Mr BENMOUNA Reda	Professor	Université de Tlemcen	Examiner

Laboratoire URMER
BP 119, 13000 Tlemcen - Algérie

Acknowledgment

First of all I thank the Almighty God for giving me the courage and the will to be able to carry out this modest work.

I especially thank my supervisors, **Pr. MERAD Laarej** and **Dr.BOUCHAOUR Mama**, for doing me the honor of mentoring me and giving me very enlightened advice that was very useful for my project.

My thanks go of course to the president of the jury **Pr. BENMOUSSA Nasr-Eddine** and the members of jury **Pr. CHEKNANE Ali**, **Pr. BOUSAID Abdelhak** and **Dr.BENMOUNA Reda** for showing interest in my PHD work and accepting to participate in this thesis.

I also express my deep gratitude for: My family and my close friends for their uninterrupted moral support and their many advices throughout my thesis.

I thank the **Association of Renewable Energies and Sustainable Development of Sidi Bel Abbes** for helping me to provide a suitable working environment and to use all means

A.Slami

LISTE OF ABBREVEATION

AC alternating current

BC conduction band

BV valence band

CSi crystalline silicon

DC direct current

ETM electron transport material

FTO fluorine tin oxide

HTM hole transport material

ITO indium tin oxide

IPCE incident photon to current efficiency

MPPT maximum power point tracking

PMW pulse width modulation

PV photovoltaic

PSCs Perovskite solar cells

SC semiconductor

SDT sustainable disinfection tunnel

TCO transparent conductive oxide

UV ultraviolet

D-SSCs Photovoltaic Dye Cells

QDSCs quantum dot solar cells

TABLE OF CONTENT

Acknowledgment..... i
Liste of Abbreveation ii
Table of content 1
List of figures..... 5
List of tables..... 7
GENERAL INTRODUCTION..... 8
References..... 11
CHAPTER 1 GENERALITIES ON THE DIVERS TYPES OF PV CELLS & DIVERS PV SOLAR INSTALLATIONS 12
I. Introduction:..... 13
II. Different generations of Cells..... 13
1- First (01) generation:..... 13
2- Second (02) generation:..... 14
3- Third (03) generation:..... 14
III. Standards of choice of materials for PV..... 15
IV. Different types of photovoltaic cells..... 15
1. Inorganic photovoltaic cells 15
a. Monocrystalline silicon :..... 15
b. Hydrogenated amorphous silicon (a-SH):..... 16
c. Poly crystalline and Microcrystalline silicon:..... 17
c.1) Polycrystalline silicon..... 17
c.2) Microcrystalline silicon :..... 17
d. Cadmium telluride solar cells (CdTe):..... 18
e. Copper Indium Gallium Selenium cells (CIGS):..... 18
2. Organic photovoltaic cells:..... 19
2.1. Structures of Organic PV Cells:..... 20
a. Monolayer structure:..... 20
b. Heterojunction structure..... 21
c. Heterojunction structure in volume:..... 21
2.2 PV effect in organic cells:..... 22
3. Hybride PV solar cells Perovskite : crystalline systeme, working principles and Characteristics..... 23
a. Perovskite crystalline systems:..... 23
b. Working principles:..... 26
c. Deposition techniques for PSC Thin Film and Fabrication of MASnI3:..... 27
c.1. Deposition techiniques for PSC thin film:..... 27
c.2. Preparation of the MASnI3 active layer..... 27

TABLE OF CONTENT

V. Different photovoltaic solar installations and mainfactors to consider..... 28

1. System configuration :..... 28

a. Off-grid PV plant..... 28

b. Grid-connected PV plant..... 29

2. Components of a PV plant..... 31

2.1 Components of the Grid connected PV plant..... 31

2.2 Components of the off Grid PV plant..... 31

a. Solar cell / solar module (configuration, function,photovoltaic effect)..... 32

b. Charge controller:..... 33

b.1. Types of charge regulator:..... 34

b.2. Requirements in charging regulators:..... 35

c. Batteries:..... 35

c.1. Types of solar batteries :..... 35

c.1.1. Flooded lead plate acid batteries :..... 35

c.1.2. Valve regulated lead acid :..... 36

c.1.3. Nickel-cadmium storage batteries:..... 36

d. Inverters (Types, self -controlled vs grid -controlled):..... 37

VI. Conclusion..... 39

VII. References:..... 40

CHAPTER 02 STRATEGIES TO PROGRES THE STABILITY OF PEROVSKITE 42

I. Introduction:..... 44

a. Stability studies:..... 44

a.1. Moisture:..... 44

a.2. UV light and Oxygen:..... 46

a.3.Temperature:..... 47

a.4.Encapsulation:..... 48

b. Strategies to develop the long term stability of PSCs..... 50

b.1. Mixed cation:..... 50

b.1.1. Binary (FM/MA)PbI3System. 50

b.1.2. Binary(MA/Cs) PbI3 System..... 50

b.1.3. Binary(FA/Cs) PbI3 System..... 51

b.1.4. Binary(FA/Rb) PbI3 System..... 51

b.2. Mixed divalent metal cation:..... 51

b.3. Mixed halide typs:..... 52

b.3.1Binary FAPb (I/Cl) and MAPb (I/Cl) Systems 53

b.3.2 Binary FAPb(I/Br) and MAPb(I/Br) Systems 53
b.3.3 Ternary MAPb(I/Br/Cl) and FAPb(I/Br/Cl) Systems 54
b.4. Mixed cation -Mixed divalent metal cations:..... 55
b.5. Mixed cation -Mixed halide:..... 55
b.6. Mixed divalent metal cations- mixed halide anions..... 56
b.7. Mixed cation -Mixed divalent metal cations -Mixed halide anions..... 56
II. Conclusion 58
III. References 59
CHAPTER 03 RESULTS & DISCUSSION 70
1. Introduction..... 70
2. Comparative study of different HTM in a PSC..... 72
2.1 Device architecture and simulation..... 72
2.2 Influence of the thickness of absorber layer onsolar cell performance with different HTM layer.75
2.3 Effect of doping of the absorber layers on the PV performances..... 76
2.4 Effect of temperature..... 77
3. Comparative study of different ETM in a Psc..... 79
3.1 Modeling of PSC and simulation..... 79
3.2 Numerical analysis for various ETM candidates..... 84
4. Wireless networklocal using perovskite solar cell. 86
4.1 Introduction 86
4.2 Diagram, device structure and simulation 87
A. Trnsmission of sound : 87
a) Emitter: 87
b) Receiver : 88
b.1 Perovskite / Silicon Solar Cell 88
b.2 Simulation Parameters: 89
b.3 Results and discussion..... 90
B. Transmission of text:..... 90
a) Emitter:..... 90
a.1 Sending and work principle..... 90
a.2 Source code..... 91
b) Receiver:..... 91
b.1 Receiving and work principle..... 91
5. Sustainable antiseptic tunneling for antivirus less harmful than covid19 93
5.1 Design and work of disinfection tunnel. 94

TABLE OF CONTENT

5.2 Solar system model. 95

5.3 Contents of the solar kit 95

5.4 Energy needs assessment 96

6. Wi-fi station & solar powered smart-phone chargers with a money multi coin selector..... 97

6.1 Design and realization of a Wifi station & smart phone charger with a multi coin selector programmed with the Arduino..... 97

6.2 Contents of the solar kit 98

6.3 Energy needs assessment 99

6.5 Schematic plan (CH-926 / Arduino) and Source code..... 100

REFERENCES: 101

GENERAL CONCLUSION..... 109

Perspective..... 110

INTERNATIONAL PUBLICATIONS..... 111

INTERNATIONAL AND NATIONAL COMMUNICATIONS..... 112

ملخص..... 113

RESUME: 113

ABSTRACT:..... 113

List of figures

Chapter 01:

Figure 1 1 Best research-cell efficiencies 14
Figure 1 2 silicon diamond structure 15
Figure 1 3 Crystalline structure and energy band diagram 16
Figure 1 4 Atomic structure and energy band diagram 17
Figure 1 5 polycrystalline silicon atomic structure 17
Figure 1 6 Microcrystalline silicon atomic structure 18
Figure 1 7 Diagram of a typical CdTe device 18
Figure 1 8 Diagram of a typical CIGS device 19
Figure 1 9 General structure of organic PV cell. 20
Figure 1 10 a) Bande diagram and b) Monolayerstructure of organic PV cell. 20
Figure 1 11 a) Bande diagram and b) Bilayer structure of organic PV cell. 21
Figure 1 12 a) Monolayer structure and b)The active layer of organic PV cell. (interpenetrating network) 21
Figure 1 13 Mobilité de la génération de photo porteurs dans une hétérojonction organique 22
Figure 1 14 Crystalline systems of perovskite type 23
Figure 1 15 Unit cell of such a crystal 24
Figure 1 16 Rapid PCE evolution of PSCs from 2009 to 2023. 24
Figure 1 17 Band diagram and working principal steps in PSC 26
Figure 1 18 Representative deposition techniques for PSC thin film. (a) OSM; (b) SDM; (c) DSVD; and (d) VASP. 27
Figure 1 19 The absorber layer of MASnI3 layer deposition. 28
Figure 1 20 Schematic view of a stand-alone system. 29
Figure 1 21 Difference between two methods (Full feed in — Net metering) 30
Figure 1 22 Components of the Grid connected PV plant 31
Figure 1 23 Components of the off Grid PV plant 31
Figure 1 24 Crystalline solar cell working principle. 32
Figure 1 25 From a solar cell to a solar array 33
Figure 1 26 Controller of charge 34
Figure 1 27 Difference between the controller PMW and MPPT 34
Figure 1 28 Flooded lead plate acid batteries 35
Figure 1 29 AGM battery 36
Figure 1 30 Nickel-cadmium batteries 36
Figure 1 31 Different types of inverters 37
Figure 1 32 SiFngle / three phase inverters 37

Chapter 02:

Figure 2- 1PCE spectrum of mixed cation perovskite devices, and MAIPbI3 FPbI3. 50
Figure 2- 2IPCE spectra of devices based on CH3NH3Sn1-x PbxI3 perovskite 52
Figure 2- 3 IPCE curves for MASn0.5Pb0.5I3/P3HT and MAPbI3/spiro-OMeTAD PSCs... 52

Chapter 03:

Figure 3 1 Architectures of different HTL materials..... 72
Figure 3 2 SCAPS working procedure. 73
Figure 3 3 Energy band alignment 73
Figure 3 4 Variation of PSCs of the thickness of absorber layer..... 75
Figure 3 5 Effect of the Absorber density of PSC absorber layer on PV performances. 77
Figure 3 6 Representation of the variation of PCE with the temperature..... 78
Figure 3 7 Architectures of twelve schematic with different HTM layer..... 82
Figure (III.8): Energy band alignment..... 82
Figure 3 9 Comparative study of ZnO et TiO_2 in a perovskite solar cell..... 85
Figure 3 10 Things we'll need..... 87
Figure 3 11 Compounds of Emitter part of transmission of sound..... 88
Figure 3 12 General diagram of the receiver part of the transmission of sound. 88
Figure 3 13 Schematic representation perovskite solar cell (PSC) and silicon solar cell (PN) 89
Figure 3 14 The emitter part. 91
Figure 3 15 General diagram of the receiver part..... 92
Figure 3 16 Schematic of Sustainable Disinfection Tunnel (SDT) 94
Figure 3 17 Cable Schematics of the solar system. 95
Figure 3 18 plan diagram of our wifi station & solar charger. 98
Figure 3 19 Cable Schematics of the solar system. 99
Figure 3 20 Schematic plan of CH-926 / Arduino..... 100

List of tables

Table 1 Parameters used in SCAPS -1D for PSCs architectures..... 74
Table 2 Performance of Psc with various HTM layers. 75
Table 3 Differents parameters used in SCAPS-1D simulator of Psc..... 84
Table 4 Efficiency of PSC with two different ETM layers. 84
Table 5Simulation parameters of MASnI3 PSC and PN junction..... 89
Table 6 Electrical equipment used in the station..... 96
Table 7 Electrical equipment used in the station..... 99

Renewable energies, like photovoltaic energy are considered as clean and sustainable energies. This solar energy converts directly light radiation in electricity. This technology showed an enormous development in the last years and represents an important part of our present and future energy mix.

Therefore, it is important to know its potential and energy conversion mechanism. The solar cell is an essential device in this area.

At the time of today we distinguish three generations of photovoltaic cells according to their technologies.

Third generation solar cells like Organic Cells (OPVs) [2], Photovoltaic Dye Cells (D-SSCs)[3], quantum dot solar cells (QDSCs) [4] and perovskite solar cells (PSCs) aim to pass the Shockley-Queisser limit [1].

These next-generation cells boast several advantages over conventional inorganic solar cells. They excel at capturing sunlight due to their impressive light absorption ($1.50 \times 10^{4} cm^{-1}$), the charges generated within the cell travel further thanks to diffusion lengths exceeding 1 micrometer for both electrons and holes [5,6]. This efficient light capture and charge transport translate to significantly higher open circuit voltage, reaching over 1 Volt compared to the typical 0.7 Volts in silicon cells.

While perovskite solar cells (PSCs) show impressive efficiency, their limited lifespan under real-world conditions hinders their widespread use. Research has pinpointed moisture as a key culprit, with chemical breakdown occurring rapidly in humid environments. The key to unlocking the long-term potential of perovskite solar cells (PSCs) lies in finding either stable perovskite materials or designing devices that resist degradation, as highlighted in [8].

Moreover, PSCs are delicateto elevated temperatures, humidity, oxygen andUV-light: factors that are delaying their commercialization [9].

While a compound called methylammonium lead iodide ($CH_3NH_3PbI_3$) has been the star player in PSCs, it comes with a downside: lead is toxic to humans. So, scientists are on a global mission to find a suitable alternative that shines just as bright, but without the harmful side effects. [10]

Replacing the toxic materials in perovskite solar cells with $CH_3NH_3PbI_3$ is possible. This compound, has a direct bandgap of 1.3 eV, acts as an absorber layer and avoids the toxicity of typical perovskite materials [11].

Spiro-OMeTAD, a hole-transport material (HTM), has earned widespread popularity in the fields of organic photovoltaics (OPV) and organic optoelectronics [12], but it is the reasons forthe deterioration in the devices performance and the field is still research active [13]. Finding alternatives to spiro-OMeTAD is crucial for the advancement of perovskite solar cells.

Our thesis is split into three chapters. We present in the first chapter the generalities on the different generations of photovoltaic cells. After a description of the different types of inorganic cells and organic cells, and we develop more specifically the hybrid cells based on perovskite. Finally, we introduce the various solar photovoltaic systems. Off-grid photovoltaic installations and On-grid photovoltaic installations (connected to the network).After a presentation on the main factors to consider.

We detail in the second chapter the strategies of developing the long-term stability of the PSCs. Particularly (mixed cations), (mixed cations of divalent metals), (mixed halides), (mixed cations with mixed cations of divalent metals), (mixed cations with mixed halides), (mixed cations of divalent metals with mixed halides) and also (the mixed cations with the mixed cations of divalent metals with the mixed halides).

The third chapter is divided into two parts:

We presented in the first part, one hand, modelization of Tin based perovskite solar cell using three different HTMs layers (PEDOT: Pss, Spiro-OMeTAD and Cu_2O). We proposed the ZnO (Zinc Oxide) as an (ETM). We present key findings on the impact of active layer doping level, thickness, and temperature on device performance, summarized for clarity. On the other hand, two kinds of electron transport materials (ETMs) have been compared and analyzed with a diverse Hole transport materials (HTMs) and two different active layers ($MAPbI_3$ and $MASnI_3$).

This comparative work has been done between eleven structures (five of our own structures and six we used as a reference) by replacing TiO_2 with ZnO as ETM layer with perovskite ($MAPbI_3$ and $MASnI_3$) and (Spiro-OMeTAD, PEDOT:PTT, Cu_2O and CuI) as HTM layers.

We present in the second part of the third chapter, a novel simple process for encoding voices and text onto a laser beam and transmitting them over long distances using a perovskite solar cell (Wireless local network based on PSC programmed with the Arduino), is described. We presented a comparative simulation between the PSC and the silicon (monocrystalline) solar cell. First, the simulation and the prototype with the silicon-based solar cell were made. And until now, only the simulation part has been validated with the perovskite solar cell.

While economically impractical, the prototype holds research potential for laboratory implementation. On the one hand, a study and realization of sustainable disinfection tunnel (SDT) to reduce viruses less harmful than Covid19 which are transmitted by touch, with the use of solar energy. On the other hand, a study and realization of a wifi station and solar powered smart-phone chargers with a multi coin selector. This makes it possible to highlight the two principles of environmental conservation, the green economy (using the solar PV) as well as the opening of the workstation.

References

[1] Hibberd, Christopher J., et al. "Non-vacuum methods for formation of Cu (In, Ga)(Se, S) 2 thin film photovoltaic absorbers." Progress in Photovoltaics: Research and Applications 18.6 (2010): 434-452.

[2] Chung, In, et al. "All-solid-state dye-sensitized solar cells with high efficiency." Nature 485.7399 (2012): 486-489.

[3] Ko, Dong-Kyun, et al. "Photovoltaic performance of PbS quantum dots treated with metal salts." ACS nano 10.3 (2016): 3382-3388.

[4] Shockley, William, and Hans Queisser. "Detailed balance limit of efficiency of p–n junction solar cells." Renewable Energy. Routledge, 2018. Vol2_35-Vol2_54.

[5] Kim, Hui-Seon, et al. "Lead iodide perovskite sensitized all-solid-state submicron thin film mesoscopic solar cell with efficiency exceeding 9%." Scientific reports 2.1 (2012): 591.

[6] Hodes, Gary. "Perovskite-based solar cells." Science 342.6156 (2013): 317-318.

[7] Burschka, Julian, et al. "Sequential deposition as a route to high-performance perovskite-sensitized solar cells." Nature 499.7458 (2013): 316-319.

[8] Li, Faming, and Mingzhen Liu. "Recent efficient strategies for improving the moisture stability of perovskite solar cells." Journal of Materials Chemistry A 5.30 (2017): 15447-15459. [9] Mesquita, Isabel, Luísa Andrade, and Adélio Mendes. "Perovskite solar cells: Materials, configurations and stability." Renewable and Sustainable Energy Reviews 82 (2018): 2471-2489.

[10] Liu, Chong, et al. "Highly efficient perovskite solar cells with substantial reduction of lead content." Scientific Reports 6.1 (2016): 35705.

[11] Mhaisalkar, Subodh Gautam, et al. "Lead-free halide perovskite solar cells with high photocurrents realized through vacancy modulation." (2014).

[12] Hossain, Mohammad I., Fahhad H. Alharbi, and Nouar Tabet. "Copper oxide as inorganic hole transport material for lead halide perovskite based solar cells." Solar Energy 120 (2015): 370-380.

[13] Nogueira, A. F., C. Longo, and M-A. De Paoli. "Polymers in dye sensitized solar cells: overview and perspectives." Coordination Chemistry Reviews 248.13-14 (2004): 1455-1468.

CHAPTER 1

GENERALITIES ON THE DIVERS TYPES OF PV CELLS & DIVERS PV SOLAR INSTALLATIONS

I. Introduction:

Semiconductors are categorized according to chemical compositions. There are simple semiconductors such as Si, Ge, Sn (Tin), which all fit in to group IV of the periodic table. There are also composite semiconductors, binary, ternary, quaternary respectively consisting of two, three and four different chemical species.

These elements can be from group IV, such as Silicon Carbide (CSi), may also be from group (II-VI / CdTe), (I-VII / Copper chloride), (IV-VI / sulphide of Lead PbS), (V-VI/Bi2Te3), the most common being III-V semiconductors due to their properties:

- Robust - High thermal conductivity - high melting point.

We begin this first chapter by presenting the different generations of solar PV cells. Then we are interested in the state of the art and generalities of different types of photovoltaic cells including inorganic, and organic produced until today. Then we present the hybrid perovskite photovoltaic cells, we start with its crystalline structures, its operating principles. This will be followed by defining the techniques and methods most requested for the deposition of this material

II. Different generations of Cells.

1- First (01) generation:

The first generation of solar cells uses crystalline silicon (monocrystalline-polycrystalline) as the absorbent material. The junction is the homojunction (n-Si / p-Si).

This material has a lot of advantage, on the one hand it exhibits stable photo-conversion efficiency and being very abundant in the earth's crust. On the other hand, it is a non-toxic and very reliable PV cell material [1] and the technology of this material is mature and is well developed in microelectronic field.

The disadvantage of the technology of this material is the use of a very pure Si with a thickness of about 200 µm, which results in high production costs. This material is a poor light absorber due to its indirect energy bandgap of about 1.1 eV at chamber temperature [2].

2- Second (02) generation:

A second generation of cells based on thin film materials. The principle of thin-film cells is the economic use of materials in relation to the physical properties and the simplicity of the technologies used for their realization(easy and inexpensive elaboration)and to use much thinner absorber materials, around 2 µm thick [3].

The main materials used as thin film absorbers are amorphous Si (a-Si), micro-crystalline Si(µc-Si), CdTe, CIGS, CZTS, GaAs,alloys (binary, ternary, quaternary), refractory compounds (oxides, nitrides, carbides),intermetallic compounds and polymers.

3- Third (03) generation:

This generation is focused on attainment a high efficiency (PCE) than compounds mono cells and reducing the cost per watt typically by the progress of new materials [4], such as Thin film, solar inks, organic, nanostructure, polymere, moleculare, dye sensitized, perovskite.

All these types of solar cells are of specific interest because of their simple and modest fabrication method and high conversion efficiency [5].

- **Development photovoltaic efficiency**

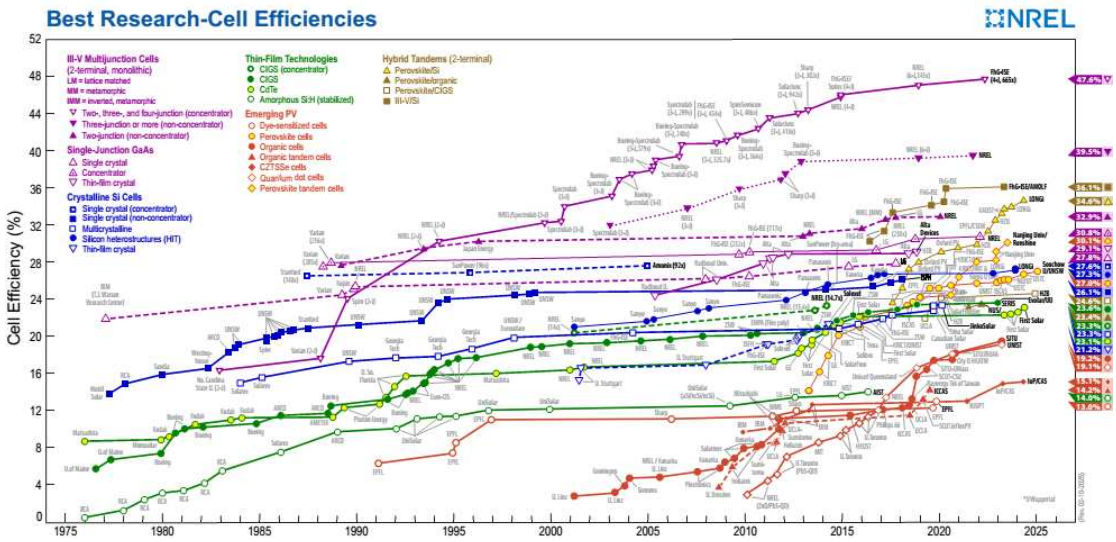

Figure 1 1 Best research-cell efficiencies[5]

III. Standards of choice of materials for PV.

1) PV conversion:

* Efficiency = P provided / P incident
* Adaptation of the material to the radiation

2) Material cost:
* Availability
* Amount of material required

3) Energy payback time:
* 01 to 03 years

4) Component toxicity:

5) Integration / Aesthetics

IV. **Different** types of photovoltaic cells:

1. Inorganic photovoltaic cells :

a. Monocrystalline silicon :

The perfect silicon has atoms that are regularly organized according to the structure of the diamond. A double cubic network with a centered face [19].Thus each atom of silicon, element of column IV of the periodic table, is positioned in a tetrahedral environment shown schematically in Figure 3 below, whose inter-atomic distance of these four neighboring atoms is d = 1.35A ° thus creating covalent bonds and that the angle formed amid two atoms is 109.28 °.[20]

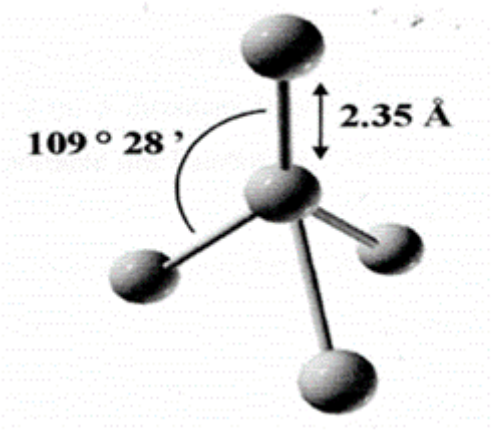

Figure 1 2 silicon diamond structure [20]

Monocrystalline silicon is a material that is characterized by a forbidden energy band "gap", Eg = 1.12 eV at room temperature as shown in Fig 03 below.

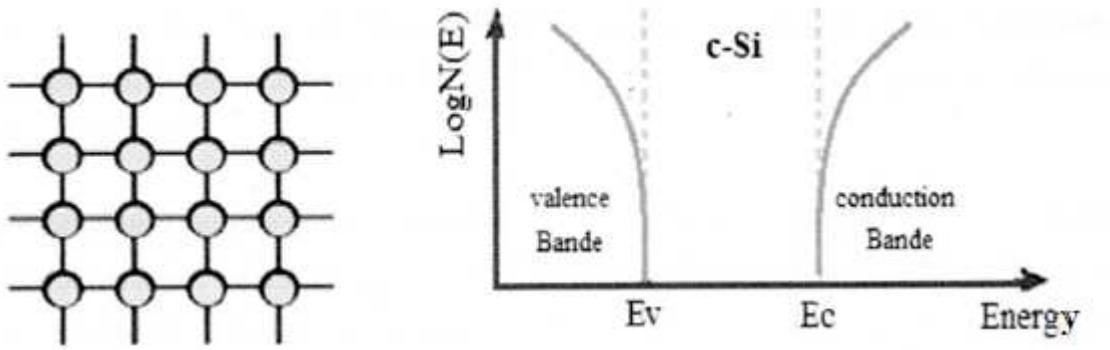

Figure 1 3 Crystalline structure and energy band diagram [20]

b. Hydrogenated amorphous silicon (a-SH):

On the other hand with crystalline silicon, the atomic organization in amorphous silicon is not regular [20], its structure is preserves the tetrahedral configuration, but not crystallized and glassy, this dispersion increases with distance, only after 4 or 5 inter atomic distances, a large fraction of the covalent bonds are cut and the positions are randomly distributed (figure 04) below.

These distortions in the network result in the appearance:

- These distortions can become large enough to prevent a bond from forming, and thus give rise to **dangling bonds** [5,6]
- On the other hand, localized states with energies located in the gap. These states form what are called the **tails of bands**. (figure 04),

These bonds provide spaces for Electrons to recombine with Holes but the hydrogen passivated them, producing what is called hydrogenated amorphous silicon (a-SH) (Staebler-Wronskieffect) [7].

(a-SH) are well suited for small power and consumption applications [8]. The highest recorded yield is 14.0% for a triple junction laboratory sample [9].

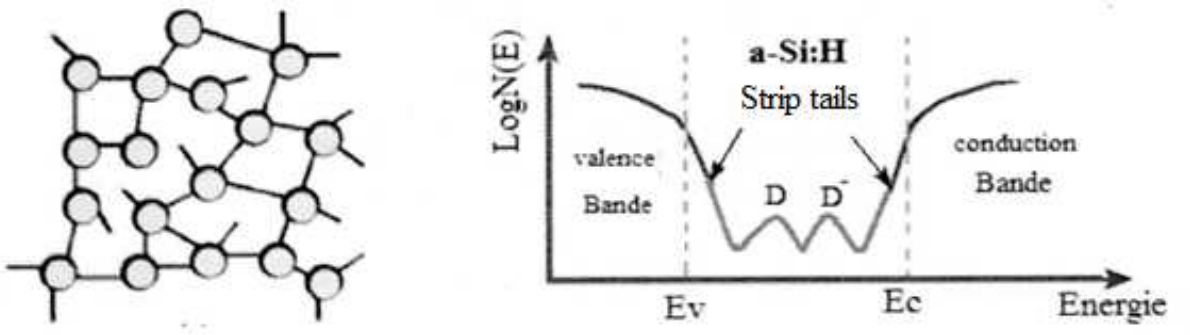

Figure 1 4 Atomic structure and energy band diagram [20]

c. Poly crystalline and Microcrystalline silicon:

Polycrystalline or microcrystalline siliconis a silicon which occurs in an intermediate state,between the crystalline state and the amorphous state.

c.1) Polycrystalline silicon.

The model of polycrystalline silicon is a material considered to be composed of small crystallites joined togetherby grain boundariesas is shown below (figure 05). Crystallites are therefore grains whose arrangement is periodic, thus forming small single crystals.

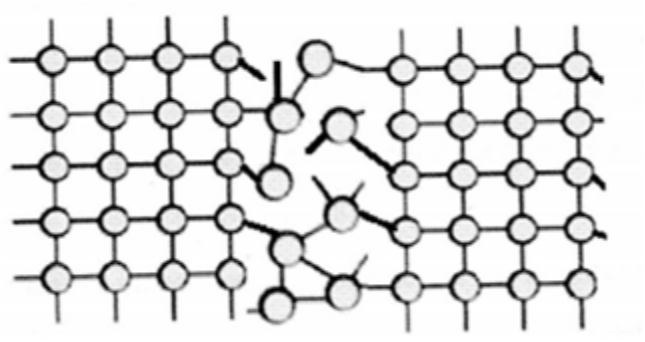

Figure 1 5 polycrystalline silicon atomic structure [20]

c.2) Microcrystalline silicon :

It is a material made up of a set of crystallites of different sizes and orientations, encrusted in an amorphous fabric, with vacuum and weakly bound hydrogen, see (figure 06). It has a gap equal to about 1.4 eV.

Figure 1 6 Microcrystalline silicon atomic structure [20]

d. Cadmium telluride solar cells (CdTe):

It is a set of TCO (conductive oxide transport) layer,middle layer is CdTe film.Which form an E-field that invert the light absorbed in the CdTe layer into current and voltage, The CdTe has an ideal direct bandgap of Eg = 1.45 eV (which approaches the theoretical optimum Eg =1.4 eV [21]) and a high absorption coefficient (Figure 07).

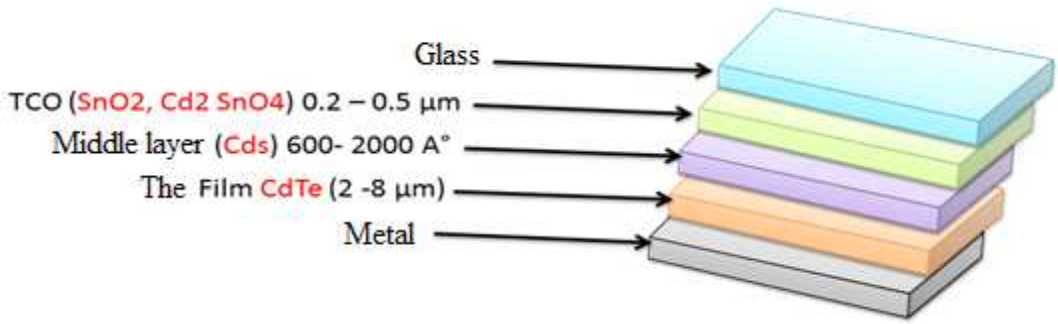

Figure 1 7 Diagram of a typical CdTe device [21]

•**TCO** : Are transparent to visible light and highly conductive for current transport.

• **Mid layers:** Help the growth of electrical properties between TCO and CdTe.

• **The CdTe Film:** As a primary photoconversion layer and absorbs the most visible light.

e. Copper Indium Gallium Selenium cells (CIGS):

The CIGS alloy uses the principle of the PN junction (Heterojunction-complex junction) of CIGS (p) / Cds (n) / ZnO (n) type. The record efficiency of 22.3% was reached at the end of 2015 by a solar cell of about 0.5 cm² from Solar Frontier-Japan

[22], and 25% by simulation [23]. Scientific research is working to replace the middle layer with an ecological layer (Zn, Mg, O, S).

- The heterojunction is formed between CIGS and ZnO semiconductors with Cds and ZnO.

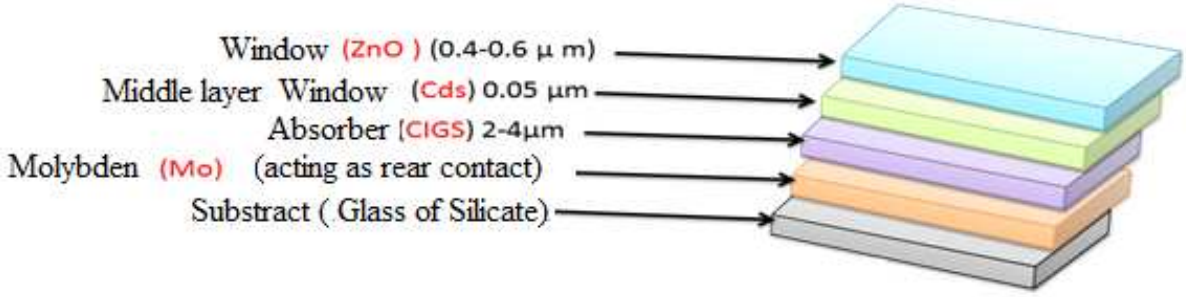

Figure 1 8 Diagram of a typical CIGS device [23]

CIGS has a type (P) doping resulting from essential defects. While Type (N) ZnO thanks to the integration of Aluminum (Al), this asymmetry doping which extends more from the ZCE in the CIGS than in the ZnO.

2. Organic photovoltaic cells:

Are PV cells of which at least the active layer consists of organic molecules. Which are sturdy, sustainable, Respect the environment -the electricity produced is clean and the manufacturing process relies on abundant and recyclable materials [24].

Can be classified into two types of semiconductor:

- **Small molecules (oligomers and monomers):** are pigments and dyes, generally deposited by vacuum evaporation

- **Polymers:** according to molecular structure and their chemical composition. Theyare deposited by the liquid spin coating technique on large surfaces.

2.1. Structures of Organic PV Cells:

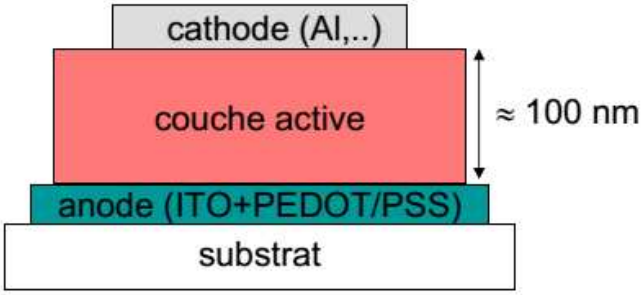

Figure 1 9 General structure of organic PV cell [24]

- **Substrate:** rigid or flexible

- **Transparent anode:** generally ITO (indium-doped tin oxide) (the most widely used compound, it has semi-transparency and good ohmic contact with hole-carrying materials) / conductive polymers.

- **Active layer:** small molecules or polymers.

- **Cathode:** allows ohmic contact to be obtained with electron transporting materials, deposited by vacuum evaporation (Al, Ag, etc.)

a. Monolayer structure:

These cells are described as being of the shottky type.

The choice of metals is decisive in achieving an ohmic contract on one side and non-ohmic on the other. The advantage of this type is the simplicity of manufacture, but the very low efficiency.

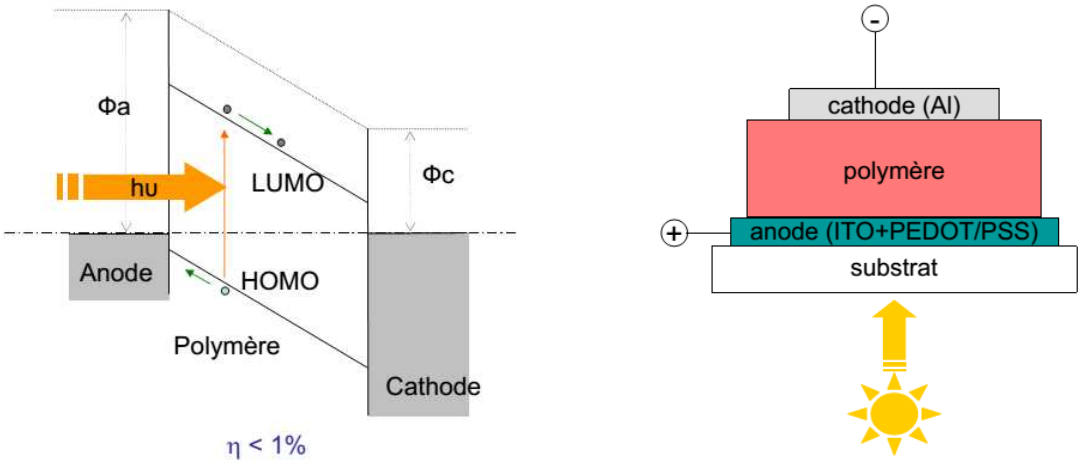

a b

Figure 1 10 a) Bande diagram and b) Monolayerstructure of organic PV cell. [24]

The dissociation of excitons in the volume is less than at the electrodes. And the electric field rarely enough to separate the excitons (because only the excitons generated near the ZCE can participate in the PV conversion)

b. Heterojunction structure.

It is composed of two materials of different nature (donor and acceptor) brought into contact between two electrodes. They have a much larger absorption zone width than shcottky cells

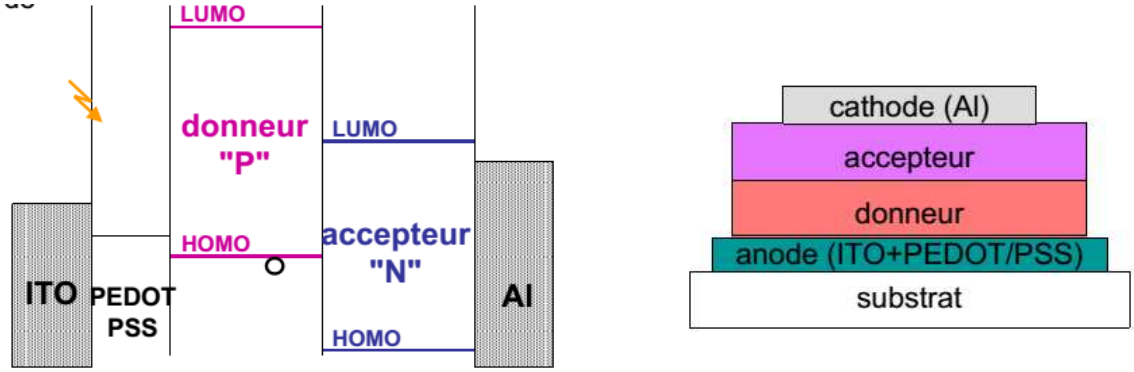

a b

Figure 1 11 a) Bande diagram and b) Bilayer structure of organic PV cell [24]

Electric field at the interface induces the separation of charges → dissociation of the exciton more efficient than in the case of homojunctions.

c. Heterojunction structure in volume:

This network constitutes a layer which is a mixture of two organic materials D and A, deposited between two electrodes.

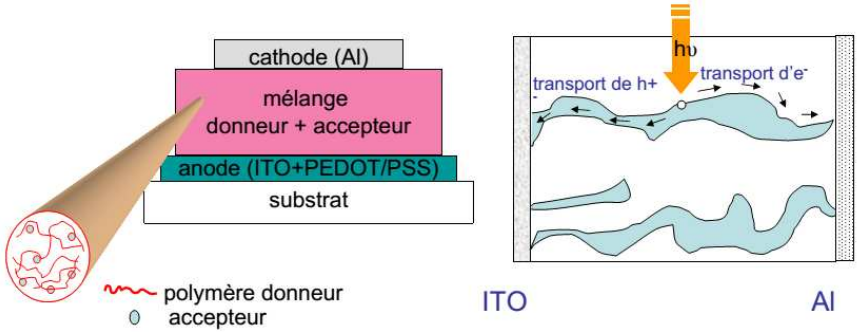

a **b**

Figure 1 12 a) Monolayer structure and b)The active layer of organic PV cel [24]. (interpenetrating network)

The mixing makes it possible to reduce the problem of losses by recombination of the photogenic excitons. And also allows increasing the number of interfaces (Donor /Acceptor).

2.2 PV effect in organic cells:

When light enters an organic PV converter, several steps act successively until the last step where electrons are collected on the electrodes.

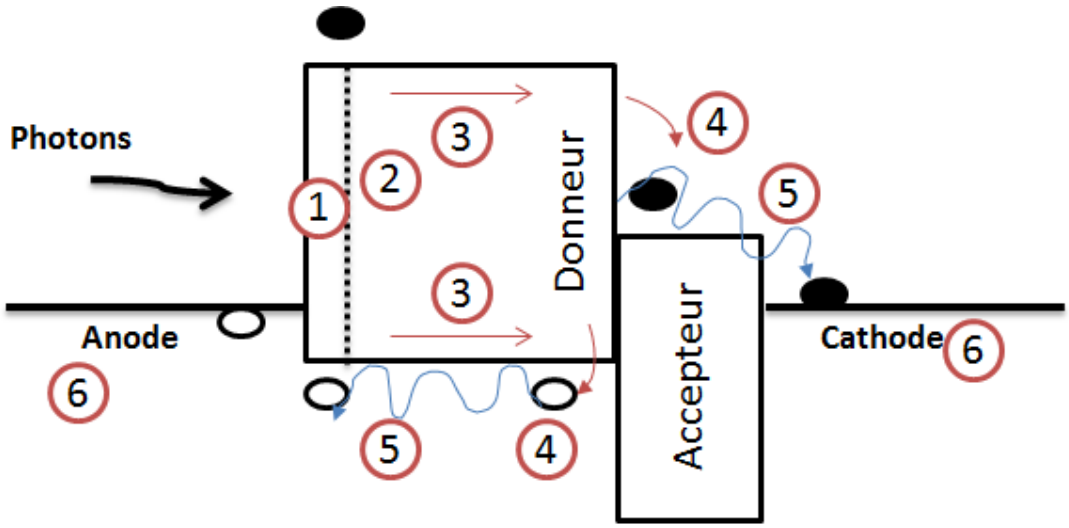

Figure 1 13 Mobilité de la génération de photo porteurs dans une hétérojonction organique

1 → Absorption photonique ηA

2 → Génération des excitons

3 → Diffusion des excitons $\eta diff$

4 → Séparation des excitons ηTc

5 → Transport des charges vers les électrodes ηTr

6 → Collecte de charges aux électrodes ηCc

3. Hybride PV solar cells Perovskite : crystalline systeme, working principles and characteristics.

a. Perovskite crystalline systems:

Perovskites are crystalline organic-inorganic compounds on a trimethylammonium base generally associated with lead and halogen [12]. They are divided into inorganic perovskite oxide and perovskite halide [10] (fig 14).

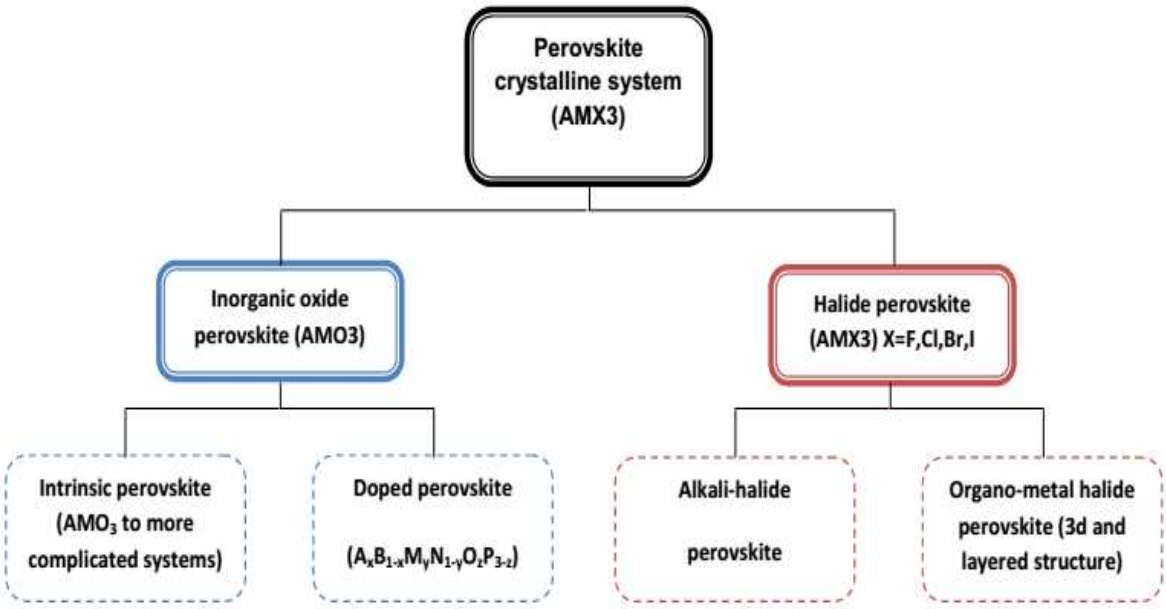

Figure 1 14 Crystalline systems of perovskite type [10]

Halide perovskites (AMX_3) can be divided into organometallic halide perovskite and alkali-halide perovskite [10]. The first category is mainlyformed from divalent M^{II} (Ni^{2+}, Ca^{2+}, Be^{2+}, Ba^{2+}, Mg^{2+}, Zn^{2+}, Sn^{2+}, Ge^{2+}, Fe^{2+}, Co^{2+}, Pb 2+ , Sr^{2+}) and monovalent alkali metal A^{I} (Rb^{+}, Li^{+}, Cs^{+}, Na^{+}, K^{+}) with X representing halide anions (Cl^{-}, I, Br^{-}, F^{-}).

Their chemical formula is CH3NH3PbX3 (MAPbX3) where X is a halide ion (I^{-}, Br^{-} or Cl). Figure 15 shows a unit cell of such a crystal [12].

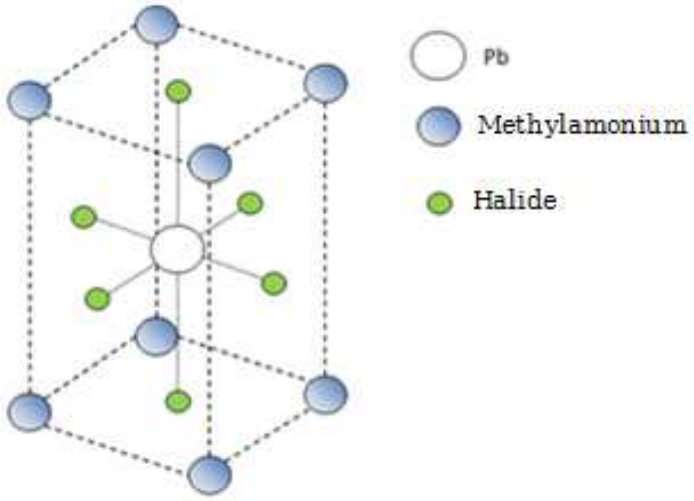

Figure 1 15 Unit cell of such a crystal [12]

The synthesis of a perovskite layer is relatively easy and very cheap and since it was shown by Kojima et al. That it was possible to integrate such a layer as an absorber of a solar device [14], PSCs have experienced the fastest development of conversion efficiency of all solar technologies.

Yields rose from (3.8%) in 2009 at values greater than (25.7)% in 2023 as shown in figure 16.

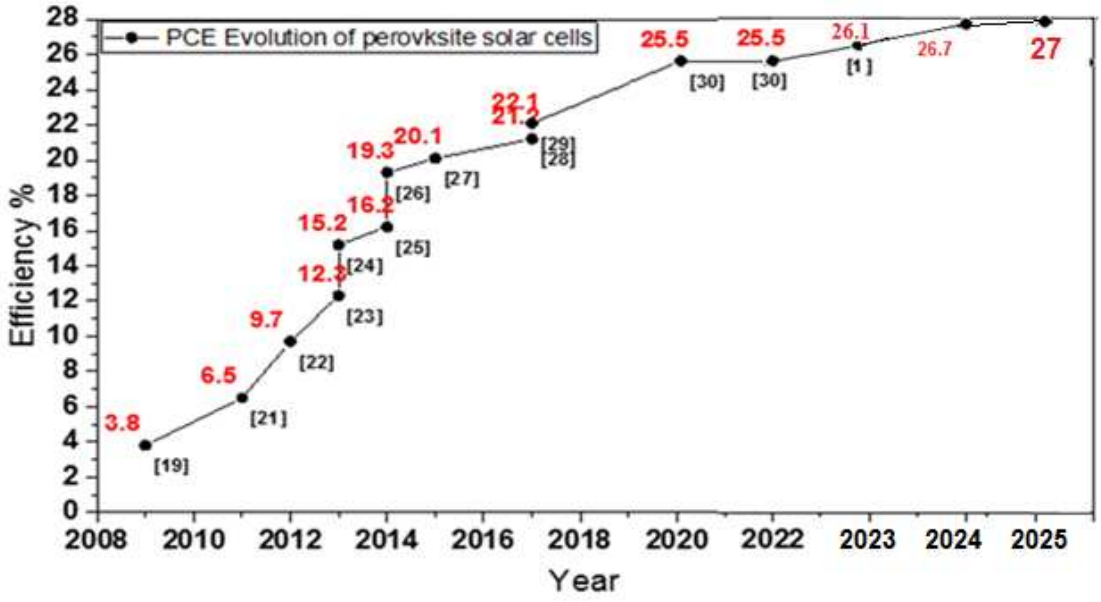

Figure 1 16 Rapid PCE evolution of PSCs from 2009 to 2025.

Most of the research focused on cell architectures, on performance reproducibility and especially on the stability of devices.

At the same time, Perovskites have been shown to drive both electrons and holes, which made it possible to greatly simplify the structure of the collection electrodes to lead to a simple transverse "planar" structure. A review of the evolution of solar device structures was made by M. Grätzel [16].

In the same article, MrGrätzel highlighted some of the remaining problems in making perovskite based cells. Serious competitors of more mature sector such as crystalline silicon. In addition to the problems of long-term stability, which must be solved so that these devices can be viable for many years in outdoor use. The problem of toxicity arises since this material contains lead. Attempts to replace lead with tin have remained made but, to date, with equal conversion yields (6%) [17].

Finally, measurements of characteristics I(V) often have hysteresis dependent on the meaning and the scanning speed of the I (V) curve [13]. These hysteresis also seem to depend on the architecture of the cell, simple planar structures with more hysteresis than mesoscopic structures in which the perovskite and the electron-collecting conductor are nested at the nanoscale.

One possible interpretation is the value of the diffusion length carriers who, if short, could limit the collection of carriers in "planar" structures. Nevertheless, recent estimates of diffusion length by transient absorption measurements and photo-luminescence it was on the order of a micrometer both for holes and electrons[18].

It would seem, therefore, that the diffusion length argument limiting collection is not sufficient. It is clear that studies on internal structure and transport mechanisms have remained extremely limited so far. However, we have some information about some characteristics of these materials.

Perovskites are considered as a direct gap semiconductor material with a bandwidth between 1.6 eV and 2.3 eV.

This material can lead both holes and electrons with mobilities of the order of a few cm 2.0V $^{-1}s^{-1}$ for electrons and up to a few tens of cm 2.0 $V-^{1}s-^{1}$ for holes and lifetimes of the order of several hundred nanoseconds [11, 12].

Another important feature of these materials is the carrier generation mechanism by photons.This generation involves excitons generated by the absorbed photons and their subsequent dissociation gives rise to charge carriers, electron and holes.

The binding energy of these excitons is of the order of 30 meV which allows them to be thermally dissociated at room temperature. Such a material therefore has characteristics close to those of an inorganic semiconductor such as hydrogenated amorphous silicon

b. Working principles:

In PSCs, absorbing light with the active layer material (often methylammonium lead iodide, MAPbI3) doesn't generate long-lived excited states (excitons). Despite this limitation, PSCs still achieve high efficiency by effectively separating these short-lived excitons into individual charged particles using layers like mesoporous or planar TiO2 (ETL) and a separate hole transporting layer (HTL) as shown in Figure 17 [26].

Standard solar cells use a transparent glass window coated with tin oxide (FTO) at the front and a thin gold film deposited at the back.

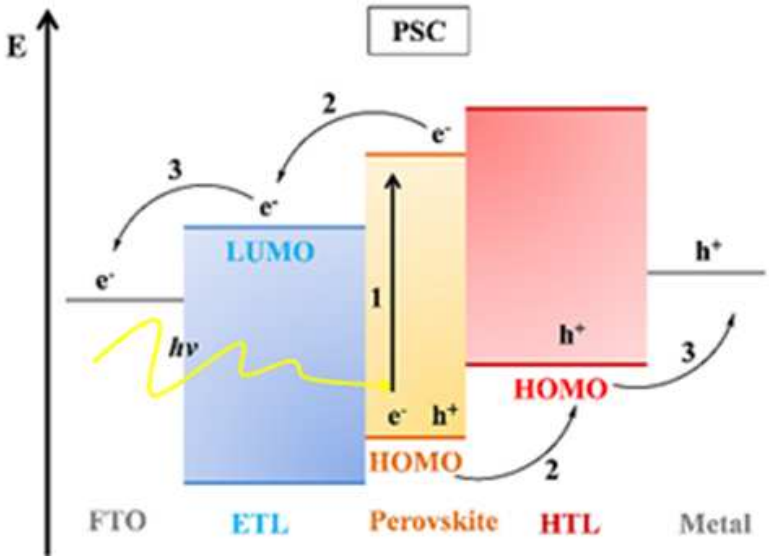

Figure 1 17 Band diagram and working principal steps in PSC [26]

c. Deposition techniques for PSC Thin Film and Fabrication of $MASnI_3$:

c.1. Deposition techiniques for PSC thin film:

The deposition techniques for Psc thin films can be almost classified into two methods: dual-source vapour deposition (DSVD), vapour-assisted solution processes (VASP), one-step spin-coating methods (OSM), and sequential deposition methods

(SDM), as shown in (Figure 06) [28]. The one-step coating method closely rivals other techniques as the preferred process [15]. Notably, DSVD is a vapour process, whereas SDM and OSM are solution processes. Both require a spin-coating process to place PSC thin films and metal halide thin films such as PbI2 or SnI2, respectively

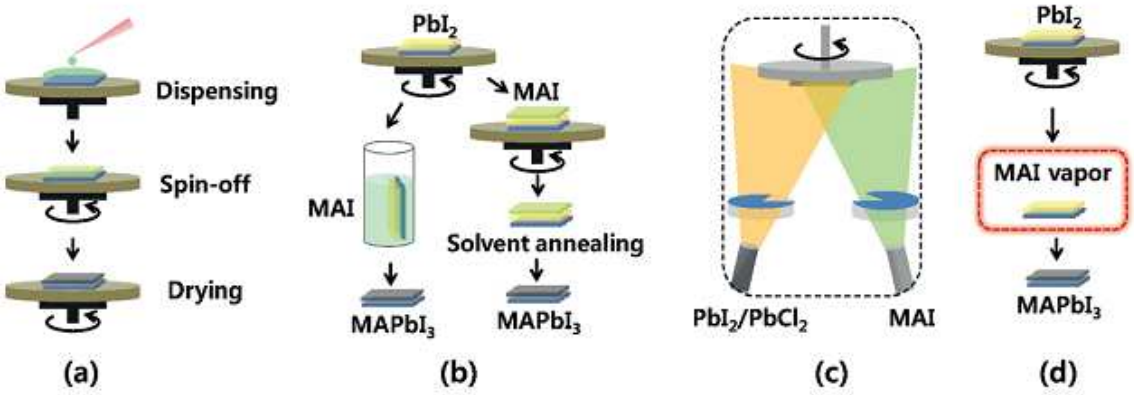

Figure 1 18 Representative deposition techniques for PSC thin film. (a) OSM; (b) SDM; (c) DSVD; and (d) VASP. [15]

c.2. Preparation of the $MASnI_3$ active layer.

Two main approaches exist for synthesizing MASnI3 perovskite: (1) a single-step spin-coating technique using a combined between the CH3NH3 and SnI2, and (2) a two-step method involving initial SnI2 deposition followed by CH3NH3 deposition. To get ready this solution, equimolar quantities of CH_3NH_3I (MAI) and SnI_2 with 40.0 wt % as a concentration was melt in a DMF and DMSO-GBL. (Figure 19) present the absorber layer deposition [27].

The precursor solutions were spin coated onto ETM (TiO_2) coated substrates to form a dark-brown tin perovskite layer. Since the $MASnI_3$ increasingly decomposed in air, all the preparation of $MASnI_3$ films were performed in nitrogen glove box to avoid oxidation of tin perovskite layer in contact with ambient air and hydrolysis.

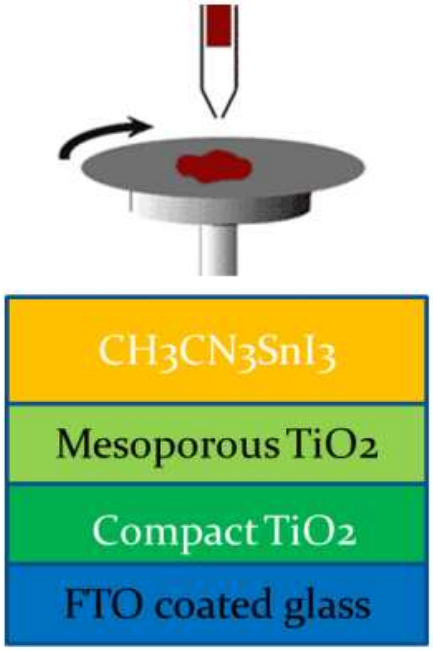

Figure 1 19 The absorber layer of MASnI3 layer deposition. [27]

V. Different photovoltaic solar installations and main factors to consider.

1. System configuration :

In this section the working principle of grid-connected and off-grid PV power plants is described and thus the process of energy conversion from sun radiation to energy fed into the grid illustrated.

a. Off-grid PV plant

The working principle of an off-grid PV plant, also called stand-alone system, strongly differs from grid connected PV systems. In this case, the energy is not fed into a grid, but is either stored in batteries or it is locally consumed immediately. The PV array slightly differs from the grid-connected systems and its size is typically much smaller, especially for small stand-alone applications like solar home systems.

PV modules are interconnected using copper cables and are mounted on stain steel structures as in grid-connected systems. Overvoltage protections, fuses, and eventually lightning protections have to be installed as well in both DC and AC side if available. The output of the PV array is then connected to a controller that controls the charging and discharging of the batteries, the temperature, the state of charge, and the discharge velocity. The batteries are thus connected to an inverter that converts the

incoming DC into AC. The inverter is only necessary if AC loads are used. (Fig 20) shows schematically a stand-alone system.

With Batterie Without Batterie

Figure 1 20 Schematic view of a stand-alone system.[29]

There are lots of different stand-alone systems which might incorporate only some of the components previously mentioned. For example, water pumps powered by PV usually do not include batteries and inverters, but only a controller and a DC water pump. On the other hand, PV stand-alone systems can become extremely complicated and serve, for example, as back-up systems for mini-grids. The automatic control of such mini-grids,which usually include diesel generators and other renewable energy sources like small wind generators, is generally complicated but there are good technical solutions available on the market.

b. Grid-connected PV plant.

The principle of photovoltaic system is very simple: PV cells are connected to obtain the preferred voltage and current properties. Modules are also connected to obtain the preferred output voltage or current for the PV array.

The structures of the modules are in aluminum are mounted in the the ground or in the roof. Roof mounted PV systems habitually fix the modules to the roof for good radiation levels. Ground mounted systems typically use the inclination angle of 33° (in Algeria) in order to increase the rays input in the year. Some PV plants use trackers (two or on-axes) in order to track the irradiation of the sun.

The connexion between modules with electric copper cables. The cross section of the cables depends on the power of the PV array. Overvoltage and lightning protections have to be installed at the latest by this time. The input of the inverter is connected with The PV array output.

The inverter acts as a translator, taking the DC electricity generated by solar panels and turning it into AC. It's like having a built-in smart assistant that constantly tracks the changing power output of the panels due to sunlight and temperature fluctuations. This MPPT ensures to capture the most available energy at any given moment. A meter connected in the inverter output for registers the quantity of energy fed into the grid.

There are two connection methods to the grid: Full feed-in or net metering. The first method is commonly used in Germany and the second method is mainly used in the US, although it is now also permitted in Germany. Full feed-in means that the total production of the PV array is fed into the grid and there is no possibility of own consumption. There is one meter in order to measure the sold energy and one meter for energy consumption. On the other hand, net metering uses a single consumption and production meter. The produced energy is first consumed on-site. In case of exceeding energy, it is fed into the grid; in case of the amount of locally required energy exceeding the production of the PV array, the additional energy is supplied by the grid. (Fig 21) shows schematically the differences between these two methods.

Figure 1 21 Difference between two methods (Full feed in — Net metering)

2. Components of a PV plant.

Photovoltaic (PV) solar cell convert the sunlight electricity , with the photovoltaic effect. The connection of the solar cells in parallel or series to form panels, which are then either connected to a regulator for charging batteries and for using a DC load. The batteries connected to the inverters to convert the DC into AC. The output from the inverters is thus fed into the AC junction for security the grid for consumption. This section presents the main components of a PV plant in detail

2.1 Components of the Grid connected PV plant.

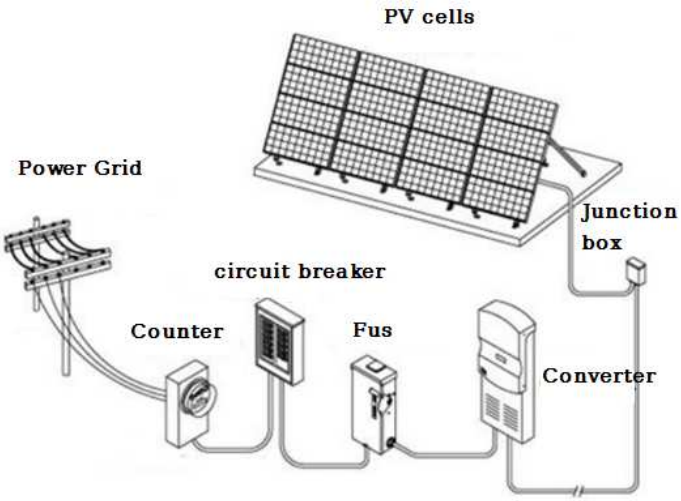

Figure 1 22 Components of the Grid connected PV plant

2.2 Components of the off Grid PV plant.

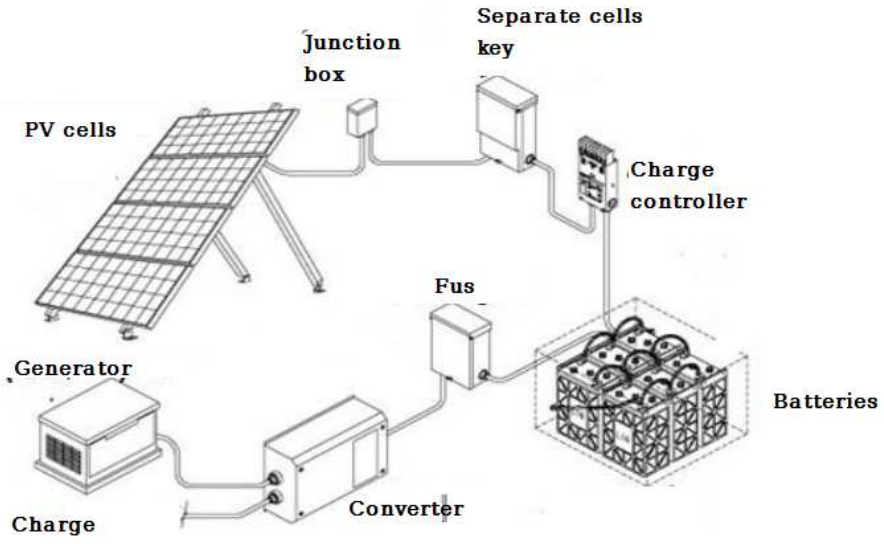

Figure 1 23 Components of the off Grid PV plant

a. Solar cell / solar module (configuration, function, photovoltaic effect).

Electrons excite from the BV to the BC holes when Semi-Conductor materials are exposed to the light.

Introducing tiny amounts of impurities like phosphorus or boron into silicon's crystal structure creates n-type or p-type SC, respectively.

P-N junction formed by combining two types of semiconductors (n-type and p-type), creating an electric field that separates electrons and holes, generating a direct current (DC) in solar cells (Fig. 24).

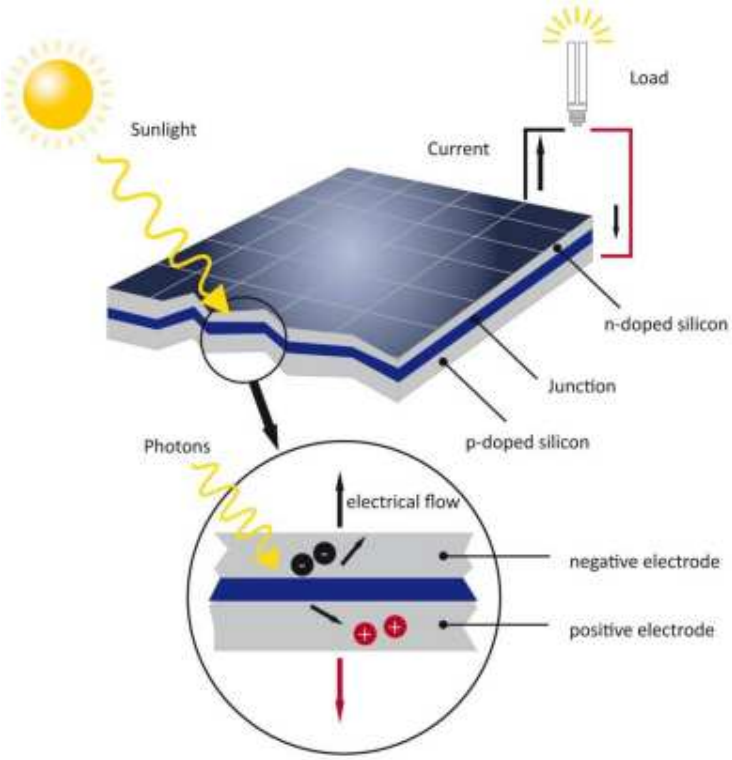

Figure 1 24 Crystalline solar cell working principle.[30]

Sunlight hitting solar cells gets partially reflected, partly passes through, and mainly gets absorbed, generating electron-hole pairs. An electric field separates these pairs, and before arriving at the contacts and heat the solar cell some electron-holes pairs recombine.

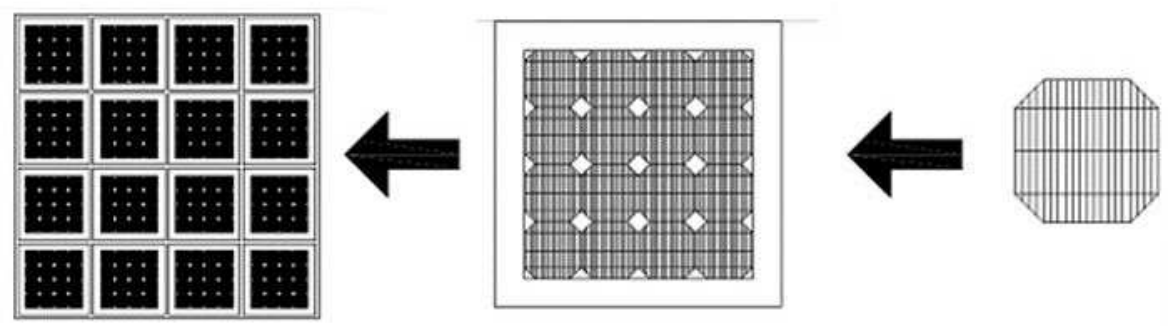

Figure 1 25 From a solar cell to a solar array

Arrangement of the solar cells in series and parallel to compose solar panel and to obtain a desired final power, which is determined by a module's current and voltage. The solar cells are embedded in a glass-EVA-solar cell-Tedlar sheet-Aluminium frame in order to protect them from weather conditions. To avoid high power output losses due to shadowing. Bypass diodes are placed on the back side of the panel.

Solar cells act like miniature batteries, and their electrical behavior can be mapped using a current-voltage (I-V) curve. The most common type, crystalline silicon (cSi), makes up about 80% of the market. They can be either monocrystalline or multicrystalline.

Thin-film solar cells are gaining popularity because they're cheaper to make and easier to produce. They are promising option for the future.

The share of thin-film solar cells in the PV market is growing as manufacturing costs have been significantly reduced and their production is easy.

b. Charge controller:

The batteries can be damaged in the following cases:

- If the battery continues to charge after being fully charged.
- If the charge (discharge) is removed from the battery when it is almost empty.

Hence the importance of having a regulator or controller that disconnects the battery once it is charged, or the battery voltage reaches a value above or below the charge level and stop the load picking operation. It also providers protection for all components of PV system.

Figure 1 26 Controller of charge [31]

b.1. Types of charge regulator:

Common types of controllers include:

- **Pulse width modulation (PWM) :**

It mainly relies on a switch to connect the photovoltaic matrix to the batteries. The result is that the grid voltage will drop to a value close to the battery voltage.

- **MPPT (Maximum Power Point Tracking) controller**

It is more complex and adjusts the input voltage and current to get the maximum power of the PV panel, then converts the input voltage into the voltage required for the DC rods and charges the batteries with high efficiency.

Charge controllers are used with off-grid systems.

Figure 1 27 Difference between the controller PMW and MPPT

b.2. Requirements in charging regulators:

- Protection against overcharging.
- Protection against deep discharge
- Preventunintendedemptying
- Perfectbatterycharging.
- Protection against short circuit
- Protectagainstpolarity reversal
- Battery indicator

c. Batteries:

The battery consists of two electrodes of two different materials which conduct electricity and are immersed in an electrolyte solution,and one of the electrodes becomes positive and the other negative, depending on the charge carried by each of them[28].

It is used to store electrical energy safely so that it can be used anytime and as needed. Solar-powered batteries store electrical energy produced by photovoltaic solar panels during the glare of the sun (during the day) in order to benefit from this electrical energy stored during the absence of the sun (at night). It is used in stand-alone systems.

c.1. Types of solar batteries :

c.1.1. Flooded lead plate acid batteries :

Lead wafers must be completely immersed in a liquid capable of electrical ionization, taking into account that this type gives off explosive hydrogen gas during its work, and therefore sufficient care is taken so that no kind of flame or spark is present next to him during his work.

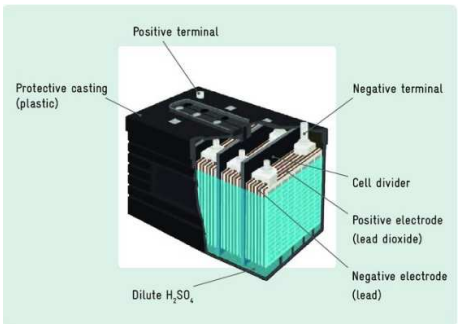

Figure 1 28 Flooded lead plate acid batteries[32]

c.1.2. Valve regulated lead acid :

It uses a technology that freezes the acid in the form of jelly or gel, which is a mixture of water, sulfuric acid and silicate particles from which the acid does not spill at any stage of the operation.

There are three main types:

- **Wet**: it can perform 500 deep discharges of almost 80% It is designed for navigation.
- **AGM**: an electrophoresisable liquid that has been absorbed into a sponge mat.
- **Gel**: liquid transformed into gel or ointment, considered the most effective, the depth of discharge reaches 95%.

Figure 1 29 AGM battery[33]

c.1.3. Nickel-cadmium storage batteries:

They operate on the same general basis as lead acid batteries. But different chemicals are used there, the cathode is cadmium, the anode is nickel oxide, and the potassium hydroxide solution is used as an electrolyte. It is airtight, which prevents it from leaking outside.

Figure 1 30 Nickel-cadmium batteries [35]

d. Inverters (Types, self -controlled vs grid -controlled):

Inverters are static direct-alternating converters making it possible to obtain an alternating voltage and current (AC) source from a direct voltage and current (DC) source and regulates the frequency. There are two types of inverters: three-phase inverters and mono-phase inverters.

Figure 1 31 Different types of inverters[34]

Single-phase inverters power one line, while three-phase handle all three lines. Smaller systems (usually under 5 kWp) use single-phase due to lower power load. For larger systems, three-phase inverters (distributing power across all grid phases) offer greater flexibility in system scale compared to single-phase versions. It is also possible to form a three phase system with connection of many single phase inverters. But the power not surpass 05 Kw.

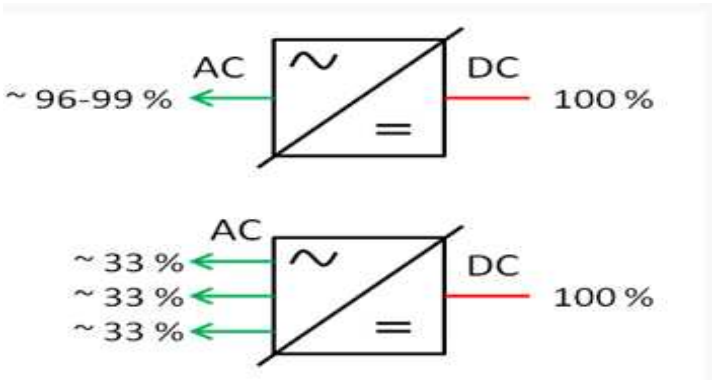

Figure 1 32 SiFngle / three phase inverters

To maximize power output, inverters need to track the constantly shifting Maximum Power Point (MPP) of the PV array due to changing irradiance levels, requiring adaptable electronic components.

Inverters with MPPT technology automatically track shifting sunlight conditions, maximizing solar panel output. Faster tracking, higher accuracy, and better efficiency in MPPTs lead to more efficient inverters.

Certain inverters add transformers for voltage adjustment and safety isolation for the thin-film installations. But they cause additional costs.

The quest for more efficient and compact inverters has driven intense research into transformerless designs.

Companies are already offering transformerless options with features matching traditional transformer-based inverters.
However, grid operators do not accept inverters without transformers in some countries.

Conclusion

In this chapter, we have presented preliminary knowledge on the generations of photovoltaic cells. We have mentioned their different photovoltaic sectors. After, we presented Perovskite-based Hybrid solar cells where we gave general overviews on structural, optical and electrical properties. This, to better understands their operating principle and behavior and mastered them in order to introduce them into photovoltaic cells and improve their electrical efficiency.

The PSCs thin films can be deposited by the vapour-assisted solution processes, dual-source vapour deposition, sequential deposition methods, and one-step spin-coating methods. PSCs have shown special sensitivity to moisture, UV light, temperature and oxygen are still under scrutiny.

Prior to commercialization, it is crucial to establish well-defined metrics for both environmental and photo stability of the device.

Finally, we have presented preliminary knowledge on the different photovoltaic installations.

References:

[1] Schmalensee, Richard. The future of solar energy: an interdisciplinary MIT study. Energy Initiative, Massachusetts Institute of Technology, 2015.

[2] Brooks, Will SM, Dan A. Lamb, and Stuart JC Irvine. "IR reflectance imaging for crystalline Si solar cell crack detection." IEEE journal of photovoltaics 5.5 (2015): 1271-1275.

[3] CHADEL, Asma. Optimisation et simulation numérique du profil de la couche absorbante et des différentes couches des cellules photovoltaïques à base de CIGS. Diss. Université de Tlemcen-Abou Bekr Belkaid, 2011.

[4] Chebrolu, Venkata Thulasivarma, and Hee-Je Kim. "Recent progress in quantum dot sensitized solar cells: an inclusive review of photoanode, sensitizer, electrolyte, and the counter electrode." Journal of Materials Chemistry C 7.17 (2019): 4911-4933.

[5] Zhou, Yong, ed. Eco-and renewable energy materials. Springer, 2015.

[6] Kilner, John A., et al., eds. Functional materials for sustainable energy applications. Elsevier, 2012.

[7] Staebler, 1_D L., and C. R. Wronski. "Reversible conductivity changes in discharge□produced amorphous Si." Applied physics letters 31.4 (1977): 292-294.

[8] Jean, Joel, et al. "Pathways for solar photovoltaics." Energy & Environmental Science 8.4 (2015): 1200-1219.

[9] Levi, Dean H., et al. "Solar cell efficiency tables (version 51)." Progress in Photovoltaics 26.NREL/JA-5J00-70757 (2017).

[10] Kojima, Akihiro, et al. "Organometal halide perovskites as visible-light sensitizers for photovoltaic cells." Journal of the american chemical society 131.17 (2009): 6050-6051.

[11] Etgar, Lioz, et al. "Mesoscopic CH3NH3PbI3/TiO2 heterojunction solar cells." Journal of the American Chemical Society 134.42 (2012): 17396-17399.

[12] Grätzel, Michael. "The light and shade of perovskite solar cells." Nature materials 13.9 (2014): 838-842.

[13] Noel, Nakita K., et al. "Lead-free organic–inorganic tin halide perovskites for photovoltaic applications." Energy & Environmental Science 7.9 (2014): 3061-3068.

[14] Stranks, Samuel D., et al. "Electron-hole diffusion lengths exceeding 1 micrometer in an organometal trihalide perovskite absorber." Science 342.6156 (2013): 341-344.

[15] Liu, Mingzhen, Michael B. Johnston, and Henry J. Snaith. "Efficient planar heterojunction perovskite solar cells by vapour deposition." Nature 501.7467 (2013): 395-398.

[16] De Wolf, Stefaan, et al. "Organometallic halide perovskites: sharp optical absorption edge and its relation to photovoltaic performance." The journal of physical chemistry letters 5.6 (2014): 1035-1039.

[17] Ito, Seigo, et al. "Effects of surface blocking layer of Sb2S3 on nanocrystalline TiO2 for CH3NH3PbI3 perovskite solar cells." The Journal of Physical Chemistry C 118.30 (2014): 16995-17000.

[18] Chen, Tianran, et al. "Origin of long lifetime of band-edge charge carriers in organic–inorganic lead iodide perovskites." Proceedings of the National Academy of Sciences 114.29 (2017): 7519-7524.

[19] Aida, Mohamed Salah, and Assia Bouraiou. "Elaboration et caractérisation des couches minces CuInSe2 par électrodéposition." (1945).

[20] Stephan, U., et al. "Large area deposition technique for PECVD of amorphous silicon [solar cells]." Conference Record of the Twenty Sixth IEEE Photovoltaic Specialists Conference-1997. IEEE, 1997.

[21] He, Y. B., et al. "Heteroepitaxial growth of CuInS 2 thin films on sapphire by radio frequency reactive sputtering." Applied physics letters 83.9 (2003): 1743-1745.

[22] El Jouad, Zouhair. Réalisation et caractérisation des cellules photovoltaïques organiques. Diss. Angers, 2016.

[23] Ullah, Hanif, Bernabé Marí, and Hai Ning Cui. "Investigation on the effect of Gallium on the efficiency of CIGS solar cells through dedicated software." Applied Mechanics and Materials 448 (2014): 1497-1501.

[24] LIU, YINGHUI. "FLEXIBLE SOLAR CELLS WITH IMPROVED EFFICIENCY BY INTEGRATION OF LIGHT-TRAPPING NANOSTRUCTURES." (2012).

[25] NREL Efficiency Chart. This Plot Is Courtesy of the National Renewable Energy Laboratory, Golden, CO. Available online : https://www.nrel.gov/pv/assets/pdfs/best-research-cell-efficiencies.20190802.pdf (accessed on 30Dec 2020).

[26] Pellet, Norman, et al. "Mixed□organic□cation Perovskite photovoltaics for enhanced solar□light harvesting." Angewandte Chemie International Edition 53.12 (2014): 3151-3157.

[27] Kim, Hui-Seon, et al. "Lead iodide perovskite sensitized all-solid-state submicron thin film mesoscopic solar cell with efficiency exceeding 9%." Scientific reports 2.1 (2012): 591.

[28] Y.M.Kamilia ,M.S. Essebki, Energy photovoltaic Book (Arabic version)

[29] Poitiers Academy (2010), Photovoltaic solar energy, Ed Quali'Pv, France, pp. 1-7

[30] Khalifa Aliu Ibrahim et al, THE EFFECT OF SOLAR IRRADIATION ON SOLAR CELLS, Science World Journal Vol 14(No 1) 2019, PP. 20-22

[31] M.A Khan et al, Green Auto Mobile Vehicle Design, ISSN: 2600-7495 eISSN: 2600-9633 IJEEAS Vol. 6, No. 2, October 2023

[32] Andreas Manhart et al, End-of-Life Management of Batteries in the Off-Grid, Deutsche Gesellschaft fürInternationale Zusammenarbeit (GIZ) GmbH, Eschborn, October 2018.

[33] Saher Mahmood Jawd, Nabaa Hameed Chekhyor,Aryaf Mahmood .. Types of Solar Cell Batteries and theirEnergy Charging Methods., Journal of Thermal Engineeringand Applications. 2021; 8(2): 16–22p

[34] Ciprian Ionut Paunescu et al, Laboratory smart home energy management system, DOI: 10.1109/ISGT-Asia.2015.7386987, November 2015

[35] Ayodele O. Soge , P.W. Lefley, A.O. Soge and J. Starkey “Rechargeable batteries: the evolution and beyond – Nickel-based batteries”, part of a four-series article published in Energize Journal by EE Publisher, South Africa. March 2012 editions.Nov/Dec 2012 - Vector - Page 54

CHAPTER 2

STRATEGIES TO PROGRESS THE LONG TERM STABILITY OF PSC

I. Introduction:

With the aim of producing efficient and inexpensive perovskite solar cells, manufacturers should offer warranties that ensure the product's long-term stability and provide measures to extend its lifespan."

In this chapter, we outline systematically the low stability of perovskite and the profit to use (mixed cations), (mixed cations of divalent metals), (mixed halides), (mixed cations with mixed cations of divalent metals), (mixed cations with mixed halides), (mixed cations of divalent metals with mixed halides) and also (the mixed cations with the mixed cations of divalent metals with the mixed halides) in perovskite materials.

a. Stability studies:

The number of publications on the PCE is still numerous compared to the publications focused on long-term stability.

unluckily, perovskite solar cells face a major difficulty: stability. These cells are highly susceptible to degradation from environmental factors like UV light, oxygen, temperature, and humidity. Additionally, the selection of materials and the production techniques used to create these devices play a crucial role in their lifespan.

Stability of PSCs-based DSSC was limited in 2011 (~10 min) ahead of degradation for the reason that PSCs QDs dissolved into redox electrolyte [57]. Stability of PSCs was improved from few minutes to more than 500h using spiro-MeOTAD as HTM , in 2012 [58]

a.1. Moisture:

Research has identified moisture as a significant hurdle for the practical use of MAPbI3, as it readily triggers degradation of the material [01][02]. Too much water disrupts the ordered crystal structure of the perovskite, compromising its performance[03].

While degradation mechanisms for perovskites are explored, some studies suggest low humidity (<30%) during fabrication enhances crystal formation and device performance [4, 5], making the optimal moisture level a topic of debate.

Series of reactions for the moisture catalysed decomposition of the perovskite layer, are proposed by the authors:

$$MAPbI_3 \overset{H_2O}{\Longleftrightarrow} MAI(aq) + PbI_2 \quad (1)$$
$$MAI(aq) \leftrightarrow CH_3NH_2(aq) + HI(aq) \quad (2)$$
$$4HI(aq) + O_2 \leftrightarrow 2I_2(s) + H_2O \quad (3)$$
$$2HI(aq) \overset{hv}{\Leftrightarrow} H_2(g) + I_2(s) \quad (4)$$

[4]

The water is the catalyst required for the irreversible degradation of the perovskite material. It's suggested in many reports.

Under high humidity (70%) for 60 hours, Leguy et al. [06] observed the absorption of water by CH3NH3PbI3 and forming CH3NH3PbI3·H2O–Eq (5) with increasing its band gap to 3.1 eV.

While briefly drying can reverse initial water uptake, prolonged exposure to a dry atmosphere triggers irreversible breakdown (PbI2 formation, CH3NH3+ dissolution). Even moderate light in dry conditions can cause this decomposition [07].

$$4(CH_3NH_3)PbI_3 + 4H_2O \leftrightarrow 4[CH_3NH_3PbI_3.H_2O]$$
$$\leftrightarrow (CH_3NH_3)_4PbI_6 2H_2O + 3PbI_2 + 2H_2O \quad (5)$$

The formation of a hydrated product after $CH_3NH_3PbI_3$ was exposed to moisture [08], it's observed by Christians et al. The authors propose that perovskite resistance to moisture might be linked to how strongly its atoms bond with (H2o) or the organic cation (CH3NH3+). Their idea is that strengthening the bond between the metal halide (PbI6) and the cation could create a more water-resistant material.

Wolf et al observed a surprising change when they exposed a dark brown film to humidity: it turned pale yellow. This color shift matched a drop in light absorption by a hundredfold in the blue and green part of the spectrum (1.5 to 2.5 eV). Interestingly, the edge of light absorption also moved, suggesting the formation of a new material called PbI2. [09]

These authors employed photothermal deflection spectroscopy (PDS), a highly sensitive technique capable of detecting minute changes in absorption, to directly measure the moisture-induced decomposition of CH3NH3PbI3 [62].

a.2. UV light and Oxygen:

In addition to moisture, lighting with UV light also can cause poverty in PSCs, especially in devices containing a TiO2 mesoporous layer. TiO2, known for its water and organic compound oxidation capabilities under UV light due to its 3.2 eV band gap, can generate electron-hole pairs upon illumination. However, recombination at the oxygen adsorption site often hinders efficiency [10].

P. Sullivan et al, concluded that there are two degradation mechanisms: i) oxidation of the active layer by oxygen, responsible for the decrease in the photogenerated current in the cells- ii) degradation by light independently of the presence of oxygen [11].

Ito et al. aimed to tackle the ultraviolet (UV) light instability of the TiO2 layer in PSCs. They applied a technique previously used in inorganic cells, incorporating a thin layer of antimony sulfide (Sb2S3) at the interface between TiO2 and the light-absorbing material (CH3NH3PbI3). This "blocking layer" effectively reduced UV-induced degradation and improved the overall stability of the device [12].

Extraction of electrons from iodide anion to forming I2at the TiO2/ perovskite interface–Eq.(01) is supposed by these authors– and from the reaction presented in Eq (02) they can deconstructing the perovskite crystal. The electron extracted by the TiO2 it could jump back, triggering a reaction that releases harmful HI gas Eq (03). This, in turn, depletes the positive hydrogen ions (H+) needed for another crucial reaction Eq(04). As a result, the balance shifts, and the material releases methylamine (CH3NH2) due to its low boiling point, potentially escaping as a gas (17°C). [61].

$$2I^- \rightleftharpoons I_2 + 2e^- \qquad (01)$$

$$3CH_3NH_3^+ \rightleftharpoons 3CH_3NH_2(g) + 3H^+ \qquad (02)$$

$$I^- + I_2 + 3H^+ + 2e^- \rightleftharpoons 3HI(g) \qquad (03)$$

To combat TiO2-related instability, Chander et al. [14] suggest UV filters, while Leijtens et al. [13] attain +1000 hours of stable photocurrents by replacing TiO2 with an insulating- Al2O3 scaffold.

Replacing the ETL with Zn2SnO4 improved both perovskite crystallization and UV stability in Bera et al.'s [15] work, but resulted in a lower PCE

(13.3%). However, the device displayed minimal hysteresis and remarkable stability (>1 month) without encapsulation.

a.3.Temperature:

As the degradation of PSCs is caused by exposure to oxygen, water and light . It is also accelerated by the temperature.

Effects of temperature on the degradation of PSCs in two ways: on hand affecting the perovskite material and other hand impacting the hole-transporting material (HTM).

While some studies claim perovskite materials can withstand very high temperatures (over 300°C), others show the organic parts break down much sooner, even below 140°C.

PSCs are particularly susceptible to damage by heat. Studies have shown that the key light-absorbing material, MAPbI3, starts to break down (decompose) when heated above 85°C [18,19].

According to Pisoni et al. [20], uneven heat distribution creates mechanical stress, reducing PSC lifespan. This means that a Both polycrystals and single crystals structures exhibit very low thermal conductivity.

The influence of elevated temperatures on both CH3NH3PbI3 and $CH_3NH_3PbI_{3-x}Cl_x$ films is investigated by Phillippe et al. [21]. To isolate the impact of temperature on film degradation, the authors eliminated water and air exposure. Under these controlled conditions, they observed the perovskite film decomposing upon heating to 100°C [63].And they recommended this reaction for the temperature induced decomposition:

$$CH_3NH_3PbI_3 \rightarrow PbI_2 + CH_3NH_2 \uparrow + HI \uparrow \qquad (4)$$

Conings et al. investigated the thermal stability of incomplete PSCs (ITO/TiO2/MAPbI3 structure) by annealing them at 85°C for 24 hours under various environmental conditions [64].

Misra et al. [67] investigated PbI2 and PbBr2 as precursors for perovskite preparation. And after doing experiments ,Sealed CH3NH3PbI3 solar cells degraded within 60 minutes at 44-55°C, while CH3NH3PbBr3 devices remained stable in aging tests. The observed behavior can be attributed to the differences in bond strength

between Pb and I compared to Pb and Br. Due to their larger size, iodine atoms form longer and weaker bonds with lead compared to bromine atoms, making the Pb-I compound less stable [68].

While inorganic precursor substitution improves thermal stability, organic precursors also significantly contribute to overall device robustness and stability.

To isolate the breakdown of the perovskite layer itself, the researchers removed the HTM and top electrode. This is because previous studies have shown that the underlying layer can influence how the PSCs decomposes under heat [65, 66].

While early research utilized a titanium dioxide (TiO2) scaffold, the push for lower manufacturing temperatures led to its replacement with ZnO. However, the ZnO/CH3NH3PbI3 interface appears to promote faster thermal decomposition of the perovskite layer, resulting in reduced thermal stability compared to the TiO2-based structure [65, 66].

To assess perovskite solar cell (PSC) stability in real-world settings, Li et al. [69] exposed devices to outdoor environment in Jeddah, Saudi Arabia, for a week.

The light-absorbing layer, made of perovskite material, was carefully filled into a sponge-like structure composed of titanium dioxide and zirconium dioxide (TiO2/ZrO2). A layer of carbon black was added at the back for electrical contact, and the entire device was sealed with a glass cover using epoxy resin.

After seven days the structure observed the similar Performances. Using the thermally carbon materials contributed for The absence of Hole Transport Materiel (HTM) in this case, and attributed the exhibited good stability,

a.4.Encapsulation:

Different encapsulation techniques for PSCs are used to avoid contact between ambient air and the active layer. In 2006 the team of N.S. Sariciftci [22] presented a technique of encapsulation of organic photovoltaic cells based on MDMO-PPV: PCBM.

This technique involves sealing a flexible barrier (the same material as the substrate) above the cathode with an epoxy resin. This flexible barrier is an organic-inorganic multilayer PEN / (SiOx / PEN) * 5, developed by Novaplasma (a Canadian start-up company) with a thickness of 500 nm for a visible transmission of about 85%.

For small-scale devices, researchers have typically relied on a basic encapsulation method: covering the device with a thin glass cover slip and sealing it with a UV-curable epoxy resin [14, 23, 24].

Han et al compared two encapsulation methods [25], the first technique employed a simple method; a filling the UV curable epoxy resin between the plain glass cover and a silver contact. The other technique was adopted from OLED technology.

Shao et al. presented a groundbreaking, cost-effective method for encapsulating and forming the top electrode of small-scale, lab-made solar cells in one go [26]. They replaced the traditional thermally evaporated top contact with a readily available conductive copper tape, offering a simpler and more economical approach. These authors [72] demonstrated that a readily available carbon conductive tape, adhered well to perovskite layers, serving as both back contact and encapsulant , simplifying fabrication and reducing costs.

Traditional encapsulation for perovskite solar cells involves a top glass substrate separated by Surlyn® sealant (DuPont, USA). The encapsulation of the device which is sandwiched and protected to avoid the supply of moisture and oxygen [69,70] with a polymer resin was only good for a few days. Comparing thermal plastics and light-curable resins for sealing is explored in [71] by, Matteocci et al.

To assess durability, devices underwent accelerated aging tests (temperature stress, damp-heat , light-soaking), with their power conversion efficiency (PCE) degradation monitored.

The optimal sealing combined (Kapton®, DuPont, United States) adhesive with light- curable glues and UV- (Henkel, Germany and ThreeBond, United States) for edge sealing. Although plastic barrier films are common for flexible PSCs [61], hot-pressing Surlyn foil actually decreased efficiency compared to unsealed devices. Weerasinghe et al. [73] explored two encapsulation methods for flexible devices: incomplete and complete, both utilizing a saleable plastic obstacle adhesive (Mitsubishi Plastic, Inc, Japan) covered at 100°C onto the back contact. However, advancements have led researchers to adopt conductive tapes for back contacts, offering potential advantages.

b. Strategies to develop the long term stability of PSCs

The advantages to employ mixed cations, mixed divalent metal cations and mixed halides in PSCs materials. For highlight the next advantages: (i) increased stability, (ii) enabling band gap tuning, (iii) enhanced carriers charge transport, (iv) higher performance, (v) less pronounced hysteresis.

b.1. Mixed cation:

b.1.1. Binary (FM/MA)PbI_3System.

While FAPbI3, with its narrower band gap, could theoretically generate more current in solar cells, it's less stable than the commonly used MAPbI3. [27] Pellet et al. found that combining two different materials, MAPbI3 and FAPbI3, in solar cells improves their ability to capture light, leading to more efficient devices. This is measured by the IPCE. PSCs made with a mix of two materials (MA0.6FA0.4PbI3) performed better than those using just one. This mixture captures more red light, leading to stronger electric currents without reducing voltage (Fig 1)[27,28].

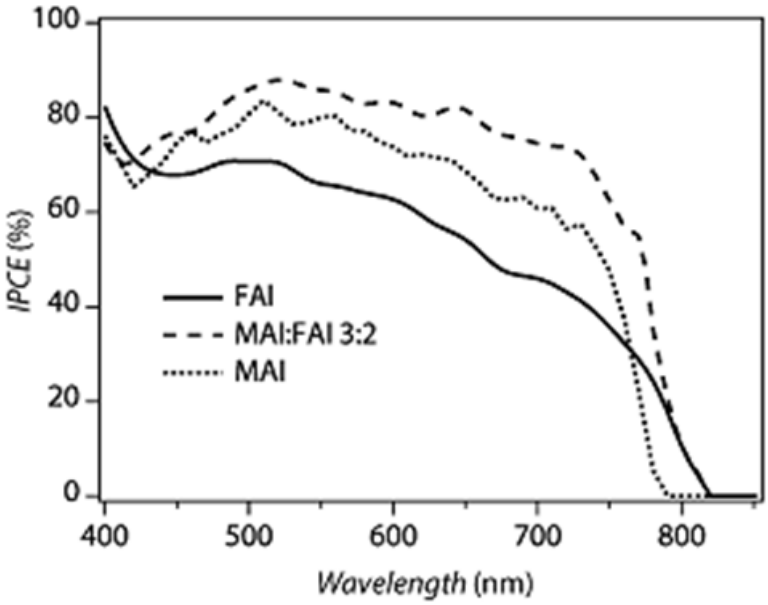

Figure 2- 1PCE spectrum of mixed cation perovskite devices, and MAIPbI3 FPbI3.

Binek et al. [74] investigated that the integration of MA+ into $FAPbI_3$ structure results a stable MAxFA1-xPbI3perovskite structure,[75,76,77]

b.1.2. Binary (MA/Cs) PbI_3 System

Scientists took perovskite solar cells a step further by using a mix of different atoms (including cesium Cs+ and rubidium Rb+) instead of just one. This new approach led to record-breaking efficiency of 21.6%, [29, 30].

Niu et al. [79] showed superior thermal stability of Cs_x $MA_{1-x}PbI_3$ with x = 0.09 and x = 0.20 than that of $MAPbI_3$, contrary to MA+, they reporting a higher efficiency of 18.1% in their optimized $Cs_xMA_{1-x}PbI_3$ devices. Choi et al.[78], devloped $Cs_xMA_{1-x}PbI_3$ devices with x = 0.1, they achieved a PCE of 7.68%. By swapping some of the lead in the cell for a mix of cesium and methylammonium, they saw efficiency improvements of around 20% and 15% in two different studies [78, 79].

b.1.3. Binary (FA/Cs) PbI_3 System.

Scientists haven't explored the (FA/Cs)PbI3 system as much as the CsxMA1-xPbI3 one, but there are still some promising results [80,81,82,83]. Similar to the other system, adding a bit of cesium (Cs) to FAPbI3 seems to boost its efficiency. Studies have shown improvements of 5% to 16% when using about 10-20% Cs [80,81,82].

b.1.4. Binary (FA/Rb) PbI_3 System.

Researchers are exploring the potential of rubidium (Rb+) cations, even smaller than cesium (Cs+) with its 0.152 nm radius, to further improve the efficiency and stability of perovskite solar cells [84,85,86]. The promising results suggest Rb+ could be a viable alternative for enhancing these key performance metrics. Zhang et al [85] and Park et al [86] studied The (FA/Rb) PbI3 system systematically and independently. Incorporation of Rb (5%) in the $Rb_xFA_{1-x}PbI_3$perovskite is reported in both studies

b.2. Mixed divalent metal cation:

While lead (Pb) dominates as the metal cation in PSCs, its toxicity raises concerns for environmental impact, hindering commercialization.

Zuo et al. [31] reported that the Tin (Sn) emerged as a promising alternative of lead (Pb), and achieving a PCE of 10.1%, with the proportion of 75% Pb and 15% Sn.

The minimization of the band gap of provskite is by the he augmentation of Sn concentration, it’s also responsible for the enhancement in solar light absorption [32] (Fig 2) but the existence of Pb is necessary for retarding the oxidation of Sn^{2+} to Sn^{4+} [33].

It is essential to study tin and lead mixed perovskite solar cells, Y.Ogomi et al obtained the greatest PCEs by using $MASn_{0.5}Pb_{0.5}I_3$ perovskite. 4.18% efficiency with short circuit current 20.04 mA/cm^2, open circuit voltage 0.42 V and FF 50% are reported.

If the ration is controlled between Sn and Pb in the perovskite $MASn_{1-x}Pb_xI_3$, the light absorption can be extended to the near infrared region (1060 nm), which was (260 nm) red-shifted compared with that of MAPbI3 PSC is shown in (fig 03) [34,35] and the band gap can be tune in the range 1.17-1.55 eV.

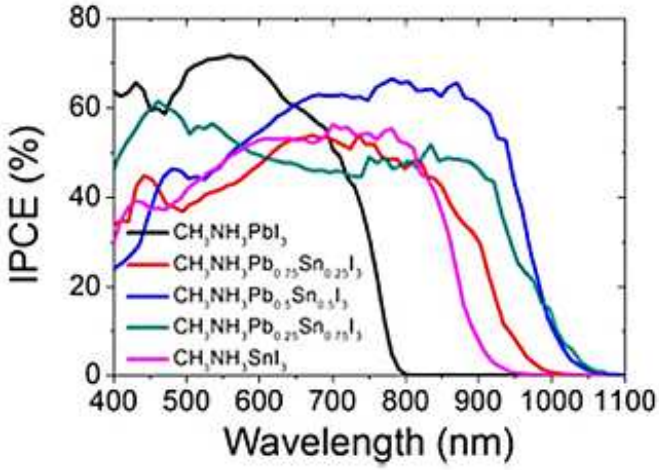

Figure 2- 2IPCE spectra of devices based on CH3NH3Sn1-x PbxI3 perovskite

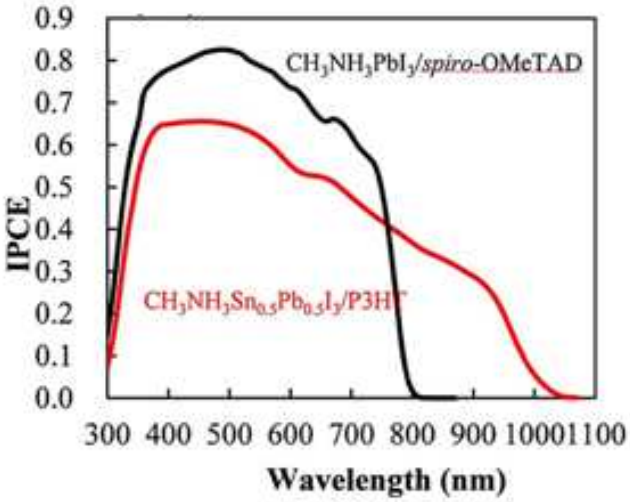

Figure 2- 3 IPCE curves for MASn0.5Pb0.5I3/P3HT and MAPbI3/spiro-OMeTAD PSCs.

b.3. Mixed halide typs:

Building upon extensive research summarized in [90 , 91, 92, 93], this section offers an up-to-date analysis of the structure-property relationship in mixed-halide perovskites, specifically focusing on FAPb(I/Cl) ,MAPb(I/Cl) , MAPb(I/Br),

CsPb(I/Cl), MAPb(I/Br/Cl) , CsPb(I/Br), CsPb(Br/Cl), FAPb(I/Br), MAPb(Br/Cl). based on recent literature.

Mixed-halide perovskites also enhanced the stability on nano-structured TiO2 [59]. Fascinatingly, PSC architectures show more stable after addition of Br into the mixed-halide, when compared to alone later than 30 days, while the efficiency of PSC without Br dropped by20% than the initial PCE [60].

Tailoring the mix of halides in perovskite materials has proven to be a powerful method for enhancing their light and electrical properties [36,37,38]. This strategy is crucial for achieving record-breaking efficiencies in perovskite solar cells (PSCs). Notably, attempts to reach 20% efficiency with pure halide perovskites, like MAPbI3, have consistently fallen short [39,40,41].

Combining different halogen elements in organic-inorganic lead halide perovskites offers numerous advantages, such as enhancing carrier transport [43,44,29], increasing open-circuit voltage [39,40], and improving the overall stability of PSCs [36,42]. Notably, substituting mixed halides within the perovskite structure has been particularly effective in improving PSC stability.

b.3.1Binary FAPb (I/Cl) and MAPb (I/Cl) Systems

Researchers have tried to stabilize the material by halide mixing or exchanging. MAPbI(I/Cl) stands out as a highly researched binary mixed perovskite, drawing significant attention for its potential applications. [98,99]

Lee et al.reported that the PSCs $MAPbI_{3-x}Cl_x$ was more stable in air than $MAPbI_3$ [45].

A few research focus on the FAPb(I/Cl) material system.[100] Lv et al.[97] using the method mixing FAI and PbCl2 in a molar ratio of 3:1 at 60 C° for 30 min in DMF with stirring.

b.3.2 Binary FAPb(I/Br) and MAPb(I/Br) Systems

The mixing of 20% Br into MAPbI3 improved the solar cell stability to a great extent [30]. They are reporting an efficiency of 12.3% is demonstrated by Noh and Jeon et al.

Zhu et al.employed a facile halide exchange route to incorporate Br into $MAPbI_3$ to form $MAPbI_{3-x}Br_x$.

PSCs based on the mixed-halide composition MAPbI3-xBrx achieved a PCE of 14.25%. Notably, these cells retained 93% of their initial efficiency after 14 days of exposure to ambient air without encapsulation [46].

This highlights the potential of mixed-halide perovskites for improved stability compared to pure halide perovskites, which are known to be susceptible to degradation under UV light and heat due to their low crystallization energy [47, 48, 49].

Scientists found that adding a small amount of bromine Br_x (0.2 parts) to the CH3NH3PbI3 improves its stability without sacrificing its efficiency in converting sunlight to electricity [36].

The proposed stabilization mechanism hinges on the contrasting crystal phases of MAPbI3 (tetragonal) and MAPbBr3 (cubic). Substituting iodine (I) with smaller bromine (Br) atoms shrinks the lattice, triggering a transition to the more stable cubic phase, ultimately enhancing material stability.

Mixed halide FAPbI3-xBrx perovskites were also synthesized with x varying from 0 to 1[94, 95].

Rehman et al. discovered that the way they focused the laser beam significantly affected how different materials within the perovskite separated [96].

Strategies to make both FAPb(I/Br) and MAPb(I/Br) systems flexible to phase segregation phenomena is wanted.

b.3.3 Ternary MAPb(I/Br/Cl) and FAPb(I/Br/Cl) Systems

The ternary MAPb(I/Br/Cl) system exhibits properties resembling a linear combination of its binary counterparts, MAPb(I/Cl) and MAPb(I/Br) [89]. Chiang et al.utilized a combined hot solution spin-coating method to fabricate the triple halide perovskites. Their inverted solar cell structures (ITO/PEDOT:PSS/MAPbI3-x-yBrxCly/PC61BM/Ca/Al) with active areas of 0.1 cm2 generated FF = 78 %, Voc = 1.10 V, Jsc = 19.25 mA/cm2 , PCE = 16.52 %.

The latest research demonstrates a significant advancement in PSC stability by exploring variations in optional layers, mixed-halide perovskites, and HTMs. This comprehensive investigation opens doors for optimizing device longevity.

b.4. Mixed cation -Mixed divalent metal cations:

Maddalena Patrini et al. carried out the first extensive investigation addressing the synthesis and characterization of the $FA_{0.8}MA_{0.2}Sn_xPb_{1-x}I_3$ solid solution showing a complete solubility of Sn on the Pb-site leading to cubic single-phase materials.

This research has identified new lead-reduced or lead-free perovskite materials with stable cubic structures and bandgaps ranging from 1.25-1.18 eV. These properties translate to enhanced near-infrared light absorption, marking a significant step towards advanced applications in perovskite solar cells.

The authors successfully crafted a PSC using a mixed absorber of 60% (FASnI3) and 40% (MAPbI3). This composition resulted in an absorption edge of roughly 1.2 eV and a noteworthy PCE of around 15%, highlighting the effectiveness of such mixed-halide approaches in solar cell technology [37].

b.5. Mixed cation -Mixed halide:

The newly composite mixed-perovskite systems where the double (FA/MA), (MA / Cs), (FA / Cs), triple (FA / MA / Cs) and even quadrupole (FA /MA /Cs/ Rb) mixed cations[87] are usually followed by the mixed (I/Br), (FA /MA /Cs/ Rb). Improve devices were reported to show the best efficiency and stability [88].

Zhiping Wang et al. presented the first long-term stability study of the new PSCs composition $FA_{0.830}Cs_{0.170}Pb(I_{0.60}Br_{0.40})3$(FA = (HC(NH2)2)) and discover that the cells are really stable when exposed to sun light in ambient conditions without encapsulation [52].

Michael Saliba et al. demonstrated a PSC which not only more stable but also is possesses higher PCEs of 21.1%, contains less sensitive to processing conditions [53, 54], and is fewer phase impurities.

They also investigated triple-cation PSC of the generic form "$Cs_x(MA_{0.170}FA_{0.830})$ $(100_{-x})Pb(I_{0.830}Br_{0.170})_3$," representing that the use of all three cations, MA, Cs, and FA, provides additional versatility in fine-tuning highquality PSC films [38].

These perovskite solar cells achieved impressive stabilized power conversion efficiencies (PCEs) exceeding 18% and 21% after 250 hours under real-world operating conditions. Additionally, the triple-cation perovskite films demonstrated

superior thermal stability and resilience to variations in external factors like temperature, solvent vapors, and heating procedures [38]. The demonstrated robustness of this approach is crucial for ensuring reproducibility, a vital factor for cost-effective, large-scale manufacturing of perovskite solar cells (PSCs).

Scientists found another way to adjust the light-absorbing properties of perovskites by combining mixed halide and mixed cation ($FAPbIyBr_{3-y)}$.[51] This led to solar cells with efficiency of 20.8%, making this new material is one of the biggest performances of PSCs right now [03].

b.6. Mixed divalent metal cations- mixed halide anions

Sun et al. have introduced a groundbreaking class of air-stable triple-cation mixed-halide perovskites capable of achieving high solar cell efficiencies without the requirement of a thermal annealing process. This feat is attributed to the incorporation of Pb(SCN)2 within the perovskite structure.

Combining formamidinium (FA), methylammonium (MA), and cesium (Cs) cations with a mixture of iodide (I) and bromide (Br) anions, the study identifies $FA_{0.7}MA_{0.2}Cs_{0.1}Pb(I_{5/6}Br_{1/6})_3$ (FMC) as the optimal composition for forming stable perovskite structures based on theoretical calculations.

Adding Pb(SCN)2 to the $FA_{0.7}MA_{0.2}Cs_{0.1}Pb(I_{5/6}Br_{1/6})_{3-x}(SCN)_x$ perovskite composition (denoted as FMC-SCN) significantly increases the size and crystallinity of the perovskite crystals, even without the typical thermal annealing process.

Furthermore, the addition of Pb(SCN)2 helps prevent the formation of unwanted defects and a harmful lead iodide phase within the perovskite material. This translates to a remarkable power conversion efficiency (PCE) of 14.09% in planar solar cells based on this composition, with a reduced hysteresis effect [54,55].

This research presents a novel and scalable approach for manufacturing efficient perovskite solar cells at room temperature, while also boasting good moisture and thermal stability.

b.7. Mixed cation -Mixed divalent metal cations -Mixed halide anions

Ueoka. N et al. explored how adding small amounts of different materials like Cesium Bromide (CsBr), Cesium Iodide (CsI) , and Tin Bromide (SnBr2) affected the light-harvesting and surface features of perovskite solar cells.

The fill factors, open-circuit voltage and short-circuit current densities increased by CsI addition, and the doping of SnBr2 also improved the surface coverage of the PSC crystals.

The cell prepared by a starting composition of MA0.95 Cs0.05 Pb0.95 Sn0.05I2.90 Br0.10 showed the best conversion efficiencies of 8.25%, and the sizes of the PSC crystals reduced [56].

Conclusion

In this work, we have presented on the basic of PCE loss during the including of (i) oxygen, heat, polarization, humidity, at solar cell and permanent degradation induced by solar cells. light leading to PbI2 and I containing volatile species [101, 102].

We have cited in this chapter different encapsulation techniques for perovskite solar cells to avoid contact between the ambient air and the active layer. And we have summarized recent advances and advantages to employing in mixed perovskite.

References

[01] Petrus, Michiel L., et al. "The Influence of Water Vapor on the Stability and Processing of Hybrid Perovskite Solar Cells Made from Non□Stoichiometric Precursor Mixtures." ChemSusChem 9.18 (2016): 2699-2707.

[02] Gottesman, Ronen, et al. "Extremely slow photoconductivity response of CH3NH3PbI3 perovskites suggesting structural changes under working conditions." The journal of physical chemistry letters 5.15 (2014): 2662-2669.

[03] Mesquita, Isabel, Luísa Andrade, and Adélio Mendes. "Perovskite solar cells: Materials, configurations and stability." Renewable and Sustainable Energy Reviews 82 (2018): 2471-2489.

[04] Zhou, Huanping, et al. "Interface engineering of highly efficient perovskite solar cells." Science 345.6196 (2014): 542-546.

[05] Leguy, Aurélien MA, et al. "Reversible hydration of CH3NH3PbI3 in films, single crystals, and solar cells." Chemistry of Materials 27.9 (2015): 3397-3407..

[06] Habisreutinger, Severin N., et al. "Carbon nanotube/polymer composites as a highly stable hole collection layer in perovskite solar cells." Nano letters 14.10 (2014): 5561-5568.

[07] You, Jingbi, et al. "Moisture assisted perovskite film growth for high performance solar cells." Applied Physics Letters 105.18 (2014).

[08] Chebrolu, Venkata Thulasivarma, and Hee-Je Kim. "Recent progress in quantum dot sensitized solar cells: an inclusive review of photoanode, sensitizer, electrolyte, and the counter electrode." Journal of Materials Chemistry C 7.17 (2019): 4911-4933.

[09] De Wolf, Stefaan, et al. "Organometallic halide perovskites: sharp optical absorption edge and its relation to photovoltaic performance." The journal of physical chemistry letters 5.6 (2014): 1035-1039.

[10] Fujishima, Akira, Tata N. Rao, and Donald A. Tryk. "Titanium dioxide photocatalysis." Journal of photochemistry and photobiology C: Photochemistry reviews 1.1 (2000): 1-21.

[11] Sullivan, P., and Tim S. Jones. "Pentacene/fullerene (C60) heterojunction solar cells: Device performance and degradation mechanisms." Organic Electronics 9.5 (2008): 656-660.

[12] Ito, Seigo, et al. "Effects of surface blocking layer of Sb2S3 on nanocrystalline TiO2 for CH3NH3PbI3 perovskite solar cells." The Journal of Physical Chemistry C 118.30 (2014): 16995-17000.

[13] Leijtens, Tomas, et al. "Overcoming ultraviolet light instability of sensitized TiO2 with meso-superstructured organometal tri-halide perovskite solar cells." Nature communications 4.1 (2013): 2885.

[14] Chander, Nikhil, et al. "Reduced ultraviolet light induced degradation and enhanced light harvesting using YVO4: Eu3+ down-shifting nano-phosphor layer in organometal halide perovskite solar cells." Applied Physics Letters 105.3 (2014).

[15] Heo, Jin Hyuck, et al. "Efficient inorganic–organic hybrid heterojunction solar cells containing perovskite compound and polymeric hole conductors." Nature photonics 7.6 (2013): 486-491.

[16] Bera, Ashok, et al. "Fast crystallization and improved stability of perovskite solar cells with Zn2SnO4 electron transporting layer: interface matters." ACS applied materials & interfaces 7.51 (2015): 28404-28411.

[17] Dualeh, Amalie, et al. "Effect of annealing temperature on film morphology of organic–inorganic hybrid pervoskite solid□state solar cells." Advanced Functional Materials 24.21 (2014): 3250-3258.

[18] Misra, Ravi K., et al. "Temperature-and component-dependent degradation of perovskite photovoltaic materials under concentrated sunlight." The journal of physical chemistry letters 6.3 (2015): 326-330.

[19] Conings, Bert, et al. "Intrinsic thermal instability of methylammonium lead trihalide perovskite." Advanced Energy Materials 5.15 (2015): 1500477.

[20] Pisoni, Andrea, et al. "Ultra-low thermal conductivity in organic–inorganic hybrid perovskite CH3NH3PbI3." The journal of physical chemistry letters 5.14 (2014): 2488-2492.

[21] He, Y. B., et al. "Heteroepitaxial growth of CuInS 2 thin films on sapphire by radio frequency reactive sputtering." Applied physics letters 83.9 (2003): 1743-1745.

[22] Dennler, Gilles, et al. "A new encapsulation solution for flexible organic solar cells." Thin Solid Films 511 (2006): 349-353.

[23] Lee, Jin□Wook, et al. "Formamidinium and cesium hybridization for photo□and moisture□stable perovskite solar cell." Advanced Energy Materials 5.20 (2015): 1501310.

[24] Guarnera, Simone, et al. "Improving the long-term stability of perovskite solar cells with a porous Al2O3 buffer layer." The journal of physical chemistry letters 6.3 (2015): 432-437.

[25] Han, Yu, et al. "Degradation observations of encapsulated planar CH 3 NH 3 PbI 3 perovskite solar cells at high temperatures and humidity." Journal of Materials Chemistry A 3.15 (2015): 8139-8147..

[26] Shao, Yuchuan, et al. "Vacuum-free laminated top electrode with conductive tapes for scalable manufacturing of efficient perovskite solar cells." Nano Energy 16 (2015): 47-53.

[27] Eperon, Giles E., et al. "Formamidinium lead trihalide: a broadly tunable perovskite for efficient planar heterojunction solar cells." Energy & Environmental Science 7.3 (2014): 982-988.

[28] Wang, Zhiping, et al. "Efficient and air□stable mixed□cation lead mixed□halide perovskite solar cells with n□doped organic electron extraction layers." Advanced Materials 29.5 (2017): 1604186.

[29] Roiati, Vittoria, et al. "Investigating charge dynamics in halide perovskite-sensitized mesostructured solar cells." Energy & Environmental Science 7.6 (2014): 1889-1894.

[30] Jeon, Nam Joong, et al. "Solvent engineering for high-performance inorganic–organic hybrid perovskite solar cells." Nature materials 13.9 (2014): 897-903.

[31] Zuo, Fan, et al. "Binary□metal perovskites toward high□performance planar□heterojunction hybrid solar cells." Advanced Materials 26.37 (2014): 6454-6460.

[32] Hao, Feng, et al. "Anomalous band gap behavior in mixed Sn and Pb perovskites enables broadening of absorption spectrum in solar cells." Journal of the American Chemical Society 136.22 (2014): 8094-8099.

[33] Ogomi, Yuhei, et al. "CH3NH3Sn x Pb (1–x) I3 Perovskite solar cells covering up to 1060 nm." The journal of physical chemistry letters 5.6 (2014): 1004-1011.

[34] Philippe, Bertrand, et al. "Chemical and Electronic Structure Characterization of Lead Halide Perovskites and Stability Behavior under Different Exposures • A Photoelectron Spectroscopy Investigation." Chemistry of Materials 27.5 (2015): 1720-1731..

[35] Jean, Joel, et al. "Pathways for solar photovoltaics." Energy & Environmental Science 8.4 (2015): 1200-1219.

[36] Burschka, Julian, et al. "Sequential deposition as a route to high-performance perovskite-sensitized solar cells." Nature 499.7458 (2013): 316-319.

[37] Yang, Woon Seok, et al. "High-performance photovoltaic perovskite layers fabricated through intramolecular exchange." Science 348.6240 (2015): 1234-1237.

[38] Kulkarni, Sneha A., et al. "Band-gap tuning of lead halide perovskites using a sequential deposition process." Journal of Materials Chemistry A 2.24 (2014): 9221-9225.

[39] Kojima, Akihiro, et al. "Organometal halide perovskites as visible-light sensitizers for photovoltaic cells." Journal of the american chemical society 131.17 (2009): 6050-6051.

[40] Saliba, Michael, et al. "Cesium-containing triple cation perovskite solar cells: improved stability, reproducibility and high efficiency." Energy & environmental science 9.6 (2016): 1989-1997.

[41] Lee, Michael M., et al. "Efficient hybrid solar cells based on meso-superstructured organometal halide perovskites." science 338.6107 (2012): 643-647.

[42] Gao, Peng, Michael Grätzel, and Mohammad K. Nazeeruddin. "Organohalide lead perovskites for photovoltaic applications." Energy & Environmental Science 7.8 (2014): 2448-2463.

[43] Shi, Dong, et al. "Low trap-state density and long carrier diffusion in organolead trihalide perovskite single crystals." Science 347.6221 (2015): 519-522.

[44] Stranks, Samuel D., et al. "Electron-hole diffusion lengths exceeding 1 micrometer in an organometal trihalide perovskite absorber." Science 342.6156 (2013): 341-344.

[45] Iefanova, Anastasiia, et al. "Lead free CH3NH3SnI3 perovskite thin-film with p-type semiconducting nature and metal-like conductivity." Aip Advances 6.8 (2016).

[46] Noh, Jun Hong, et al. "Chemical management for colorful, efficient, and stable inorganic–organic hybrid nanostructured solar cells." Nano letters 13.4 (2013): 1764-1769.

[47] Eperon, Giles E., et al. "Formamidinium lead trihalide: a broadly tunable perovskite for efficient planar heterojunction solar cells." Energy & Environmental Science 7.3 (2014): 982-988.

[48] Bi, Dongqin, et al. "Efficient luminescent solar cells based on tailored mixed-cation perovskites." Science advances 2.1 (2016): e1501170.

[49] Marinova, Nevena, Silvia Valero, and Juan Luis Delgado. "Organic and perovskite solar cells: Working principles, materials and interfaces." Journal of colloid and interface science 488 (2017): 373-389.

[50] Etgar, Lioz, et al. "Mesoscopic CH3NH3PbI3/TiO2 heterojunction solar cells." Journal of the American Chemical Society 134.42 (2012): 17396-17399.

[51] Li, Faming, and Mingzhen Liu. "Recent efficient strategies for improving the moisture stability of perovskite solar cells." Journal of Materials Chemistry A 5.30 (2017): 15447-15459.

[52] Hodes, Gary. "Perovskite-based solar cells." Science 342.6156 (2013): 317-318.

[53] Saliba, Michael, et al. "Cesium-containing triple cation perovskite solar cells: improved stability, reproducibility and high efficiency." Energy & environmental science 9.6 (2016): 1989-1997.

[54] Breakthrough Reproducibility Achieved for Perovskite Solar Cells. https:// www.perovskite-info.com/breakthrough-reproducibility-achievedperovskite-solar-cells. Accessed 2019

[55] Sun, Yong, et al. "Triple-cation mixed-halide perovskites: towards efficient, annealing-free and air-stable solar cells enabled by Pb (SCN) 2 additive." Scientific Reports 7.1 (2017): 46193.

[56] Ueoka, Naoki, et al. "Fabrication and characterization of CH3NH3 (Cs) Pb (Sn) I3 (Br) perovskite solar cells." AIP Conference Proceedings. Vol. 1807. No. 1. AIP Publishing, 2017.

[57] Im, Jeong-Hyeok, et al. "6.5% efficient perovskite quantum-dot-sensitized solar cell." Nanoscale 3.10 (2011): 4088-4093.

[58] Kim, Hui-Seon, et al. "Lead iodide perovskite sensitized all-solid-state submicron thin film mesoscopic solar cell with efficiency exceeding 9%." Scientific reports 2.1 (2012): 591.

[59] Suarez, Belen, et al. "Recombination study of combined halides (Cl, Br, I) perovskite solar cells." The journal of physical chemistry letters 5.10 (2014): 1628-1635.

[60] Prasanthkumar, Seelam, and Lingamallu Giribabu. "Recent advances in perovskite-based solar cells." Current Science (00113891) 111.7 (2016).

[61] Mesquita, Isabel, Luísa Andrade, and Adélio Mendes. "Perovskite solar cells: Materials, configurations and stability." Renewable and Sustainable Energy Reviews 82 (2018): 2471-2489.

[62] De Wolf, Stefaan, et al. "Organometallic halide perovskites: sharp optical absorption edge and its relation to photovoltaic performance." The journal of physical chemistry letters 5.6 (2014): 1035-1039.

[63] Wang, Dian, et al. "Stability of perovskite solar cells." Solar Energy Materials and Solar Cells 147 (2016): 255-275.

[64] Conings, Bert, et al. "Intrinsic thermal instability of methylammonium lead trihalide perovskite." Advanced Energy Materials 5.15 (2015): 1500477.

[65] Yang, Jinli, et al. "Origin of the thermal instability in CH3NH3PbI3 thin films deposited on ZnO." Chemistry of Materials 27.12 (2015): 4229-4236.

[66] Hu, Qin, et al. "Engineering of electron-selective contact for perovskite solar cells with efficiency exceeding 15%." ACS nano 8.10 (2014): 10161-10167.

[67] Misra, Ravi K., et al. "Temperature-and component-dependent degradation of perovskite photovoltaic materials under concentrated sunlight." The journal of physical chemistry letters 6.3 (2015): 326-330.

[68] Jin, C., et al. "Attachment of two electrons to C 60 F 48: Coulomb barriers in doubly charged anions." Physical review letters 73.21 (1994): 2821.

[69] Li, Xiong, et al. "Outdoor performance and stability under elevated temperatures and long□term light soaking of triple□layer mesoporous perovskite photovoltaics." Energy Technology 3.6 (2015): 551-555.

[70] Matteocci, Fabio, et al. "Encapsulation for long-term stability enhancement of perovskite solar cells." Nano Energy 30 (2016): 162-172.

[71] Ramos, F. Javier, et al. "Fabrication and encapsulation of perovskites sensitized solid state solar cells." 2014 IEEE 40th Photovoltaic Specialist Conference (PVSC). IEEE, 2014.

[72] Shao, Yuchuan, et al. "Vacuum-free laminated top electrode with conductive tapes for scalable manufacturing of efficient perovskite solar cells." Nano Energy 16 (2015): 47-53.

[73] Weerasinghe, Hasitha C., et al. "Encapsulation for improving the lifetime of flexible perovskite solar cells." Nano Energy 18 (2015): 118-125.

[74] Binek, Andreas, et al. "Stabilization of the trigonal high-temperature phase of formamidinium lead iodide." The journal of physical chemistry letters 6.7 (2015): 1249-1253.

[75] Weber, O. J., B. Charles, and M. T. Weller. "Phase behaviour and composition in the formamidinium–methylammonium hybrid lead iodide perovskite solid solution." Journal of Materials Chemistry A 4.40 (2016): 15375-15382.

[76] Dai, Jun, et al. "Carrier Decay Properties of Mixed Cation Formamidinium–Methylammonium Lead Iodide Perovskite [HC (NH2) 2] 1–x [CH3NH3] x PbI3 Nanorods." The Journal of Physical Chemistry Letters 7.24 (2016): 5036-5043.

[77] Slimi, B., et al. "Perovskite FA1-xMAxPbI3 for solar cells: films formation and properties." Energy Procedia 102 (2016): 87-95.

[78] Choi, Hyosung, et al. "Cesium-doped methylammonium lead iodide perovskite light absorber for hybrid solar cells." Nano Energy 7 (2014): 80-85.

[79] Niu, Guangda, et al. "Enhancement of thermal stability for perovskite solar cells through cesium doping." RSC advances 7.28 (2017): 17473-17479.

[80] Lee, Jin□Wook, et al. "Formamidinium and cesium hybridization for photo□and moisture□stable perovskite solar cell." Advanced Energy Materials 5.20 (2015): 1501310.

[81] Li, Zhen, et al. "Stabilizing perovskite structures by tuning tolerance factor: formation of formamidinium and cesium lead iodide solid-state alloys." Chemistry of Materials 28.1 (2016): 284-292.

[82] Yu, Yue, et al. "Improving the performance of formamidinium and cesium lead triiodide perovskite solar cells using lead thiocyanate additives." ChemSusChem 9.23 (2016): 3288-3297.

[83] Huang, Jiahao, et al. "Sequential Introduction of Cations Deriving Large□Grain CsxFA1− xPbI3 Thin Film for Planar Hybrid Solar Cells: Insight into Phase□Segregation and Thermal□Healing Behavior." Small 13.10 (2017): 1603225.

[84] Zhang, Meng, et al. "High-efficiency rubidium-incorporated perovskite solar cells by gas quenching." ACS Energy Letters 2.2 (2017): 438-444.

[85] Saliba, Michael, et al. "Incorporation of rubidium cations into perovskite solar cells improves photovoltaic performance." Science 354.6309 (2016): 206-209.

[86] Park, Yun Hee, et al. "Inorganic rubidium cation as an enhancer for photovoltaic performance and moisture stability of HC (NH2) 2PbI3 perovskite solar cells." Advanced Functional Materials 27.16 (2017): 1605988.

[87] Correa-Baena, Juan-Pablo, et al. "The rapid evolution of highly efficient perovskite solar cells." Energy & Environmental Science 10.3 (2017): 710-727.

[88] Saliba, Michael, et al. "Incorporation of rubidium cations into perovskite solar cells improves photovoltaic performance." Science 354.6309 (2016): 206-209.

[89] Chiang, Chien-Hung, Jun-Wei Lin, and Chun-Guey Wu. "One-step fabrication of a mixed-halide perovskite film for a high-efficiency inverted solar cell and module." Journal of Materials Chemistry A 4.35 (2016): 13525-13533.

[90] Yin, Wan-Jian, et al. "Halide perovskite materials for solar cells: a theoretical review." Journal of Materials Chemistry A 3.17 (2015): 8926-8942.

[91] Chen, Qi, et al. "Under the spotlight: The organic–inorganic hybrid halide perovskite for optoelectronic applications." Nano Today 10.3 (2015): 355-396.

[92] Luo, Shiqiang, and Walid A. Daoud. "Recent progress in organic–inorganic halide perovskite solar cells: mechanisms and material design." Journal of Materials Chemistry A 3.17 (2015): 8992-9010.

[93] Gao, Peng, Michael Grätzel, and Mohammad K. Nazeeruddin. "Organohalide lead perovskites for photovoltaic applications." Energy & Environmental Science 7.8 (2014): 2448-2463.

[94] Eperon, Giles E., et al. "Formamidinium lead trihalide: a broadly tunable perovskite for efficient planar heterojunction solar cells." Energy & Environmental Science 7.3 (2014): 982-988.

[95] Zhang, Taiyang, et al. "A facile solvothermal growth of single crystal mixed halide perovskite CH 3 NH 3 Pb (Br 1− x Cl x) 3." Chemical communications 51.37 (2015): 7820-7823.

[96] Rehman, Waqaas, et al. "Charge□carrier dynamics and mobilities in formamidinium lead mixed□halide perovskites." Advanced Materials 27.48 (2015): 7938-7944.

[97] Wang, Zaiwei, et al. "Additive-modulated evolution of HC (NH2) 2PbI3 black polymorph for mesoscopic perovskite solar cells." Chemistry of Materials 27.20 (2015): 7149-7155.

[98] Lee, Michael M., et al. "Efficient hybrid solar cells based on meso-superstructured organometal halide perovskites." science 338.6107 (2012): 643-647.

[99] Xu, Jia, et al. "Bromide regulated film formation of CH3NH3PbI3 in low-pressure vapor-assisted deposition for efficient planar-heterojunction perovskite solar cells." Solar Energy Materials and Solar Cells 157 (2016): 1026-1037.

[100] Lv, Siliu, et al. "One-step, solution-processed formamidinium lead trihalide (FAPbI (3− x) Cl x) for mesoscopic perovskite–polymer solar cells." Physical Chemistry Chemical Physics 16.36 (2014): 19206-19211.

[101] Leijtens, Tomas, et al. "Towards enabling stable lead halide perovskite solar cells; interplay between structural, environmental, and thermal stability." Journal of Materials Chemistry A 5.23 (2017): 11483-11500.

[102] Leijtens, Tomas, et al. "Stability of metal halide perovskite solar cells." Advanced Energy Materials 5.20 (2015): 1500963.

CHAPTER 3

RESULTS & DISCUSSION

1. Introduction

Recently, perovskite solar cells have shown significant improvement in theefficiency and have reached 25.7% [01]. The most universal PSC material used in solar cells is the $MAPbI_3$ (methylammonium lead Iodide). But due to toxicity of lead (Pb) to the human health, a suitable alternative of $CH_3NH_3PbI_3$ is being researched across the world in recent times [02].

Solar cells often use lead, which is harmful to the environment. This research suggests a potential solution: using $CH_3NH_3PbI_3$ as absorbing layer (direct bandgap 1.3 eV), while still capturing sufficient sunlight to generate electricity. [03]

The HTM (Spiro-OMeTAD) has been routinely used in organic photovoltaics (OPV) and organic optoelectronics [20], but it is causes degradation in the devices performance and the field is still research active [22]. So, it is necessary to choose other new HTM materials, which can replace the spiro-OMeTAD.

For any material to be hired as electron transport layer in perovskite solar cells, the material necessity satisfy few significant properties (conduction band of the ETM should be not as much of the LUMO level of the perovskite material - high electron mobility - higher band gap [27].

Now as far as the TiO_2 and ZnO are concerned in the ordinary perovskite solar cell, TiO_2 is used as an electron collecting layer. This oxide layer plays an important role in the cell; however, its growth procedure involves a high temperature annealing step. In adding to the high production costs involved, its use similarly eliminates its application to temperatures delicate substrates such as supple plastic materials [28].

In this work, on the one hand, several simulation architectures are developed using Simulator Application (SCAPS-1D) to optimize high efficiency perovskite solar cell with different ETM and HTM.

A comparative work was also carried out between eleven structures (five of our own structures and six that we used as reference) by replacing TiO_2 by ZnO as ETM layer with perovskite ($MAPbI_3$ and $MASnI_3$) and (Spiro-OMeTAD, PEDOT: PTT, Cu_2O and CuI) as HTM layers.

In this work, it was shown that the efficiency can be improved if used the HTM (Cu_2O), and the ETM (TiO_2), and the cost can be reduced if TiO_2 changes with ZnO.

In the second part, three practical works were carried out, the first project solar-powered local network that allows calls and electronic messages or texts to be

transmitted with a perovskite solar cell. The second project of sustainable disinfection tunnel (SDT) that it was designed to contribute to reduce the viruses less harmful than the corona virus that are transmitted by touch and to provide protection maximum to people going through the tunnel in about 10 seconds is by using solar PV. And the third project for a Wi-Fi station and solar-powered Smartphone chargers with a money multi coin selector which makes it possible to highlight the two principles of environmental conservation (Use of photovoltaic solar energy) and the green economy and the opening of workstations (Smartphone chargers and outdoor Wifi connection)

2. Comparative study of different HTM in a PSC

2.1 Device architecture and simulation

We have considered methylammonium tin triodide ($MASnI_3$) as absorber layer along with ZnO as Electron transport layer and three types of HTM layers are planned to study the effect of material properties and architectures on the PCE of the structure. The first structure is the solar cell with a $MASnI_3$ between the HTM (Spiro-OMeTAD) and the ETM (ZnO) as shown in the figure 1(a),in the second structure the MASnI3 is sandwiched between the HTM (PEDOT:Pss) and the ETM (ZnO) as shown in the fig 1(b) and the 3rd structure is the solar cell with a methylammonium tin triodide absorber layer between the HTM copper oxide (Cu_2O) and the ETM (ZnO) as shown in the fig 1(c).

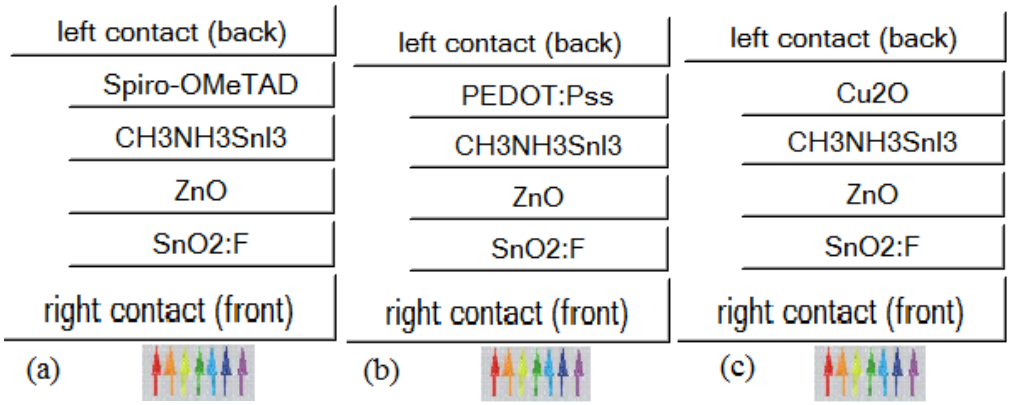

Figure 3 1 Architectures of different HTL materials

(a) Spiro-OMeTAD(HTL)/MASnI3/ ZnO/ SnO2:F

(b) PEDOT:Pss(HTL)/MASnI3/ ZnO/ SnO2:F

(c) Cu2O(HTL)/MASnI3/ ZnO/ SnO2:F

SCAPS, a 1D solar cell simulator, hails from University of Gent's ,Belgium ELIS (Electronics and Information Systems) department [23].

Beyond simulating basic photovoltaic structures, SCAPS now handles amorphous and crystalline solar cells (a-Si ,c-Si and GaAs) [26].This software has the major number of DC and AC measurements in different temperatures and also in light and dark illumination.

It solves the fundamental SC equations in 1D under steady state condition.

Fig2 explains the simulation process using SCAPS.

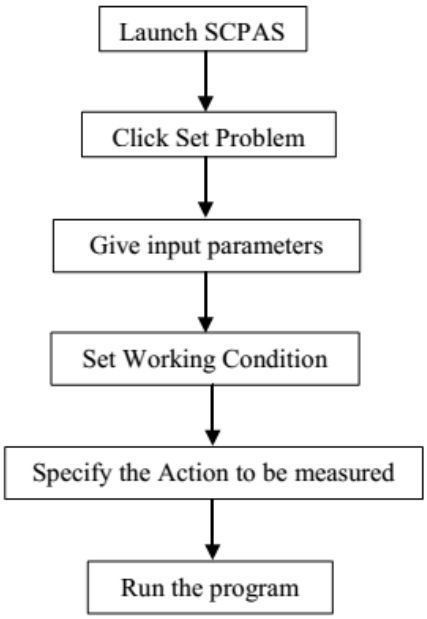

Figure 3 2 SCAPS working procedure.

To examine the effect of diverse electrical parameters on the PCE of SnO_2:f/ZnO/$CH_3NH_3SnI_3$/Spiro-OMeTAD,SnO2:f/ZnO/ $CH_3NH_3SnI_3$/PEDOT:Pss, and SnO_2:f/ZnO/ $CH_3NH_3SnI_3$/Cu_2O heterojuction-based perovskite solar cell structures. Fig 3 shows the energy band alignment of ZnO based Sn PSC along with typical perovskite materials.

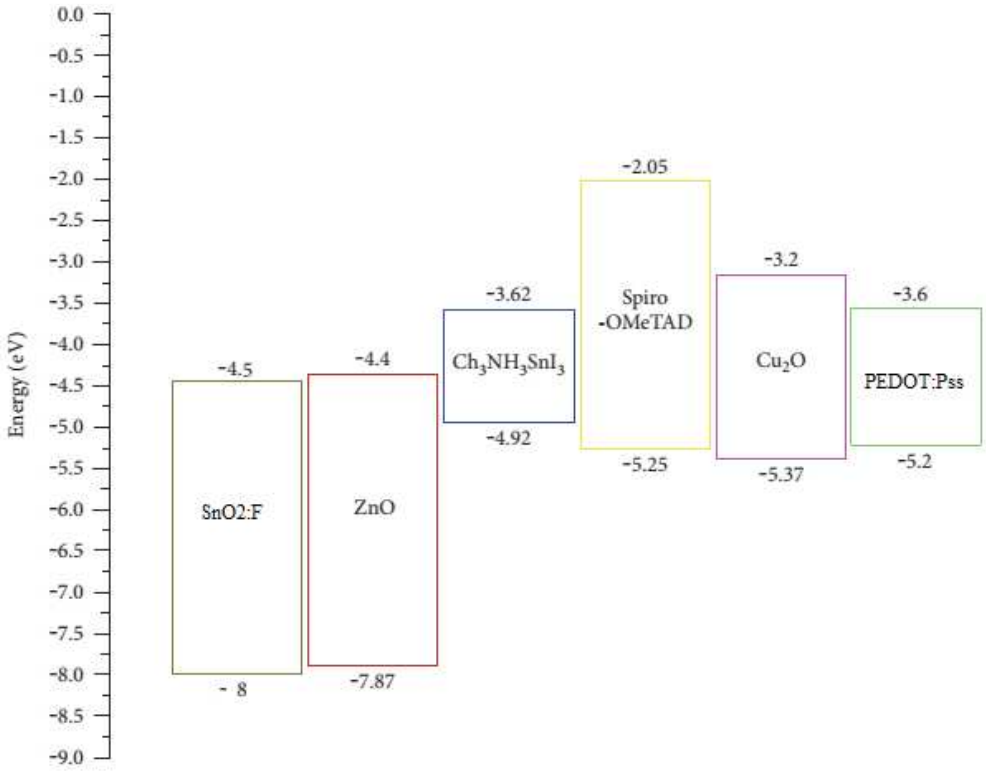

Figure 3 3 Energy band alignment

Material parameters and values of device which are the input for the simulator are cautiously adopted from those reported in theoretical results and other experimental data and extracted from published studies. The individual materials parameters for SnO_2:F, ZnO, $CH_3NH_3SnI_3$, Spiro-OMeTAD, PEDOT:Pss and Cu_2O are entered in the forms of thickness , dielectric permittivity (ε) , bandgap (Eg), valence band density of states (Nv), conduction band density of states (Nc), electron affinity (χ), hole mobility (μp), electron mobility (μn) , acœptor density, (N_A) donor density (N_D). These values are reported in Table1.

Table 1 Parameters used in SCAPS -1D for PSCs architectures

Parameters	**SnO_2 :F**	**ZnO**	**$CH_3NH_3SnI_3$**	**PEDOT :Pss**	**SpiroOMeTAD**	**Cu_2O**
Thickness(nm)	**500**	**50**	**900**	**200**	**200**	**200**
χ (ev)	**4**	**4.26**	**4.17**	**1.57**	**2.05**	**3.2**
εr	**9**	**9**	**8.2**	**3**	**3**	**7.11**
E_g(ev)	**3.5**	**3.2**	**1.3**	**3.6**	**3.17**	**2.17**
N_v (cm^{-3})	**1.81×10^{19}**	**1.81×10^{19}**	**1.00×10^{18}**	**1.80×10^{19}**	**1.81×10^{19}**	**1.11×10^{19}**
μ_h (cm^2/Vs)	**10**	**5**	**1.60**	**400**	**2.00×10^{-4}**	**80**
N_c (cm^{-3})	**2.21×10^{18}**	**2.01×10^{18}**	**1.00×10^{18}**	**2.21×10^{17}**	**2.20×10^{18}**	**2.02×10^{17}**
μ_e (cm^2/Vs)	**20**	**200**	**1.60**	**10**	**2.00×10^{-4}**	**200**
N_D (cm^{-3})	**2.00×10^{19}**	**1.50×10^{17}**	**-**	**-**	**-**	**-**
N_A (cm^{-3})	**-**		**1.50×10^{16}**	**2.00×10^{19}**	**2.00×10^{19}**	**2.00×10^{19}**
References	**[04,10,11,]**	**[07,08,09]**	**[25,05,06]**	**[12,13]**	**[14,15,16 ,17,18]**	**[17,18]**

From Table 2, it can be perceived that the device including Cu_2O as hole transport material (SnO_2:F/ZnO/$MASnI_3$/Cu_2O) has given the best performance. This suggests Cu_2O as a appropriate HTM layer.

Along, the result justifies the possibility of our proposed structure with ETM (ZnO) to be considered as a possible alternative to conventional PSCs [24].

Table 2 Performance of Psc with various HTM layers.

PSC	J_{sc} (mA/cm^{-2})	Voc(V)	FF (%)	PCE (%)
SnO2:F/ZnO/MASnI3/PEDOT:Pss	**41.72**	**0.7853**	**73.77**	**24.17**
SnO2:F/ZnO/MASnI3/Spiro-OMeTAD	**41.85**	**0.7868**	**74.41**	**24.5**
SnO2:F/ZnO/MASnI3/Cu2O	**42.47**	**0.8044**	**74.23**	**25.36**

2.2 Influence of the thickness of absorber layer on solar cell performance with different HTM layer.

Thickness of $MASnI_3$ is one of the major parameters and plays a vital role on the overall performance of the solar cell.

To absorb the maximum number of photons and to generate electron-hole pair, absorber layer should set for optimum thickness [19].

Thickness of $CH_3NH_3SnI_3$ has been varied from 50 nm to 900 nm with the PEDOT:Pss/ spiro-OMeTAD / Cu_2O HTM layers and ZnO as the ETM layer.

By varying the thickness of $MASnI_3$, all the parameters of the PSCs such as (VOC), (JSC), (FF) and the (PCE) are changing. The result is shown in Fig 4.

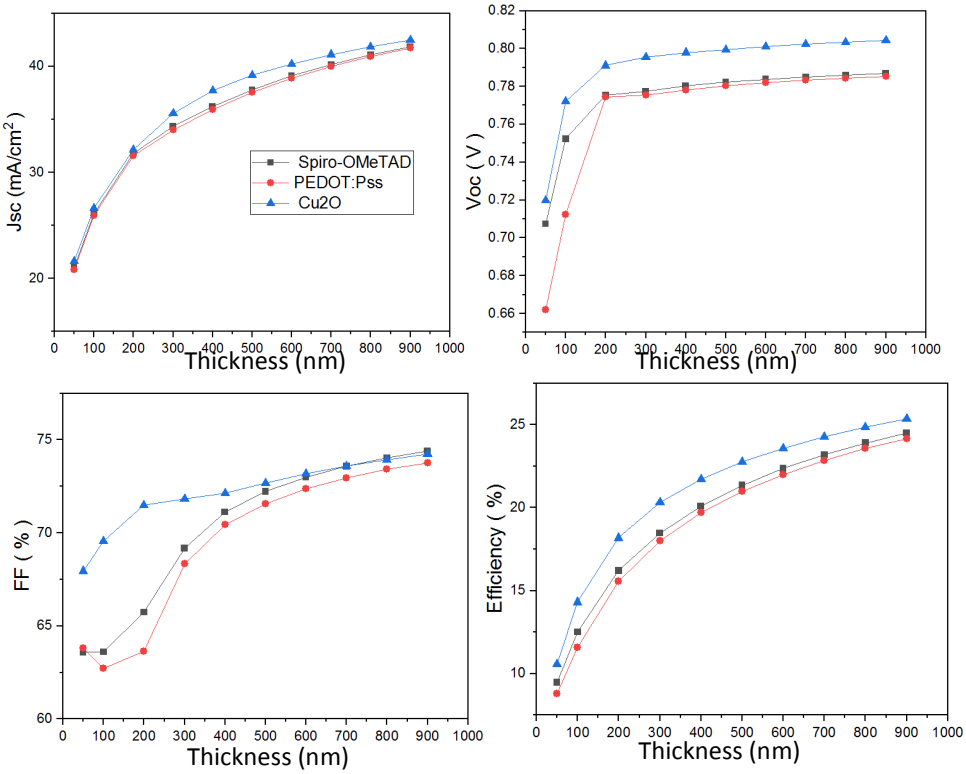

Figure 3 4 Variation of PSCs of the thickness of absorber layer.

From the above graphs; the thickness changed from 50 nm to 900 nm. It is noticed that the efficiency increases and all parameters are highest at 900nm. The PCE Increases with increasing the thickness. It can be explained by the augmentation of creation of the electron- hole pairs in the active material. It means the increase of optical density.

$CH_3NH_3SnI_3$-based solar cells exhibit an efficiency sweet spot with respect to absorber layer thickness. While increasing thickness short-circuit current (Jsc) enhances due to the greater photon absorption and charge generation, it also increases recombination losses when charge carriers have to travel further for diffusion [24].

The results show clearly that the structure including Cu_2O as HTM layer has the highest performance.

2.3 Effect of doping of the absorber layers on the PV performances.

To understand how the acceptor doping concentration (N_A) of the perovskite absorption layer with different HTM layers (Spiro-OMeTAD, PEDOT:Pss, and Cu_2O) can affect the performances of solar cells, $CH_3NH_3SnI_3$ layers with the values of N_A varying from $10^{15}cm^{-3}$ to $10^{17}cm^{-3}$ are considered. Doping of a photoactive material in the solar cell structure decides the electrical behavior of the layers which will affect the PCE of the device [19]. Fig 5 provides the PCEs of solar cells with different acceptor densities of the perovskite and with different HTM layers, and the maximum value of PCE appears at the N_A of $1.51x10^{16}$ cm^{-3} for both devices with HTM layers (PEDOT:Pss, and Spiro-OMeTAD) respectively and the N_A of $1.0x10^{16}$ cm^{-3} for device with Cu2O as HTM layer. FF also related to the change of N_A for the perovskite, and all structures (SnO_2:f /ZnO / $CH_3NH_3SnI_3$/ Spiro-OMeTAD, SnO_2:f /ZnO/ $CH_3NH_3SnI_3$/ PEDOT:Pss, and SnO_2:f/ZnO / $CH_3NH_3SnI_3$/Cu_2O) arrive at their maximum values when the N_A is approximately $1.5x10^{16}$ cm^{-3}. Hence, an appropriate doping concentration of the perovskite absorption layer is beneficial to the improvement of the photo-absorption efficiency and the Jsc. However, the Voc drops rapidly when the N_A exceeds $1.0x10^{16}cm^{-3}$ in all three models mentioned earlier.

Doping concentration plays a double-edged sword role in (Voc). While higher doping initially enhances the built-in E-field, it also fuels a rise in Auger recombination, ultimately hindering further Voc improvements.

The differing performance observed in the three cells across varying doping levels can be attributed to this interplay between field and recombination dynamics.

The improvement of the E-field promotes the partition of carriers and then the development of the PCE [21].

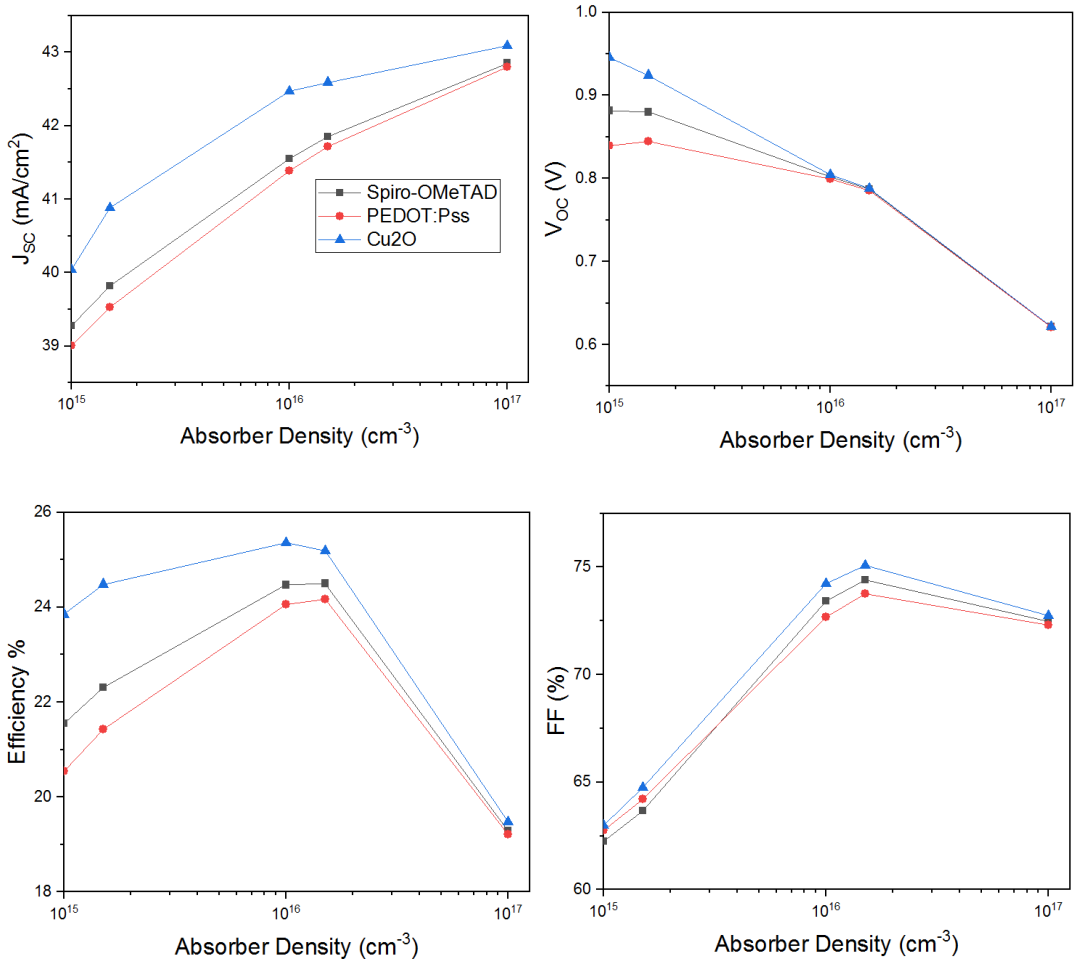

Figure 3 5 Effect of the Absorber density of PSC absorber layer on PV performances.

2.4 Effect of temperature

Temperature also effects the PCE of a solar cell Structure. General operating temperature of the device is 300 K, but at the real conditions, the temperature is higher than 300°K. Temperature changes influence the diffusion length and series resistance eventually leading to the changes in the PCE of the structure [19].

The temperature of the software representation is varied from 300K to 450K. Fig 6 shows the distinction of PCE as a function of temperature for HTM layers. All

HTM layers show similar attitude: inverse proportion (temperature increases-performances decreases).

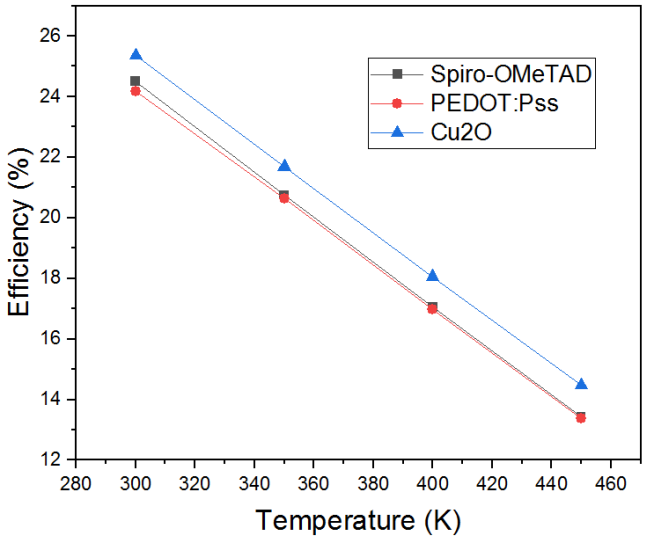

Figure 3 6 Representation of the variation of PCE with the temperature.

As shown in the graph, as the temperature increases, the efficiency increase by increasing the series resistance. At the high temperature deformation stress will be more and less connectivity between the layers [19]. leads to the more interfacial defects.

In the high temperature (450 K), the perovskite solar cell with the copper oxide (Cu_2O) as HTM layer, is better at higher temperature when compared to the remaining two PSCs with PEDOT:Pss and Spiro-OMeTAD as HTM layer. However, the best working temperature of PSCs is 300 K.

3. Comparative study of different ETM in a Psc

3.1 Modeling of PSC and simulation

We have considered TiO_2 and ZnOas Electron transport layer withmethylammonium lead iodide (MAPbI3) and methylammonium tin triodide ($MASnI_3$) as active layers along with four types of HTM layers are planned to study the effect of ETMs properties and architectures on the efficiency of the device.

The first structure is the device with a ($CH_3NH_3SnI_3$) is inserted between the Spiro-OMeTAD and ZnO as shown in the figure 1(a), in the second device the MASnI3 is sandwiched between the HTM (PEDOT:Pss) and the ETM (ZnO) as shown in the figure 1(b) , the third structure is the device with a methylammonium tin triodide absorber layer between the copper oxide (Cu_2O) as HTM layer and ZnO as shown in the figure 1(c), in the fourth and fivth structures the active layers are inserted between the Spiro-OMeTAD and TiO_2 as shown in the figure 1(d) and 1 (e) respectivly.

In the sixth and siventh architectures Najmin Ara Sultana et al, used the absorber layers ($CH_3NH_3PnI_3$) between the n-type material (TiO_2) and the p-type Spiro-OMeTAD layer and between the n-type material (ZnO) and the p-type Spiro-OMeTAD layer as shown in the figure 1(f) and 1(g) respectivly.

M.I. Hossain et al used themethylammonium lead iodide absorber layer between the copper oxide (Cu_2O) as HTM layer and TiO_2 in the eighth structure as shown in the figure 1(h).

The nineth architecture Hui-Jing Du et al, used the active layer ($CH_3NH_3SnI_3$) with TiO_2 as ETM layer as shown in the figure 1(i).

Both teams of T.Chakrabarti and U.Mandadapu used the absorber layer ($CH_3NH_3SnI_3$), the first team used it between the HTM (Spiro-OMeTAD) and the ETM (ZnO) and the seconde team used it between the HTM (CuI) and the ETM (TiO_2) in the Tenth and eleventh structures as shown in figure 1(j) and 1 (k) respectivly.

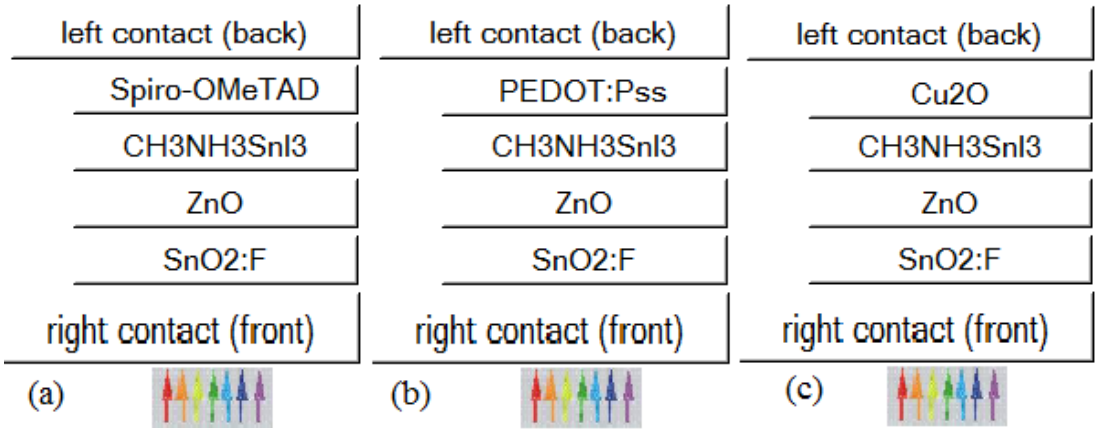

(a) Spiro-OMeTAD(HTL)/MASnI3/ ZnO , (b) PEDOT:Pss(HTL)/MASnI3/ ZnO ,

(c) Cu2O(HTL)/MASnI3/ ZnO

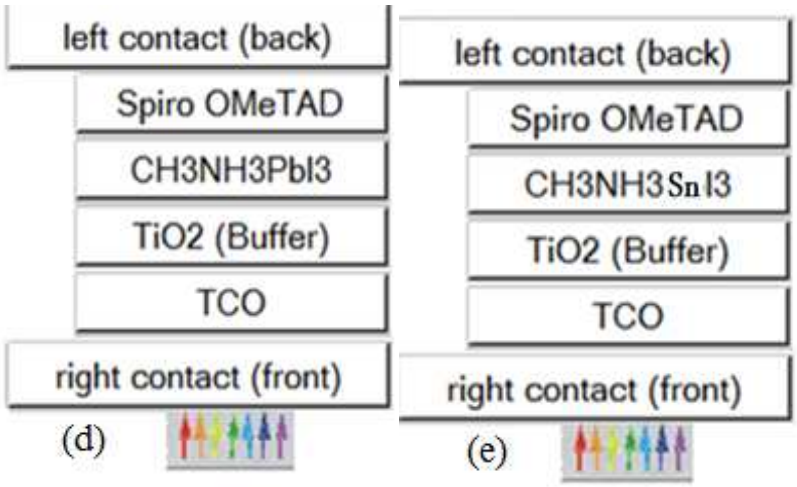

(d) Spiro-OMeTAD(HTM)/MAPbI3/ TiO2 [29] *(e) Spiro-OMeTAD(HTM)/MASnI3/ TiO2*

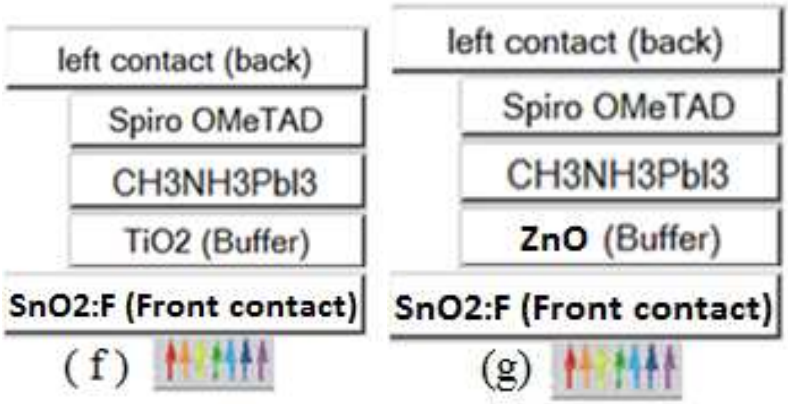

(f) (Color online) Cross-sectional schematic diagram of p-i-n perovskite solar cell[30],

(g) (Color online) Model cell,

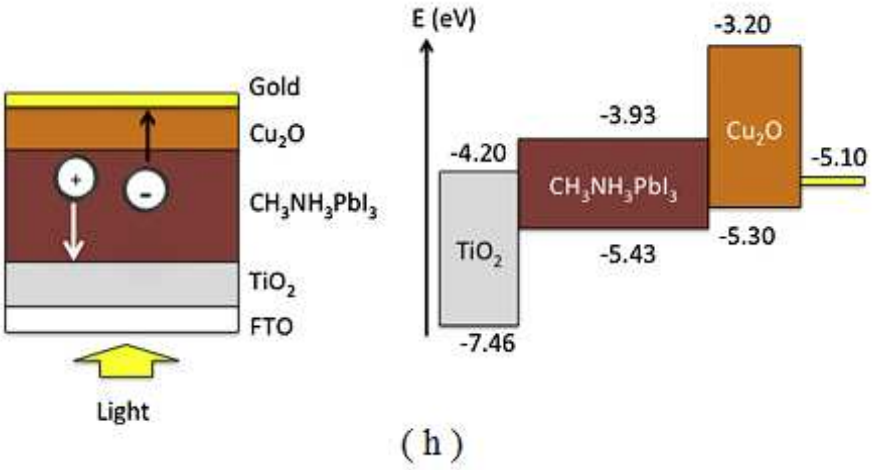

(h) (Color online) Device structure and energy level diagram of the TiO2/CH3NH3PbI3/Cu2O/Au[31]

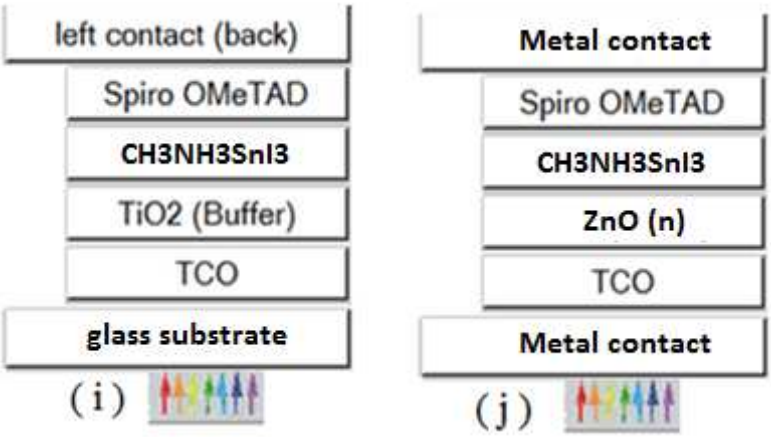

(i) (Color online) Shematic diagram of the CH3NH3SnI3 PSC[32], (j) Shematic diagram of the proposed cell [33]

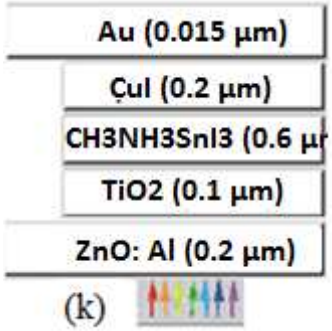

(k) Shematic diagram of the CH3NH3SnI3 PSC with CuI as HTM model (see online version for colours)[34]

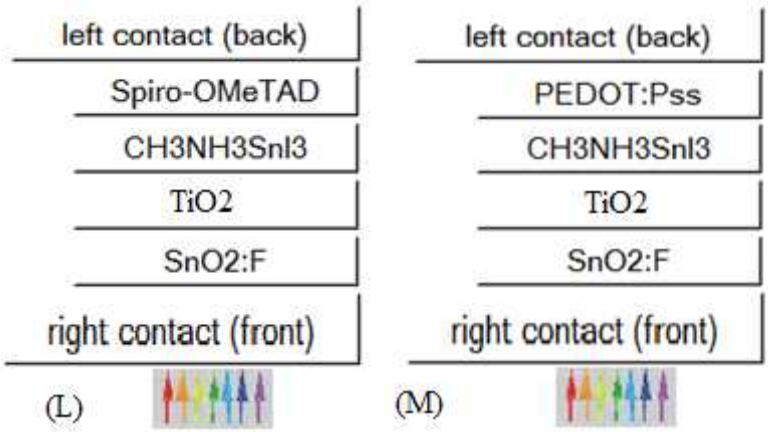

(L)) PEDOT:Pss(HTM)/MASnI3/ ZnO , (M) Cu2O(HTM)/MASnI3/ ZnO.

Figure 3 7 Architectures of twelve schematic with different HTM layer

To compar between ZnO and TiO_2 and to examine the effect of different electrical parameters on the efficiency of all heterojuctions-based perovskite solar cell structures we and all authors used the SCAPS-1D as numerical simulation. Fig 2 shows the energy band alignment of ZnO and TiO_2 along with typical perovskite materials used in conventional PSCs.

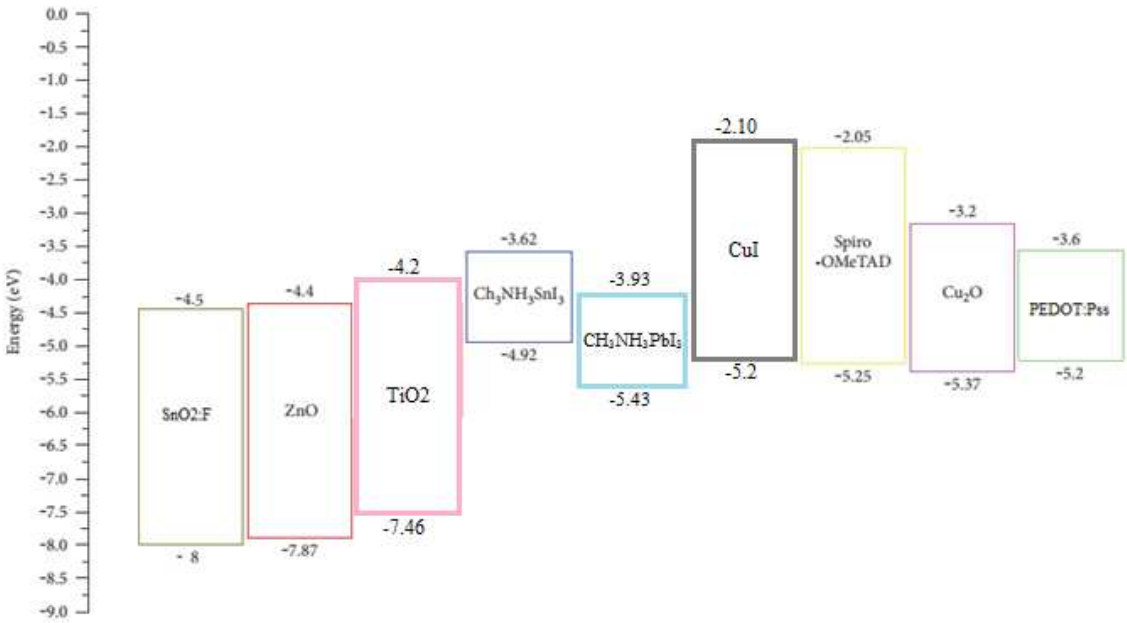

Figure (III.8): *Energy band alignment [24]*

In this part, we have used ZnO and TiO_2 as Elecrton Transport Material layers for the simulation of PSCs. All the ETM layers used in this work have been reviewed in many publications as the ETM layer along with Spiro-OMeTAD, PEDOT:Pss, CuI and Cu_2O as the HTM layer of $MASnI_3$ and $MAPbI_3$ based PSCs.

Material parameters and values of device which are the input for the simulator are carefully adopted from theoretical and experimental results.

The individual materials parameters for SnO_2:F, ZnO,TiO_2 $CH_3NH_3PbI_3$, $CH_3NH_3SnI_3$, Spiro-OMeTAD, PEDOT:Pss, CuI and Cu_2O have to be inserted in (N_D), (N_A), (Eg), (χ), (ε), (Nc), (Nv), (μn), (μp). These values are reported in Table3.

Table 3 Differents parameters used in SCAPS-1D simulator of Psc

Parameters	SnO2 :F	ZnO	TiO2	CH3NH3SnI3	CH3NH3PbI3	SpiroOMeTAD	PEDOT :Pss	Cu2O	CuI
Thickness(nm)	500	50	50	900	900	200	200	200	200
E_g(ev)	3.5	3.2	3.2	1.3	1.55	3.17	3.6	2.17	3.1
χ (ev)	4	4.26	4	4.17	3.90	2.05	1.57	3.2	2.1
εr	9	9	9	8.2	6.5	3	3	7.11	6.5
N_c (cm^{-3})	2.20×10^{18}	2.00×10^{18}	1.00×10^{19}	1.00×10^{18}	1.80×10^{18}	2.20×10^{18}	2.20×10^{17}	2.02×10^{17}	2.2×10^{19}
N_v (cm^{-3})	1.80×10^{19}	1.80×10^{19}	1.00×10^{19}	1.00×10^{18}	1.80×10^{19}	1.80×10^{19}	1.80×10^{19}	1.10×10^{19}	1.8×10^{19}
μ_e (cm^2/Vs)	20	200	0.02	1.60	0.5	2.01×10^{-4}	10	200	20
μ_h (cm^2/Vs)	10	5	2	1.60	0.5	2.01×10^{-4}	400	80	4.39
N_D (cm^{-3})	2.00×10^{19}	1.50×10^{17}	1.00×10^{19}	-	-	-	-	-	-
N_A (cm^{-3})	-		-	1.50×10^{16}	1.00×10^{19}	2.00×10^{19}	2.00×10^{19}	2.00×10^{19}	1.00×10^{18}
References	[40,45,35,]	[43,31,44]	[45]	[39,41,42]	[46,47,48]	[38,39,40,41,42]	[36,37]	[15,16]	[10]

3.2 Numerical analysis for various ETM candidates.

From Table 4, it can be perceived that the devices containing TiO_2 as Electron Transport Material (TiO_2/$MAPbI_3$/Spiro-OMeTAD,TiO_2/$MASnI_3$/CuI and TiO_2/$MASnI_3$/Spiro-OMeTAD) have given the best PCE among all the PSCs versus the cells that contain ZnO as ETM.

Table 4 Efficiency of PSC with two different ETM layers.

	Our results (Efficiency %)	Literature (Efficiency %)
Sn / TiO_2	Sn / TiO2 / Spiro-OMeTAD (25.29 %)	23.36 % [32]
	Sn / TiO2 / PEDOT :Pss (24.95 %)	18.34 % [74]
	Sn / TiO2 / Cu2O (26 %)	24.82 % [19]
Sn / ZnO	Sn / ZnO / Spiro-OMeTAD (24.5 %)	22.9 % [33]
	Sn / ZnO / PEDOT :Pss (24.17 %)	23.69 % [75]
	Sn / ZnO / Cu2O (25.36 %)	20.23 % [24]

Cellule solaire pérovskite	PCE (%)	References
Spiro/Pb/TiO_2	30.35	[29]
Spiro/Pb/TiO_2	27.6	[30]
Spiro/Pb/ZnO	27.5	[30]
CuI/Sn/TiO_2	25.91	[34]
Cu_2o/Sn/ZnO	25.36	[49]
Spiro/Sn/ZnO	24.5	[49]
Pedot/Sn/ZnO	24.17	[49]
Spiro/Sn/TiO_2	23.36	[32]
Spiro/Sn/ZnO	22.9	[33]
Pedot/Sn/TiO_2	**24.95**	-
Cu_2O/Sn/TiO_2	**26**	-
Spiro/Sn/TiO_2	**25.29**	-

The tin oxide $MASnI_3$ PSCs with different parameters are analyzed by using 1D-device simulation in the first part in this work. ZnO is proposed as the ETM for $MASnI_3$ based PSC and the PCE of the device is also studied with three different

HTM layers. Doping level of the active layer, the thickness , and temperature are varied to study the optimized PCE.

The results show that solar cell containing Cu_2O as HTM outperform all other devices with organic or inorganic HTM hitherto tested [44]. A Power conversion efficiency exceeding 26% was obtained (figure 9). The results of this proposed structure will become a good conduct for the plan of low-cost high efficiency tin halide PSCs in future,

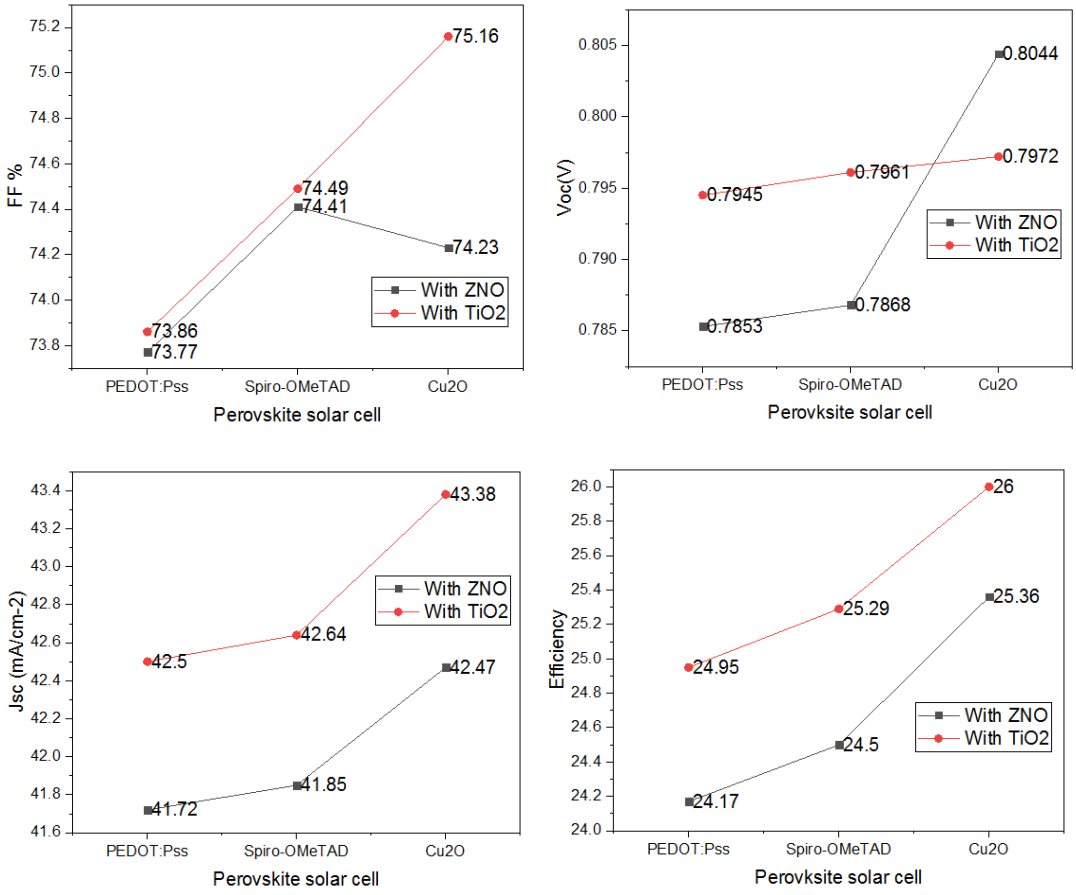

Figure 3 9 Comparative study of ZnO et TiO_2 in a perovskite solar cell

In the second part, two different candidates for ETM were employed and basic cells parameters were disputed.

The results illuminate that the solar cells with the ETM (TiO_2) can attain relatively higher efficiency but current studies have revealed that the ETM (ZnO) can be used as a proper substitute of TiO2 without affecting the PCE of PSC significantly. Furthermore, using the ETM (ZnO) nanorods instead of the ETM (TiO_2), the processing price of PCS can be reduced.

4. Wireless network local using perovskite solar cell.

4.1 Introduction

Telecommunications connect us remotely, sending information electronically or digitally through wires, light, or radio waves.This field deals with information transfer, defining standards for transmission media, measuring relevant physical properties, and analyzing signal propagation [60].

The method and the composition according to this work make it possible to sent data, like as text and sound to one Pc to another PC or to one smarphone to another smartphone respectively, through laser and PV solar power. With the use of simple and inexpensive tools such as lasers, Bluetooth, Arduino, solar cells personal computer and smartphones and helps to achieve the sustainable development goals.

This work is divided in two parts, one hand, to transmit the sound; the audio source translates music into tiny, fluctuating electrical signals sent to a laser through a cable.

These signals represent the exact sound waves a speaker connected directly to this source would produce,

Rapid changes in voltage from the audio source control the laser's intensity, transforming sound waves into light fluctuations.

Brighter laser pulses trigger stronger electric currents in the perovskite cell, mimicking the audio signal's ups and downs.

The electrical signal, shaped by the music, flows through the speaker, causing its membrane to vibrate in sync.

These vibrations generate sound waves mimicking the original music, just like a regular speaker connected to the audio device.

On the other hand, to transmit the electronic messages or the texts, by a simple communication system transmits serial data by air from a transmitter to a receiver via a laser beam powered directly from an output pin of an ATmega328 (Arduino) based microcontroller board. Because the laser draws only 30 mA from the processor which has outputs rated at 40 mA.

The ATmega328 is the central controller for the entire smart card unit. It has 14 digital input/output pins, 6 analog inputs, 16 MHz quartz crystal, USB connection, power jack and reset button.

The board can be programmed with Arduino software (IDE). It can operate on an external power supply of 6 to 20 volts.

The solar cell as a receiver, it converts the energy of the laser beam into a current which passes through the second Arduino.

Computers with keyboard and screen are required for this project. One is for giving input and the other is for getting output. Fig. 1 displays the all things we'll need.

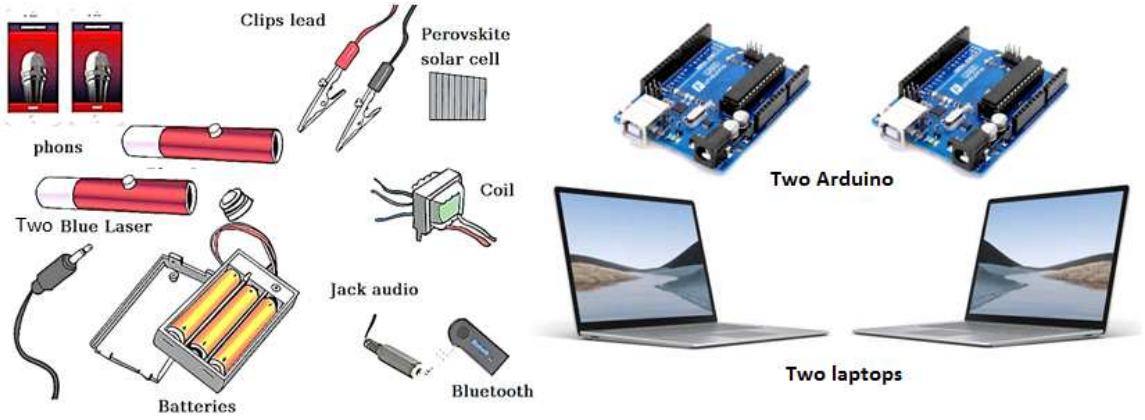

Figure 3 10 Things we'll need.

4.2 Diagram, device structure and simulation

A. Trnsmission of sound :

a) Emitter:

The microphone application opens on the smartphone connected to the Bluetooth device.

Bluetooth is associated via a coaxial electrical connection (audio jack) with a coil to make sure the exclusion of interference from a power supply or an analog signal, to create a filter for a particular frequency band.

And to smooth direct currents (noise is eliminated). The coil is connected in series to a battery and the laser to turn it on (preferably a blue laser) (more efficient

than other colors), which converts electric current into light photons at a distance of more than 1 or 2 km .Fig.2 shows the emitter part.

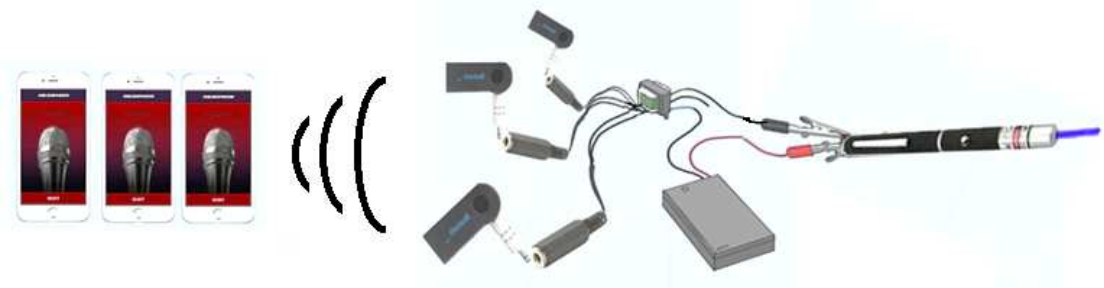

Figure 3 11 Compounds of Emitter part of transmission of sound

b) Receiver :

The simplest part is the receiver. Connect the PSc to the mic audio Jack, and plug it into the stereo phono input or amplifier.

The photons generated by the laser are received by the PSC which has a high absorption coefficient. These photons are transformed into electric current, until the amplifier passes which converts the electric current into sound waves. Figure 3 shows the diagram of the receiver part [73].

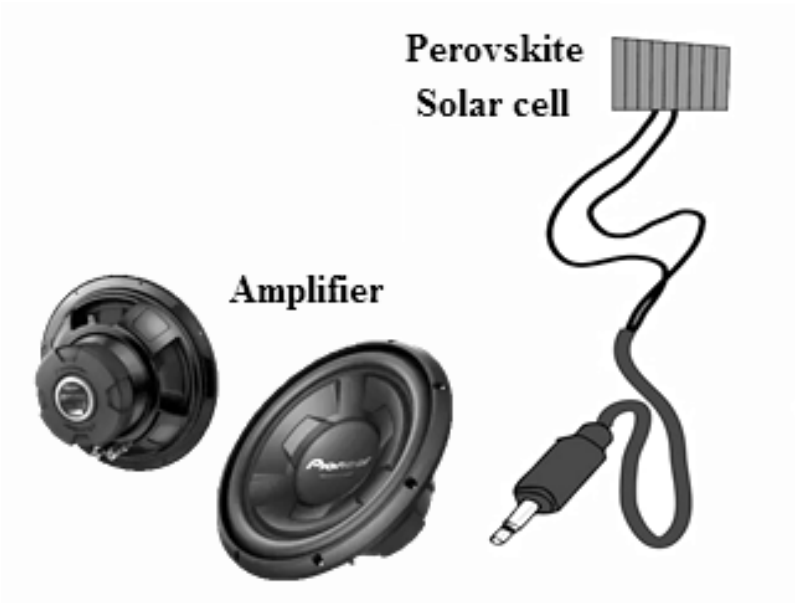

Figure 3 12 General diagram of the receiver part of the transmission of sound.

B.1 Perovskite / Silicon Solar Cell

A comparative study is presented in this work between two structures. On the one hand the silicon solar cell and on the other hand the PSc.

The proposed PSc device is "back contact /TCO/(ETM) ZnO(n) / (Active layer) $CH_3NH_3SnI_3$ / (HTM) PEDOT:Pss(p) / front contact." In this PSc, a planer p-i-n heterojunction structure with the layer arrangement of p-doped PEDOT: Pss and n-doped ZnO layers are used as HTL and ETL, respectively.

This structure as shown in Figure.4(a). The proposed silicon solar cell architecture is "metal contact / p-layer / n- layer / metal contact, as shown in Fig.4 (b).

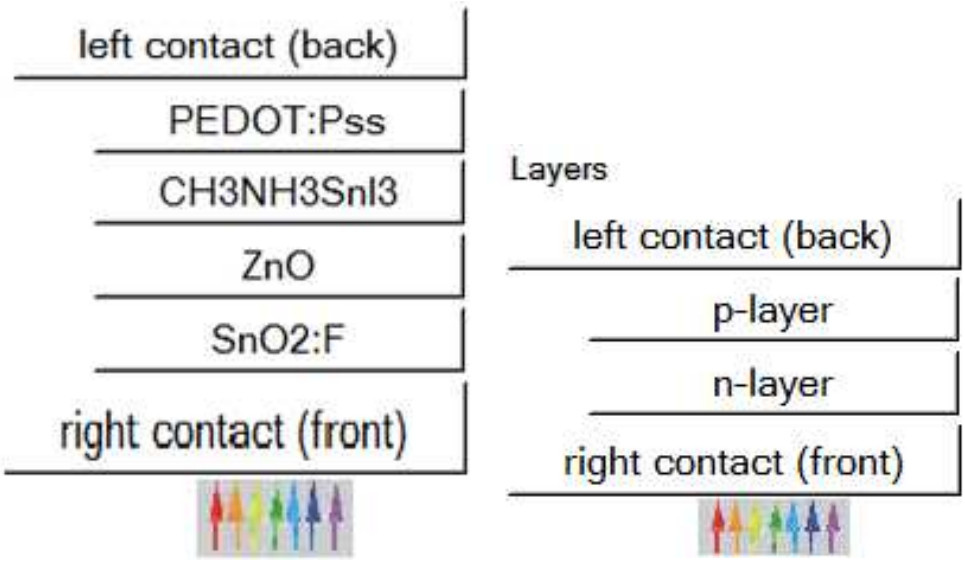

(a) (b)

Figure 3 13 Schematic representation perovskite solar cell (PSC) and silicon solar cell (PN)

B.2 Simulation Parameters:

The values of material parameters used in the simulator are exported from literatures and theories are exposed in the next Table 5.

Effective Nv and Nc densities of 1.80 x $10^{19}cm^{-3}$and PEDOT:Pss are 2.20 x $10^{17}cm^{-3}$, respectively, and are measured in this planned device [69].Thermal velocities of the hole and electron of (ETM) ZnO are both rest to be equivalent to10^{7}cm/s for this device. The defects are set to be neutral defect and single with a (Ev) of 1.6 eV, located at total density of 1.00 x 10^{15} cm. The constant A(α), is equal 1x10^{5} to obtain the absorption coefficient, alpha (α), where $\alpha = A\alpha * (hvEg)^{1/2}$ [69].

Table 5Simulation parameters of $MASnI_3$ PSC and PN junction

Parameters	SnO2 :F	ZnO	CH3NH3SnI3	PEDOT	P-layer	n-layer
Thickness(nm)	500	50	900	200	2000	500
χ (ev)	4	4.26	4.17	1.57	4.5	4.5
εr	9	9	8.2	3	10	10
E_g(ev)	3.5	3.2	1.3	3.6	1.2	1.2
N_v (cm^{-3})	1.81×10^{19}	1.80×10^{19}	1.00×10^{18}	1.81×10^{19}	1×10^{19}	1×10^{19}
N_c (cm^{-3})	2.21×10^{18}	2.01×10^{18}	1.01×10^{18}	2.21×10^{17}	1×10^{19}	1×10^{19}
N_D (cm^{-3})	2.00×10^{19}	1.50×10^{17}	-	-	-	1×10^{17}
N_A (cm^{-3})	-		1.50×10^{16}	2.01×10^{19}	1×10^{15}	-
μ_h (cm^2/Vs)	10	5	1.60	400	5	5
μ_e (cm^2/Vs)	20	200	1.60	10	5	5
References	[63,69,70,]	[66,67,68]	[62,64,65]	[61,71,72]		

B.3 Results and discussion.

To accurately represent real-world conditions, we simulated the proposed devices in SCAPS software, incorporating comprehensive data on defect states. The efficiency of the silicon (pn) solar cell is achieved 21.84 %, the Voc of 0.7397 V and the FF of this solar cell is 82.18 %. The Jsc of 35.91 mA/cm^2

Concerning the PSc (p-i-n), is achieved 24.17% of efficiency, along with the FF of this structure is observed as 73.77%. and the Voc of 0.7853V. The Jsc of 41.72 mA/cm^2 .

The work relates to a method for using perovskite solar cells to transmit sound remotely, using blue color laser and Bluetooth to connect it to any smart phone and use it as a microphone solar powered.

B. Transmission of text:

A) Emitter:

a.1 Sending and work principle

The transmitter consists of a PC with a keyboard and an Arduino. The input is given during the keyboard (example: AbCdE). The Arduino (1) converts the text into 8 bit binary. On the transmit surface, a UART (Universal Asynchronous Receiver

Transmitter) must create the data packet appending sync and parity bits and send that packet out the transmission line with precise timing via a laser beam. Fig.5 shows the emitter part.

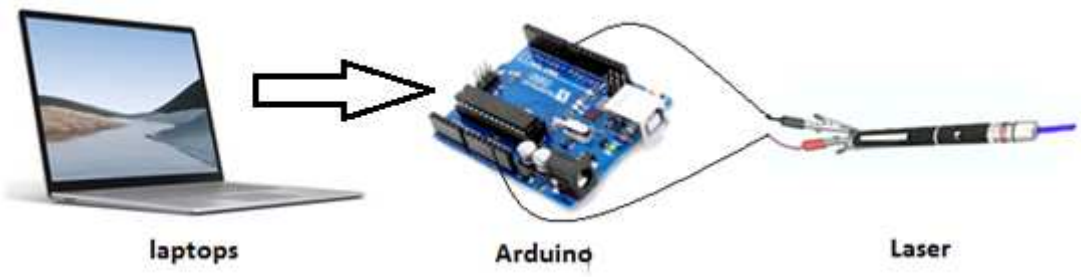

Figure 3 14 The emitter part.

Arduino-1 is used to convert the alphanumeric characters into 8 bit ASCII code. For the code, we have to do the followings:

- Take the characters as input.
- Convert the characters into ASCII code (Character Sets) of which the start bit is1.
- The delay is set 10ms between two consecutive bits.
- Set the delay of 100ms between two consecutive Bytes (1 Byte = 8 Bits)
- Upload the code

a.2 Source code

The Arduino IDE is a software application used for developing programs for Arduino microcontroller boards. It provides a text editor for writing code, a message area for displaying notifications and errors, and various menus for managing projects and settings. Additionally, it allows users to upload programs to the Arduino hardware and communicate with the board to monitor its operations.

B) Receiver:

b.1 Receiving and work principle

The receiver contains a solar cell, an Arduino and a PC with a monitor. When the laser beam is incident on the solar cell, it converts the data containing light signal into a current and this current flow through the Arduino (2).

This Arduino converts the bits into corresponding alphanumeric characters and the computer monitor shows them. Fig.6 shows the receiver part.

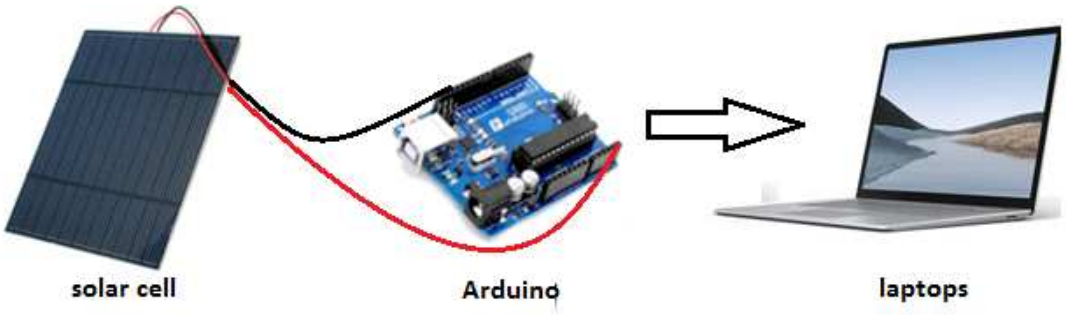

Figure 3 15 General diagram of the receiver part

Laser beam is sent to the solar cell and solar cell now receives the information. The solar cell is associated with the A1 pin and ground.

After read-through the value of the solar cell using built in “Analog Read Signal” both when there is no light on the laser, and when there is light on the laser.

We then set the THRESHOLD value for the solar cell by examining the value from “Analog Read Signal”.

In setup, we consider the solar pin A1 as input and fix the Serial.begin to 9600. Then we take the reading from the solar pin. If the Reading from the solar pin is greater than the threshold, then we consider it to be ‘1’, if not it is considered as ‘0’.

These binary bits are stored in an array. We set the delay to ‘100’ to match the delay of the sending side. Anything other than 50, the interpretation will not be right and it can produce false result.

The binary bits are converted to ASCII value. Then the ASCII values give us suitable characters.

Future research should focus on integrating this PSc with the proposed wireless technology to validate its ability to transmit sound or data signals via the system's laser beam.

The field to which the present study relates to the wireless network local based on perovskite solar cell, in several fields such as education, training and scientific research

5. Sustainable antiseptic tunneling for antivirus less harmful than covid19

The COVID-19 pandemic is devastating, and other viruses are less harmful but dangerous.we can help slow down its spread by following the infection control practices and by using a sustainable system to disinfect and sterilize outgoing and incoming people in areas that must work in hygienic conditions such as: hospitals, establishments, laboratories, schools, barracks… etc.

And abiding by the rules and instructions issued by the authorities, which will ultimately take the pressure off [50].

Often the virus spread between people via small droplets produced during coughing, sneezing, talking, or contact [51,52], if they are touching a contaminated surface and then their faces, they are may also become infected[53].

The first disinfectant tunnel was installed is in China amid the coronavirus outbreak on February 10, 2020 [54]. This was imitated by other countries. In Algeria, the first “disinfection tunnel” of this kind was launched in early April,2020.

Major health organizations, including the World Health Organization (WHO), the Pan American Health Organization (PAHO), and the Africa Centres for Disease Control and Prevention (CDC), have all issued strong statements against the use of humanspraying [57].

The Allergy Society of South Africa expresses significant concerns regarding the practice of humanspraying, highlighting potential adverse effects on individuals with asthma, allergic rhinitis, allergic conjunctivitis, and eczema, according to reports provided by the World Health Organization.

The Algerian Ministry of Health decided to withdraw sterile passages, as they are dangerous to the safetyof the sector's users, as well as the citizens coming to hospitals.

In this work, we combined the solar photovoltaic energy in the disinfection tunnel to use it as a source of energy for the triggering of the pump of the disinfectant liquid spraying circuit and the detector (photocells) of the passage of the persons or of equipment.

The sustainable unit works with the principle of eliminating harmful bacteria that they transport people, during the transition of individuals carrying microorganisms, if a cleansing substance not harmful to human health is discovered.

5.1 Design and work of disinfection tunnel.

The rigidity of the structure of this unit, made of aluminum, stainless steels or other non-corrosive material, allows it better stability and are PVC piped with the distance varying from 1meter to 2 meters.The unit is mobile, with four wheels equipped with a braking system, to facilitate its movement and its positioning in complete safety.

These tunnels are equipped with infrared detector (sensor) which activate the pump of the disinfectant liquid spraying circuit and the detector (photocells) whenever a person enters[58].

Type we used of These spray stations isDynamic type, these tunnels or walk-through passages in which the person moves for 1-2 meters andthe device sprays disinfectant throughout the path [59]. Opposite of the second Static type being a circular enclosure in which the person rotates inside the station for 10-15 seconds and the disinfectant is sprayed from all nozzles. A temperature sensor can also be installed at the entrance to ensure the feverish state of the person passing through the disinfection unit, as shown in figure 1.

Figure 3 16 Schematic of Sustainable Disinfection Tunnel (SDT)[76]

5.2 Solar system model.

The purpose of an autonomous solar system is to provide electrical power everywhere and at any time to secure sensitive devices when the network fails. The size of the system varies greatly depending on consumption and geographic location.

5.3 Contents of the solar kit

- Two polycrystalline solar panels 150 Wp - 12 V.
- Specific solar cable between the panel and the regulator.
- Solar regulator 30 A - 12/24 V.
- Two sealed slow discharge batteries, 12 V - 110 Ah.
- Inverter that converts the 24 V DC (direct current) from the battery into 220 V AC (alternating current) identical to the network – 600 VA (600 W).
- Protection box that can accommodate up to 4 circuit breakers, 2 16 A circuit breakers and a 10 A are integrated in the kit to protect the panel, the battery and the 24 V output. A circuit breaker can be added for an inverter by example.

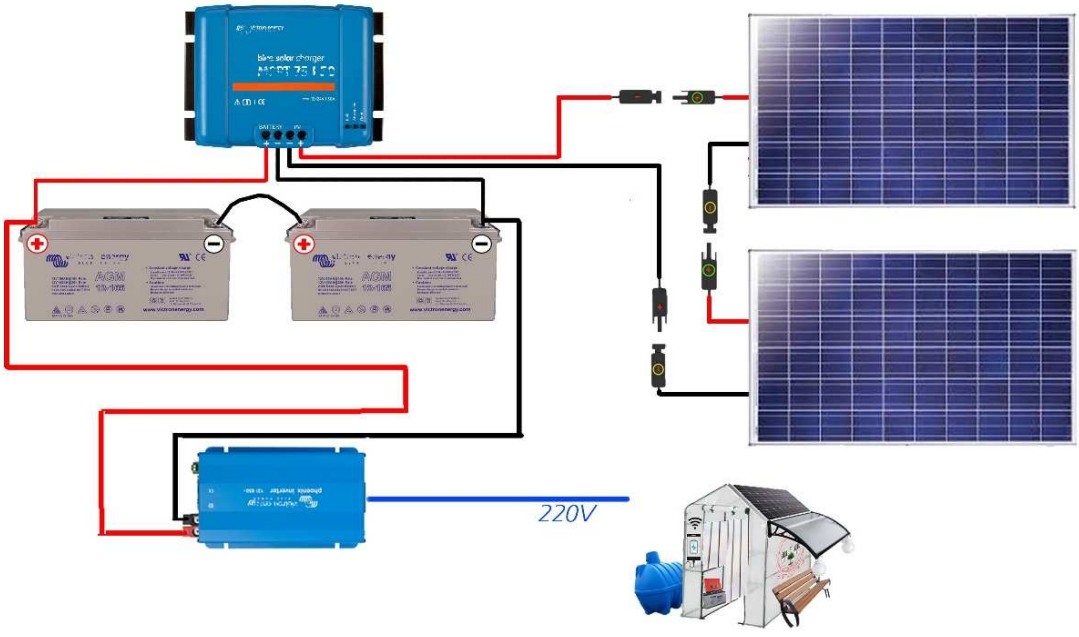

Figure 3 17 Cable Schematics of the solar system.

5.4 Energy needs assessment

Generally, in disinfection tunnels, we are interested in equipment using current from the sector. From this material, we calculated the energies consumed during each use. These results are reported in Tables 1.

Table 6 Electrical equipment used in the station

Device	**Energies (Wh)**
Water Pump (motor)	370 w x 4 hours
2 Spots (Led)	12 x 4 hours

The COVID-19 pandemic is devastating, but by following the infection control practices and abiding by the rules and instructions issued by the authorities, we can slow down its spread [50].

6. Wi-fi station & solar powered smart-phone chargers with a money multi coin selector

According to the Strategy Analytics study, by 2023, the number of mobile devices will continue to increase until it reaches an average figure of 4.3 devices per person. The race towards an ever more connected, communicating and interactive world is on. However, autonomy remains the main obstacle to this development. In order to counter this problem, alternative solutions have been designed.

The Wifi station and solar-powered smart-phone chargers with a money multi coin selector is part of this line of offering Wifi for people who want to connect and recharge their computer tools quickly and efficiently in indoor or outdoor infrastructures. In addition, with the arrival of the Wi-Fi station and solar-powered smart-phone chargers.

The Wi-Fi station and solar-powered smart-phone chargers with a money multi coin selector will considerably increase visibility and the return on investment period will be greatly reduced.

If the Micro portable and the Smart-phones of today are much more powerful than the telephones of yesteryear, they consume more; and who says high consumption says reduced autonomy. Nothing is more annoying for Smartphone addicts than we are to run out of battery.

It is around this reflection that the idea of building a solar station in sight within the public tourist spaces. A project for young people who want to work at home.

An installation that will remain autonomous in all spaces that will benefit everyone (example: telephone charging points in the Oran 2022 Mediterranean games)

6.1 Design and realization of a Wifi station & smart phone charger with a multi coin selector programmed with the Arduino.

The structure of this station, in aluminum, stainless steel or other non-corrosive material, gives it greater stability. The station is mobile, with four wheels equipped with a braking system, to facilitate its movement and positioning in complete safety. These stations are equipped with multi-coin money detector programmed with the Arduino.

The type of multi coin selector we used in this station is CH-926 type. The plan diagram of our wifi station & solar charger as shown in figure 1.

Figure 3 18 plan diagram of our wifi station & solar charger.

6.2 Contents of the solar kit

- Two polycrystalline solar panels 150 Wp - 12 V.
- Specific solar cable between the panel and the regulator.
- Solar regulator 30 A - 12/24 V.
- Two sealed slow discharge batteries, 12 V - 110 Ah.
- Inverter that converts the 24 V DC (direct current) from the battery into 220 V AC (alternating current) identical to the network – 600 VA (600 W).

Protection box that can accommodate up to 4 circuit breakers, 2 16 A circuit breakers and a 10 A are integrated in the kit to protect the panel, the battery and the 24 V output. A circuit breaker can be added for an inverter by example.

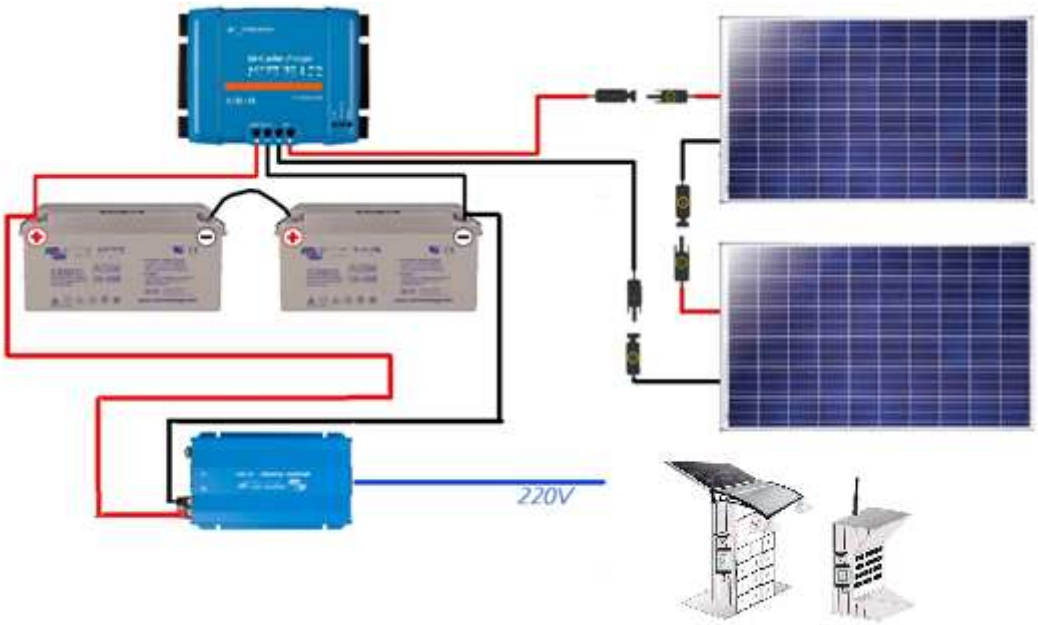

Figure 3 19 Cable Schematics of the solar system.

6.3 Energy needs assessment

Generally, in wifi & smart phone charger stations, we are interested in mobile phones and portable microphones. From this material, we calculated the energy consumed during each use. These results are reported in Table 7.

Table 7 Electrical equipment used in the station

Device	Energies (Wh)
10 Smart phones (10W for each phone)	100 w x 8 hours
4 Micro portables (40 W for each micro)	160 w x 4 hours

6.5 Schematic plan (CH-926 / Arduino) and Source code.

A coinslot is a device used in vending machines responsible for checking whether a coin conforms to a given value. More recent models usually accept a whole series of coins and sort each according to its value. The schematic plan as shown in fig 19 .

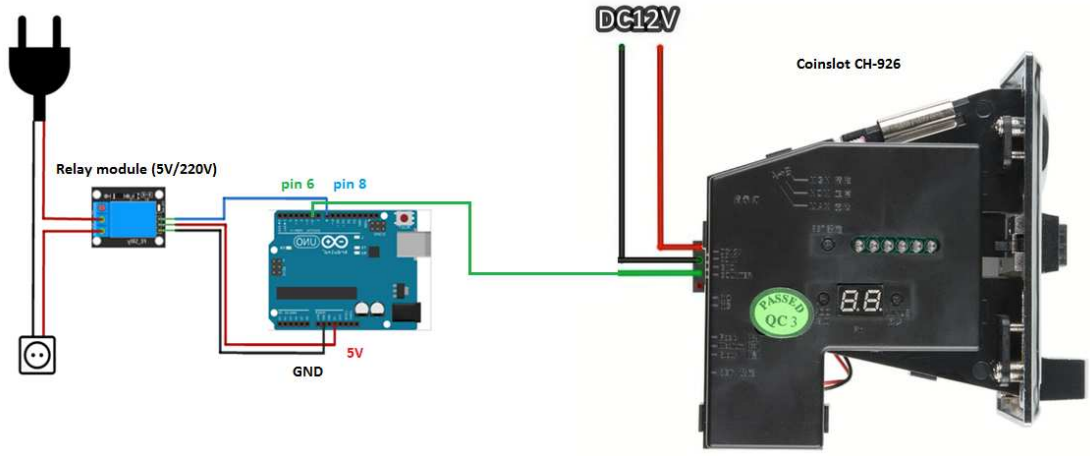

Figure 3 20 Schematic plan of CH-926 / Arduino

In this example we want to program 1 coin type: 50 DA coin1 impuls.

Here is the process how to plan the acceptor to know a set of 1 coin.

1. To start pressing plus (+) and minus (-) buttons as one until A is shown.
2. Button E should be displayed.
3. With + - buttons we select number of types of coins. 1 in our case.
4. Setup again H1 is displayed. Here with + - we select number of sample coins we would use to program this first type of coin.
5. Setup again P1 is displayed. Here we select number of impulses that would represent the first coin. In our case it will be 1 impuls for first coin.
6. Setup button F1 is displayed. Here we set sensitivity (6).
7. Setup button H2 is displayed.
8. When done LED display again shows A. After pressing Setup it changes to E. At this stage we can power off coin acceptor.
9. When pressed again we get A1 and we are ready to sample first coin. Slot the coints one by one.
10. When done indicator LEDs blink. The coin acceptor is ready to be programmed with the arduino and used with the relay module in our station.

References:

[01] NREL Efficiency Chart. This Plot Is Courtesy of the National Renewable Energy Laboratory, Golden, CO. Available online : https://www.nrel.gov /pv/assets/pdfs/best-research-cell-efficiencies.20190802.pdf (accessed on 04 Sep2019).

[02] Chong Liu, Jiandong Fan, Hongliang Li, Cuiling Zhang &YaohuaMai,"Highly Efficient Perovskite Solar Cells with Substantial Reduction of Lead Content", Scientific Reports, 6:35705,https://doi.org/10.1038/srep35705.

[03] MH.Kumar,S. Dharani,WL.Leong, PP.Boix, RR.Prabhakar, T.Baikie,C. Shi,H.Ding, R.Ramesh, M.Asta, M.Graetzel, SG. Mhaisalkar, N.Mathews,"Lead-free halide perovskite solar cells with high photocurrents",DOI:10.1002 /adma. 201401991 , Vol.26,no41,pp.712 2-71277.

[04] Chen Q Y, Huang Y, Huang P R, Ma T, Cao C and He Y 2016 Chin.Phys. B 25 027104.

[05] Noel N K, Stranks S D, Abate A, Wehrenfennig C, GuarneraS,Haghighirad A A, Sadhanala A, Eperon G E, Johnston M B, Petrozza A M, Herz L M and Snaitha H J 2014 Energy Environ. Sci. 9 3061

[06] Hao F, Stoumpos C C, Cao D H, Chang R P H and Kanatzidis M G 2014 Nat. Photon. 8 489

[07] Y.-J. Lee, D. S. Ruby, D. W. Peters, B. B. McKenzie, and J. W. P. Hsu,"ZnO nanostructures as efficient antireflection layers in solar cells,"Nano Letters, vol. 8, no. 5, pp. 1501–1505, 2008.

[08] M. Hossain, O. Daif, N. Amin, F. Alharbi, and N. Tabet,TMS Middle East - Mediterranean Materials Congress on Energy and Infrastructure Systems (MEMA 2015), 2013.

[09] S. Bansal and P. Aryal, "Evaluation of new materials for electron and hole transport layers in perovskite-based solar cells through SCAPS-1D simulations," in 2016 IEEE 43rd Photovoltaic Specialists Conference (PVSC), Portland, OR, USA, June 2016.

[10] Kemp K W, Labelle A J, Thon S M, Ip A H, Kramer I J, Hoogland S and Sargent E H 2013 Adv. Energy Mater. 3 917

[11] Hao F Stoumpos C C Chang R P H and Kanatzidis M G 2014 J. Am.Chem. Soc. 136 8094.

[12] Rutledge SA, Helmy AS. Carrier mobility esnhancement in poly(3,4-ethylenedioxythiophene)-poly (styrenesulfonate) having undergone rapid thermal annealing. Journal of Applied Physics. 2013, 114(13):133708-1–5. Crossref

[13] Mihailetchi VD, Van Duren JK, Blom PWM, Hummelen JC, Janssen RAJ, Kroon JM, Rispens MT, Verhees WJH, Wienk MM. Electron transport in methanofullerene. Advanced Functional Materials. 2003; 13(1): 43–6. Crossref

[14] L. Huang, X. Sun, C. Li, R. Xu, J. Xu, Y. Du, Y. Wu, J. Ni, H. Cai, J. Li, Sol. Energy Mater. Sol. Cells 2016, 157, 1038.

[15] S. Bansal, P. Aryal, in 2016 IEEE 43rd Photovolt. Spec. Conf., IEEE, 2016, pp. 747–750.

[16] K. Sobayel, M. Akhtaruzzaman, K. S. Rahman, M. T. Ferdaous, Z. A. Al-Mutairi, H. F. Alharbi, N. H. Alharthi, M. R. Karim, S. Hasmady, N. Amin, Results Phys. 2019, 12, 1097.

[17] A. Sahu, A. Dixit, Curr. Appl. Phys. 2018, 18, 1583.

[18] C. Malerba, F. Biccari, C. L. A. Ricardo, M. D'Incau, P. Scardi, A. Mittiga, Sol. Energy Mater. Sol. Cells 2011, 95, 2848.

[19] Usha Mandadapu et al "Simulation and Analysis of Lead based Perovskite Solar Cell using SCAPS-1D"Indian Journal of Science and Technology, Vol 10(11), DOI: 10.17485/ijst/2017/v11i10/110721, March 2017.

[20] Hossain, M.I., Alharbi, F.H., Tabet, N., 2015. Copper oxide as inorganic hole transport material for lead halide perovskite based solar cells. Sol. Energy 120, 370–380

[21] Hui-Jing Du et al 2016 Chinese Phys. B 25 108802

[22] Nogueira, A. F., Longo, C., & De Paoli, M.-A. (2004). Polymers in dye sensitized solar cells: overview and perspectives. Coordination Chemistry Reviews, 248(13-14), 1455–1468.doi:10.1016/j.ccr.2004.05.018

[23] Burgelman, M., Nollet, P. and Degrave, S. (2000) 'Modelling polycrystalline semiconductor solar cells', Thin SolidFilms, 23rd European Photovoltaic Solar Energy Conference, Valencia, Vol. 361, pp.527–532.

[24] Farhana Anwar et al, "Effect of Different HTM Layers and Electrical Parameters on ZnO Nanorod-Based Lead Free Perovskite Solar Cell for High-Efficiency Performance " International Journal of Photoenergy Volume 2017, Article ID 9846310, 9 pages https://doi.org/10.1155/2017/9846310

[25] Umari P, Mosconi E and De Angelis F 2014 Sci. Rep. 4 4467

[26] A. Niemegeers, M.Burgelman, K.Decock, J.Verschraegen, S. Degrave, SCAPS manual, May 2014.

[27] E. Constableand R. A. Lewis,"Optical parameters of Spiro-MeOTAD determined using continuous-wave terahertz radiation", JOURNAL OF APPLIED PHYSICS 112, 063104 (2012).

[28] Warda Hadouchi. Etude de l'utilisation du ZnO comme contact de type n dans des dispositifs photovoltaïques à base de pérovskite hybride. Matériaux. Université Paris-Saclay, 2017. Français. NNT :2017SACLX012ff. tel-01633008

[29] Abdelhadi SLAMI, Mama BOUCHAOUR and Laarej MERAD'Numerical Study of Based Perovskite Solar Cells by SCAPS-1D'INTERNATIONAL JOURNAL OF ENERGY and ENVIRONMENT , ISSN: 2308-1007,Volume 13, pp 17-21,2019

[30] Najmin Ara Sultana, Md.Obidul Islam, Mainul Hossain, Zahid Hasan Mahmood, comparative performance study of perovskite solar cell for different electron transport materials.Dhaka Univ. J.Sci.66(2): 109-114, 2018 (July).

[31] M. Hossain, O. Daif, N. Amin, F. Alharbi, and N. Tabet,TMS Middle East - Mediterranean Materials Congress on Energy and Infrastructure Systems (MEMA 2015), 2013.

[32] Hui-Jing Du, Wei-Chao Ang, Jian-Zhuo Zhu, Device simulation of lead-free CH3NH3SnI3 perovskite solar cells with high efficiency,Chin.Phys. B vol,25,No10(2016)108802, DOI: 10.1088/1974-1056/25/10/108802.

[33] Tapas Chakrabarti, Malay Saha, Ambar Khanda, Subir Kumar Sarkar, Modeling of lead-free CH3NH3SnI3- based perovskite solar cell using ZnO as ETL,pp 121-131 (2018).

[34] Mandadapu, U., Vedanayakam, S.V., Thyagarajan, K. and Babu, B.J. (2018) 'Optimisation of high efficiency tin halide perovskite solar cells using SCAPS-1D', Int. J. Simulation and Process Modelling, Vol. 13, No. 3, pp.221–227.

[35] G.Xosrovashvili, N.E.Gorji," Numerical analysis of TiO2/Cu2ZnSnS4nanostructured PV using SCAPS-1D", Journal of Modern Optics, DOI: Org/10.1080/09500340.2013.827252, Vol,60, N°.11,pp.936-940.

[36] Lee MM, Teuscher J, Miyasaka T, Murakami TN, Snaith HJ, Efficient hybrid solar cells based on meso-superstructured organometal halide perovskites. Science. 2012; 338:643-7.

[37] Noh JH, Im SH, Heo JH, Mandal TN, Seok SI, Chemical management for colorful, efficient, and stable inorganic- organic hybrid nanostructured solar cells. Nano letters. 2013;13:1764-9.

[38] Hirasawa M, Ishihara T, Goto T, Uchida K, Miura N. Magnetoabsorption of the lowest exciton in perovskite-type compound (CH3NH3)PbI3. Physica B: Condensed Matter. 1994;201:427-30.

[39] Umari P, Mosconi E and De Angelis F 2014 Sci. Rep. 4 4467

[40] Chen Q Y, Huang Y, Huang P R, Ma T, Cao C and He Y 2016 Chin.Phys. B 25 027104

[41] Noel N K, Stranks S D, Abate A, Wehrenfennig C, GuarneraS,Haghighirad A A, Sadhanala A, Eperon G E, Johnston M B, Petrozza A M, Herz L M and Snaitha H J 2014 Energy Environ. Sci. 9 3061

[42] Hao F, Stoumpos C C, Cao D H, Chang R P H and Kanatzidis M G 2014 Nat. Photon. 8 489

[43] Y.-J. Lee, D. S. Ruby, D. W. Peters, B. B. McKenzie, and J. W. P. Hsu,"ZnO nanostructures as efficient antireflection layers in solar cells,"Nano Letters, vol. 8, no. 5, pp. 1501–1505, 2008.

[44] S. Bansal and P. Aryal, "Evaluation of new materials for electron and hole transport layers in perovskite-based solar cells through SCAPS-1D simulations," in 2016 IEEE 43rd Photovoltaic Specialists Conference (PVSC), Portland, OR, USA, June 2016.

[45] Kemp K W, Labelle A J, Thon S M, Ip A H, Kramer I J, Hoogland S and Sargent E H 2013 Adv. Energy Mater. 3 917

[46] R.Soni, R.Eva, M.Barea, and F.Fabregat Santiago, " Analysis of the origin of Open Circuit Voltage in Dye Solar Cells" Journal of Physical Chemical Letters, DOI: 10,1021/jz3005464, Vol.3,N°.12, PP 1629-1634.

[47] G.Xosrovashvili, N.E.Gorji," Numerical analysis of TiO2 /Cu2ZnSnS4 nanostructured PV using SCAPS-1D", Journal of Modern Optics, DOI: Org/10.1080 /09500340.2013.827252, Vol,60, N°.11,pp.936-940.

[48] Lee MM, Teuscher J, Miyasaka T, Murakami TN, Snaith HJ, Efficient hybrid solar cells based on meso-superstructured organometal halide perovski.

[49] Abdelhadi SLAMI, Mama BOUCHAOUR and Laarej MERAD, Comparative study of modeling of Perovskite solar cell with different HTM layers,

INTERNATIONAL JOURNAL OF MATERIALS, DOI: 10.46300/91018.2020.7.1, Volume 7, 2020.

[50] Nabih Mohammad Lawand, Samaa Al Tabbah. 2020. Coronavirus Disease 2019 (COVID-19): Prevention and Disinfection. Int J Biol Med. 2: 10-14.

[51]. Q&A on coronaviruses. World Health Organization. 11 February 2020. Retrieved 07 Jun 2020.

[52] Coronavirus Disease 2019 (COVID-19)- Transmission. Centers for Disease Control and Prevention.17 March 2020. Retrieved 23 March 2020.

[53]. Q & A on COVID-19. European Centre for Disease Prevention and Control. Retrieved 23 March 2020.

[54] To Fight Coronavirus, Disinfectant Tunnel in China Sprays Industrial Workers | World News | US News [Internet]. [cited 2020 May 24]. Available from: https://www.usnews.com/news/world/articles/2020-02-12/to-fight-coronavirus-disinfectanttunnel-in-china-sprays-industrial-workers

[55] World Health Organization. Cleaning and disinfection of environmental surfaces in the context of COVID-19. 16 May 2020. https://www.who.int /publications/i/item/cleaning-and-disinfection-ofenvironmental-surfaces-inthe-context -of-covid-19 (accessed 07 Jun 2020).

[56] Pan American Health Organization. The use of tunnels and other technologies for disinfection of humans using chemical aspersion or UV-C light. 5 May 2020. https://iris.paho.org/ handle/10665.2/52066 (accessed 07 Jun 2020).

[57] Africa Centres for Disease Control. Position statement: The use of disinfection tunnels or disinfectant spraying of humans. 28 May 2020. https://africacdc.org /pillar/infection-prevention-and-control/ (accessed 07 Jun 2020).

[58] Ibrahim Mlaouhi, Mehdi B. H. SALAH , Haykel Khiareddine, Disinfection unit COVID-19.

[59] Manisha Biswal, RImjhim Kanaujia, Archana Angrup, Shubh Mohan Singh, Pallab Ray, “Disinfection tunnels (DT): potentially counterproductive in the context of a prolonged pandemic”, JMIR Public Health and Surveillance on: April 17, 2020.

[60] Navneesh Singh Malhotra, Harman Malhotra,Transmission of Sound Using Lasers, International Journal of Advanced Research in Computer Science & Technology, Vol. 2, Issue 3 (July - Sept. 2014)

[61] Umari P, Mosconi E and De Angelis F 2014 Sci. Rep. 4 4467

[62] Chen Q Y, Huang Y, Huang P R, Ma T, Cao C and He Y 2016 Chin.Phys. B 25 027104

[63] Noel N K, Stranks S D, Abate A, Wehrenfennig C, GuarneraS,Haghighirad A A, Sadhanala A, Eperon G E, Johnston M B, Petrozza A M, Herz L M and Snaitha H J 2014 Energy Environ. Sci. 9 3061

[64] Hao F, Stoumpos C C, Cao D H, Chang R P H and Kanatzidis M G 2014 Nat. Photon. 8 489

[65] Y.-J. Lee, D. S. Ruby, D. W. Peters, B. B. McKenzie, and J. W. P. Hsu,"ZnO nanostructures as efficient antireflection layers in solar cells,"Nano Letters, vol. 8, no. 5, pp. 1501–1505, 2008.

[66] M. Hossain, O. Daif, N. Amin, F. Alharbi, and N. Tabet,TMS Middle East - Mediterranean Materials Congress on Energy and Infrastructure Systems (MEMA 2015), 2013.

[67] S. Bansal and P. Aryal, "Evaluation of new materials for electron and hole transport layers in perovskite-based solar cells through SCAPS-1D simulations," in 2016 IEEE 43rd Photovoltaic Specialists Conference (PVSC), Portland, OR, USA, June 2016.

[68] Kemp K W, Labelle A J, Thon S M, Ip A H, Kramer I J, Hoogland S and Sargent E H 2013 Adv. Energy Mater. 3 917

[69] Hao F Stoumpos C C Chang R P H and Kanatzidis M G 2014 J. Am.Chem. Soc. 136 8094.

[70]Rutledge SA, Helmy AS. Carrier mobility esnhancement in poly(3,4-ethylenedioxythiophene)-poly (styrenesulfonate) having undergone rapid thermal annealing. Journal of Applied Physics. 2013, 114(13):133708-1–5. Crossref

[71]Mihailetchi VD, Van Duren JK, Blom PWM, Hummelen JC, Janssen RAJ, Kroon JM, Rispens MT, Verhees WJH, Wienk MM. Electron transport in methanofullerene. Advanced Functional Materials. 2003; 13(1): 43–6. Crossref

[72] L. Huang, X. Sun, C. Li, R. Xu, J. Xu, Y. Du, Y. Wu, J. Ni, H. Cai, J. Li, Sol. Energy Mater. Sol. Cells 2016, 157, 1038.

[73] Abdelhadi SLAMI, Mama BOUCHAOUR, Yacine AYACHI AMOR, Laarej MERAD: "Transmission of Sound via a Perovskite Solar Cell", INTERNATIONAL JOURNAL OF ENERGY DOI: 10.46300/91010.2020.14.12.

[74] Moh Salih, M.A.; Mustafa, M.A.;Yousef, B.A.A. DevelopingLead-Free Perovskite-Based SolarCells with Planar Structure inConfined Mode Arrangement UsingSCAPS-1D. Sustainability 2023, 15,1607. https://doi.org/10.3390/su15021607.

[75] Hossein Alipour, Abbas Ghadimi » Optimization of lead-free perovskite solar cells in normal-structure with WO 3 and water-free PEDOT: PSS composite for hole transport layer by SCAPS-1D simulation", DOI: 10.1016/j.optmat.2021.111432.

[76] SLAMI, Abdelhadi, Mama BOUCHAOUR, and Laarej MERAD. "DESIGN OF A SUSTAINABLE DISINFECTION TUNNEL OF COVID19."
Doi: 10.46657/ajresd.2022.4.2.1.

GENERAL CONCLUSION

The main goal of this thesis is to find new solar cells based on lead-free perovskite with different HTM and ETM layers. This makes it possible to optimize the stability and the cost of manufacturing these perovskite cells, as well as the technology for mass production.

The main objective of the first part of this thesis is to study and compare two active layers (MAPbI3) and (MASnI3) with several HTM and ETM in a perovskite solar cell and with different parameters are analyzed using a one-dimensional device simulation. ZnO and TiO2 are offered as electron transport layers (ETL) In the future, the results of these proposed structures will become a good guide for the design of high efficiency and low cost tin halide perovskite solar cells.

In the second part, we presented a simples process to put the voices and texts on a laser beam and transmit it remotely via a perovskite solar cell (Wireless network local based on perovskite solar cell), With the use of the Arduino.

We then proposed a new structure of a sustainable proposal tunnel (SDT) and help the community to contribute to reduce viruses, using renewable energy. If researchers find a cleaning substance not harmful to human health reverse the materials currently used condemned by the World Health Organization. Will give good results to contribute to the use of solar energy to eradicate viruses less harmful than corona virus.

In the last part, we are interested in studying a small wifi station and a smart phone charger, secured using solar energy with a money coin selector. It can be found in green spaces, public gardens and service stations outside the city as well as at bus stops.

Perspective

The prospects envisaged for pursuing this doctoral thesis are numerous. First, it is necessary to continue to develop new high-performance mixed structure. Several avenues exist for continuing the work on the research presented in this thesis,

- We will simulate and optimize a mixed structure based on MASnI3 and MAPbI3 using a SCAPS-1D dimensional simulator.
- We will simulate and optimize a mixed structure based on two HTM layers.
- Make a perovskite solar cell based on tin as the active layer, ZNO as ETM, and Cu2O as HTM, for use in our perovskite solar cell based wireless network local.

Then, regarding the development of the wireless microphone based on perovskite solar cell, other studies are currently being carried out with the aim of using the Arduino to transport data by solar cells based of perovskite.

Finally, it requires the integration of perovskite-based solar cells into stand-alone systems.

PATENT / INTERNATIONAL AND NATIONAL PUBLICATIONS

- **Abdelhadi SLAMI**, Mama BOUCHAOUR, Laarej MERAD "Numerical Study of Based Perovskite Solar Cells by SCAPS-1D ",INTERNATIONAL JOURNAL OF ENERGY and ENVIRONMENT Volume 13, 2019.
  ISSN: 2308-1007
- **Abdelhadi SLAMI**, Mama BOUCHAOUR, Laarej MERAD "Comparative study of modeling of Perovskite solar cell with different HTM layers". INTERNATIONAL JOURNAL OF MATERIALS
  DOI:10.46300/91018.2020.7.1
- **Abdelhadi SLAMI**, Mama BOUCHAOUR, Yacine AYACHI AMOR, Laarej MERAD: "Transmission of Sound via a Perovskite Solar Cell", INTERNATIONAL JOURNAL OF ENERGY DOI: 10.46300/91010.2020.14.12.
- **Abdelhadi SLAMI**, Mama BOUCHAOUR, Laarej MERAD DESIGN OF A SUSTAINABLE DISINFECTION TUNNEL OF COVID19 4(2) 2020: 122-125, Doi: 10.46657/ajresd.2022.4.2.1.
- **Abdelhadi SLAMI**, Mama BOUCHAOUR, Laarej MERAD Brevet d'invention « Microphone sans fils à base de cellule solaire perovskite ». N° 11678 https://www.univ-tlemcen.dz/fr/actualites/2405/brevet-d-invention

INTERNATIONAL AND NATIONAL COMMUNICATIONS

- **Abdelhadi SLAMI**, Mama BOUCHAOUR, Laarej MERAD 23rd International Conference On Circuits, Systems, Communications and Computer CSCC 2019 (Numerical Study of Based Perovskite Solar Cells by SCAPS-1D) at: Marathon, Athens, Greece.
- **Abdelhadi SLAMI**, Noureddine BENRAMDHANE,"Manual Method for Measuring The External Quantum Efficiency for solar cells,E3S Web of Conferences 229, 01005 (2021) ICCSRE'2020 https:// doi.org /10.1051 /e3sconf /202122901005.

Abstract

ملخص:

يتناول موضوع هذه الأطروحة تصميم وتحليل العديد من نماذج خلايا البيروفسكايت الشمسية. لدراسة كفاءة وأداء هذه الخلايا الشمسية ، يتم استخدام برنامج SCAPS-1D في المحاكاة.

تمت دراسة كفاءة الخلايا الشمسية القائمة على MASnI3 و MAPbI3 مع طبقات مختلفة من مواد نقل الثقوب (HTM) بما في ذلك Spiro-OMeTAD وPEDOT: Pss و Cu2O ، تم اقتراح طبقة أكسيد الزنك (ZnO) و TiO2 كطبقتين لنقل الإلكترون (ETM). حيث تم عرض تأثير كثافة الخلل ، سماكة طبقة الامتصاص ، و درجة حرارة العمل على أداء الجهاز.

عملية بسيطة لنقل الصوت والرسائل النصية على شعاع الليزر ونقله عبر مسافة عبر خلية شمسية من البيروفسكايت (شبكة لاسلكية محلية تعتمد على خلية شمسية بيروفسكايت مبرمجة مع الأردوينو). تعتبر هذه العملية مثالًا رائعًا لتعديل اتساع الضوء باستخدام اهتزازات الصوت. لذلك ، سيتم وصف تصميم ومحاكاة خلية بيروفسكايت الشمسية بالتفصيل في هذا العمل.

دراسة وتحقيق نفق تطهير مستدام (SDT) للحد من الفيروسات الأقل ضرراً من فيروس كورونا الذي ينتقل عن طريق اللمس ، باستخدام الطاقة الشمسية.

دراسة وتحقيق محطة واي فاي وشواحن الهواتف الذكية التي تعمل بالطاقة الشمسية مع محدد العملات المتعدد ، والذي يسلط الضوء على الاقتصاد الأخضر ، وكذلك افتتاح مناصب الشغل.

الكلمات المفتاحية:البيروفسكايت ,PEDOT:Pss, CH3NH3SnI3, أكسيد النحاس, ZnO, Spiro-OMeTAD , HTM,النجاعة، SCAPS-1D ,

RESUME:

L'objectif de cette thèse porte sur la conception et l'analyse de nombreux dispositifs de cellules solaires pérovskites. Pour étudier l'efficacité et les performances de ces cellules solaires, le logiciel SCAPS-1D est utilisé dans la simulation. L'efficacité des cellules solaires à base de MASnI3 et MAPbI3 avec diverses couches de matériaux de transport de trous (HTM), y compris Spiro-OMeTAD, PEDOT:Pss et Cu2O, est étudiée. La couche d'oxyde de zinc (ZnO) et le TiO2 sont proposés comme couches de transport d'électrons

L'influence de la densité des défauts, de l'épaisseur de la couche absorbante, et la température sur les performances de dispositifs est présentée.

Un procédé simple pour mettre les voix et les textes sur un faisceau laser et la transmettre à distance via une cellule solaire pérovskite (Réseau local sans fils à base de cellule solaire pérovskite programmer avec l'Arduino). Ce processus est considéré comme un exemple fascinant de modulation d'amplitude de la lumière à l'aide de vibrations sonores. Par conséquent, la conception et la simulation de la cellule solaire pérovskite seront décrites en détail dans ce travail.

Une étude et réalisation d'un tunnel de désinfection durable (SDT) pour réduire les virus moins nocifs que le corona virus qui se transmettent par le toucher, avec l'utilisation d'énergie solaire.

Une étude et réalisation d'une station wifi et chargeurs des smart-phones à l'énergie solaire avec un sélecteur multi pièce de l'argent, qui permet de mettre en évidence l'économie verte, ainsi que l'ouverture des postes de travail.

Mots clé: Pérovskite, CH3NH3SnI3, PEDOT:Pss, Oxyde de cuivre, Spiro-OMeTAD, ZnO, HTM, efficacité, SCAPS-1D

ABSTRACT:

The objectif of this thesise deals with the design and analysis of many devices Perovskite solar cells. To study the efficiency and the performances of thos solar cells, SCAPS-1D software is used in the simulation. The efficiency of MASnI3 and MAPbI3 based solar cell with various hole transport material (HTM) layers including Spiro-OMeTAD, PEDOT:Pss, and Cu2O is studied. Zinc oxide (ZnO) layer and TiO2 are proposed as electron

transport layers the influence of defect density, absorber layer thickness, and working temperature on the performance of the device is presented.

A simple process to put voices and texts on a laser beam and transmit it remotely via a perovskite solar cell (local wireless network based on perovskite solar cell programmed with the Arduino). This process is considered a fascinating example of amplitude modulation of light using sound vibrations. Therefore, the design and simulation of the perovskite solar cell will be described in detail in this work.

A study and realization of a sustainable disinfection tunnel (SDT) to reduce viruses less harmful than the corona virus that are transmitted by touch, with the use of solar energy.

A study and realization of a wifi station and solar-powered smart-phone chargers with a silver multi-coin selector, which highlights the green economy, as well as the opening of workstations .

Keywords: Perovskite, CH3NH3SnI3, PEDOT:Pss, Copper oxide, Spiro-OMeTAD, ZnO, HTM, efficiency, SCAPS-1D

INTERNATIONAL JOURNAL OF MATERIALS
DOI: 10.46300/91018.2020.7.1 Volume 7, 2020

Comparative study of modeling of Perovskite solar cell with different HTM layers

Abdelhadi SLAMI, Mama BOUCHAOUR and Laarej MERAD

University of Tlemcen, Faculty of Sciences, Department of Physics
Unité de Recherche « *Matériaux et Energies Renouvelables* », URMER
BP: 119, Fg. Pasteur, Tlemcen, 13000, Algeria

ABSTRACT-The efficiency of $MASnI_3$ based solar cell with various hole transport material (HTM) layers including Spiro-OMeTAD, PEDOT:Pss, and Cu_2O is studied. Zinc oxide (ZnO) layer is proposed as electron transport layer for lead-free $CH_3NH_3SnI_3$ based Perovskite solar cells. The influence of device parameters such as doping level of the active layer, thickness of the $CH_3NH_3SnI_3$ layer and working temperature is discussed. For optimum parameters of all three structures, efficiency of 24.17%, 24.50%, and 25.36% for PEDOT:Pss, Spiro-OMeTAD, and Cu_2O, respectively is achieved. To study the optimized performance of this Perovskite solar cell, SCAPS-1D software is considered.

Keywords: Perovskite, $CH_3NH_3SnI_3$, PEDOT:Pss, Copper oxide, Spiro-OMeTAD, ZnO, HTM, efficiency, SCAPS-1D.

I.INTRODUCTION

In recent years, Perovskite oxides represent a prominent of advanced compounds involved in many areas of science and technology [JTAC 2011 1–3]. Perovskite Solar Cells (PSCs) show a great performance because of their low cost fabrication than traditional solar cells [1]. The yield of PSC increases very rapidly reaching the value of 22% [2-4]. Owing the multilayer architecture of PSCs, interface has a main role to play in performance and influences long term stability [5]. The CH_3NH_3**Sn**I_3's absorber layer becomes a suitable alternative of CH_3NH_3**Pb**I_3 one because of the toxicity of this typical PSC [6].

The Spiro-OMeTAD HTM is used in organic photovoltaics (OPV) and organic optoelectronics [7], but its causes degradation in the devices performance [8]. Thus, PEDOT:Pss, or Cu_2O replace the spiro-OMeTAD HTM.

The aim of this paper is to contribute to the optimization of the efficiency of Perovskite solar cell with three different configurations: Glass/FTO/ZnO/$CH_3NH_3SnI_3$/HTM/Au, HTM being Spiro-OMeTAD. 1D solar cell capacitance simulator (SCAPS) is applied for this study.

II. NUMERICAL MODELLING AND DEVICE SRUCTURE

II.1. Numerical modeling

To analyze the effect of different electrical parameters on the efficiency of PCs, SnO_2:f/ZnO/$CH_3NH_3SnI_3$/Spiro-OMeTAD, SnO_2:f/ZnO/$CH_3NH_3SnI_3$/PEDOT:Pss, and SnO_2:f/ZnO/$CH_3NH_3SnI_3$/Cu_2O heterojuction-based perovskite solar cell structures, are adopted. SCAPS software is used for simulation. Figure 1, explains the simulation process.

SCAPS is a one dimensional solar cell simulation program developed at the department of Electronics and Information Systems (ELIS) of the University of Gent, Belgium. It allows simulating the behavior of photovoltaic structures. Since that, there are several modifications in this software such as the capability to work with crystalline solar cells (c-Si and GaAs, family) and amorphous cells (a-Si and micro-morphous Si) [9]. This simulator has the largest number of AC and DC electrical measurements which can be calculated in dark and light illumination and also at different temperatures. It (SCAPS) solves the Basic semiconductor equations in 1-Dimension under steady state condition.

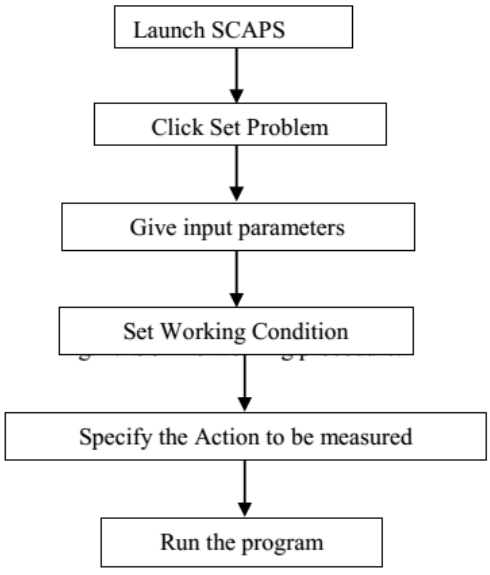

Fig. 1. SCAPS working procedure.

INTERNATIONAL JOURNAL OF MATERIALS
DOI: 10.46300/91018.2020.7.1 Volume 7, 2020

II.2. Device structure

The cell consists of Methylammonium tin triodide ($MASnI_3$); considered as absorber layer. N-type (ZnO-ETM) is arranged at the bottom side, and at the top three p-type (Spiro-OMeTAD, PEDOT:Pss and Cu_2O) are designed as HTM layer. figure 2 presents the three structures.

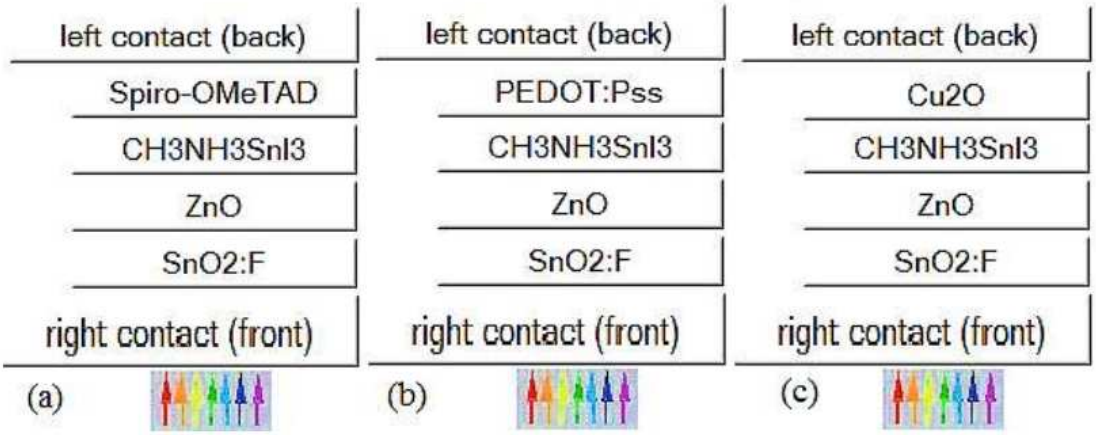

Figure 2:Schematic representation of three architectures with different HTM layers
(a) Spiro-OMeTAD(HTM)/$MASnI_3$/ ZnO/ SnO_2:F
(b) PEDOT:Pss(HTM)/$MASnI_3$/ ZnO/ SnO_2:F
(c) Cu_2O(HTM)/$MASnI_3$/ ZnO/ SnO_2:F

To run the simulation, SCAPS needs material parameters; in terms of bandgap (Eg), electron affinity (χ), dielectric permittivity (ε), conduction band density of states (Nc), valence band density of states (Nv), electron mobility (μn), hole mobility (μp), donor density (N_D), acceptor density (N_A). Table 1 summarizes data and other theoretical results extracted from published studies.

Parameters	SnO_2 :F [10, 11, 12]	ZnO [13-15]	$CH_3NH_3SnI_3$ [16, 17-18]	SpiroOMeTAD [19-23]	PEDOT :Pss [24, 25]	Cu_2O [22-23]
Thickness(nm)	500	50	900	200	200	200
E_g *(ev)*	3.5	3.2	1.3	3.17	3.6	2.17
χ *(ev)*	4	4.26	4.17	2.05	1.57	3.2
εr	9	9	8.2	3	3	7.11
$N_c\,(cm^{-3})$	2.20×10^{18}	2.00×10^{18}	1.00×10^{18}	2.20×10^{18}	2.20×10^{17}	2.02×10^{17}
$N_v\,(cm^{-3})$	1.80×10^{19}	1.80×10^{19}	1.00×10^{18}	1.80×10^{19}	1.80×10^{19}	1.10×10^{19}
$\mu_e\,(cm^2/Vs)$	20	200	1.60	2.00×10^{-4}	10	200
$\mu_h\,(cm^2/Vs)$	10	5	1.60	2.00×10^{-4}	400	80
$N_D\,(cm^{-3})$	2.00×10^{19}	1.50×10^{17}	-	-	-	-
$N_A\,(cm^{-3})$	-		1.50×10^{16}	2.00×10^{19}	2.00×10^{19}	2.00×10^{19}

Table1 : Parameters used for simulation of perovskite solar cell structures using SCAPS-1D

III. RESULTS AND DISCUSSION

III.1. Influence of Absorber layer thickness

The Thickness of $CH_3NH_3SnI_3$ is varied from [50-900] nm with the three HTM layers (PEDOT:Pss/Cu_2O/spiro-OMeTAD) and ZnO as the ETM layer.

The simulated parameters such as Power Conversion Efficiency (PCE), Fill Factor (FF), Short circuit current density (Jsc), open circuit voltage (Voc) of the $CH_3NH_3SnI_3$ solar cells, are shown in Figure 3.

All photovoltaic parameters are maximum at 900nm. The efficiency increases with increasing thickness. It will be explained by the increase in generation of electron-hole pairs in the absorber layer. Therefore, the optical density increases. Also, with increasing thickness, the short circuit current (J_{sc}) increases because the thicker absorber layer absorbs more photons, which creates more electron-hole pairs. Moreover, with a thicker absorber layer the chance of recombination increases too; as the charges cross a long distance for diffusion [26]. The results show that the device including Cu_2O as Hole Transport Material (HTM) has the highest performance.

INTERNATIONAL JOURNAL OF MATERIALS
DOI: 10.46300/91018.2020.7.1 Volume 7, 2020

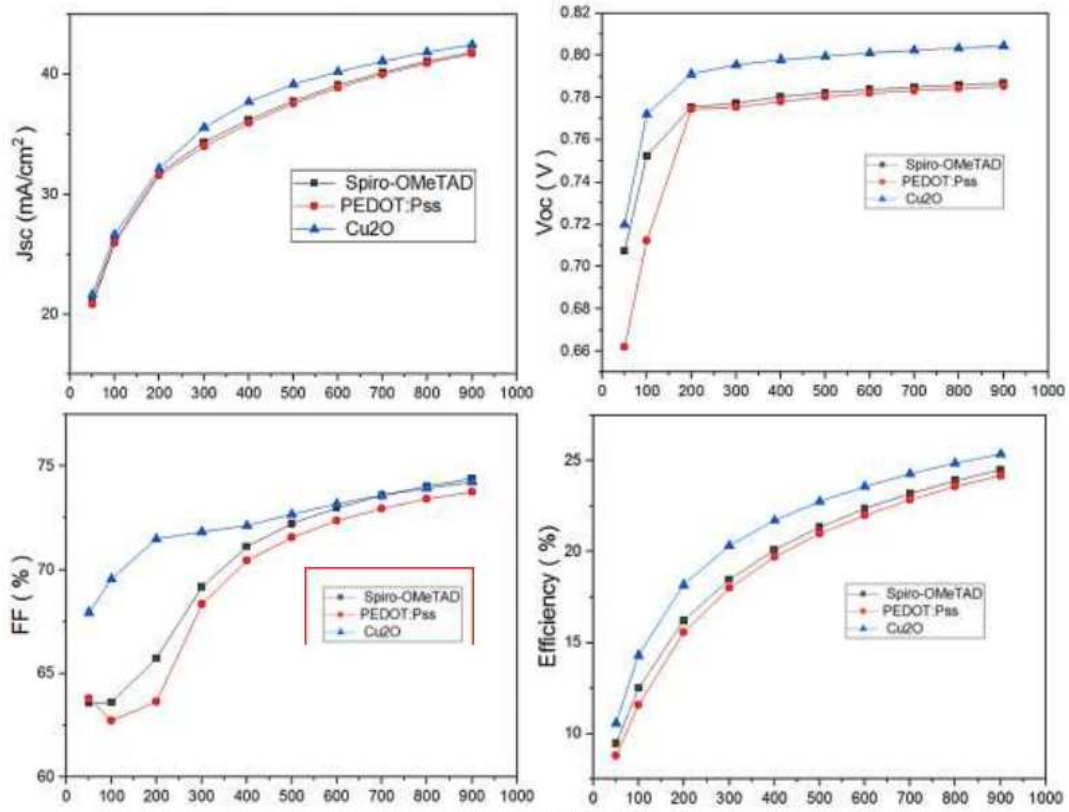

Figure 3: Variation of device performance of absorber thickness layer.

Table 2 recaps all results of PV parameters.

Perovskite solar cell	Voc (V)	J_{sc} (mA/cm^{-2})	FF (%)	PCE (%)
SnO_2:F/ZnO/$MASnI_3$/PEDOT:Pss	0.7853	41.72	73.77	24.17
SnO_2:F/ZnO/$MASnI_3$/Spiro-OMeTAD	0.7868	41.85	74.41	24.5
SnO_2:F/ZnO/$MASnI_3$/Cu_2O	0.8044	42.47	74.23	25.36

Table 2: Parameters of PSC with different HTM layers.

III.2. Influence of doping of the active layers on the PV parameters

Figure 4, presents the effect of dopant concentration (doping) of Perovskite absorber layer on PV parameters. Acceptor doping concentration (N_A) is varying from 10^{15}cm^{-3} to 10^{17}cm^{-3}. The maximum value appears at N_A of 1.5x10^{16} cm^{-3} for both structures with HTM layers (Spiro-OMeTAD, and PEDOT:Pss). On the other hand, for structure with Cu_2O as HTM layer N_A is 1.0 10^{16} cm^{-3}. FF changes also when N_A is varying. And all structures (SnO_2:f/ZnO/$CH_3NH_3SnI_3$/Spiro-OMeTAD, SnO_2:f/ZnO/$CH_3NH_3SnI_3$/PEDOT:Pss, and SnO_2:f/ZnO/$CH_3NH_3SnI_3$/Cu_2O) reach their maximum values when the N_A is approximately 1.5 10^{16} cm^{-3}. Hence, an appropriate doping concentration of the Perovskite absorption layer is favorable to the amelioration of the photo-absorption efficiency, Jsc and FF. However, the Voc drops rapidly when the N_A exceeds 1.0x10^{16}cm^{-3} in all three considered models. Its can be explained by Auger recombination rate. Indeed, increasing doping concentration causes higher Auger recombination rate. The enhancement of the electric field is the consequence of the increase of doping concentration. This characteristic favors the separation of carriers and thus the improvement of the cell performance [21].

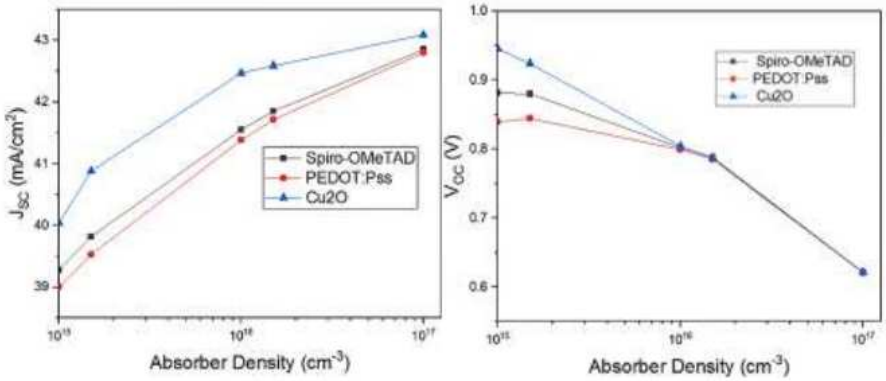

INTERNATIONAL JOURNAL OF MATERIALS
DOI: 10.46300/91018.2020.7.1 Volume 7, 2020

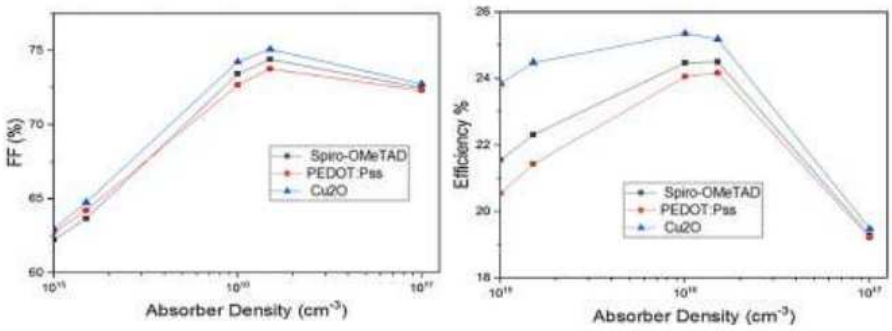

Figure 4: Effect of dopant concentrations of Perovskite absorber layer on PV parameters.

III.3. Influence of temperature

To understand the effect of temperature on the electrical performance of the solar cell, the temperature of the simulated model is changed from 300K to 450K. Figure 5 shows the variation of PCE versus temperature for all HTM layers. All the three HTM layers simulation models show similar behavior: as the temperature increases the PV parameters are decreasing not shown in this paper.

As the temperature increases, defect density inside the layers increases and then reduces the efficiency. It can be explained by the fact the defect density inside the layers increases with the temperature. It acts on deformation stress [19]. According to figure 5 ; the PSC with (Cu_2O) as HTM layer shows the better performance at high temperature (450K). Also the PSC with (Cu_2O) as HTM layer remains the more better than the two others Spiro-OMeTAD and PEDOT:Pss as HTM layers. The best operating temperature is 300K. Temperature is an important parameter; it was found that decrease in diffusion length increases of series resistance. By this fill factor and efficiency will be decreased according to papers [26-28].

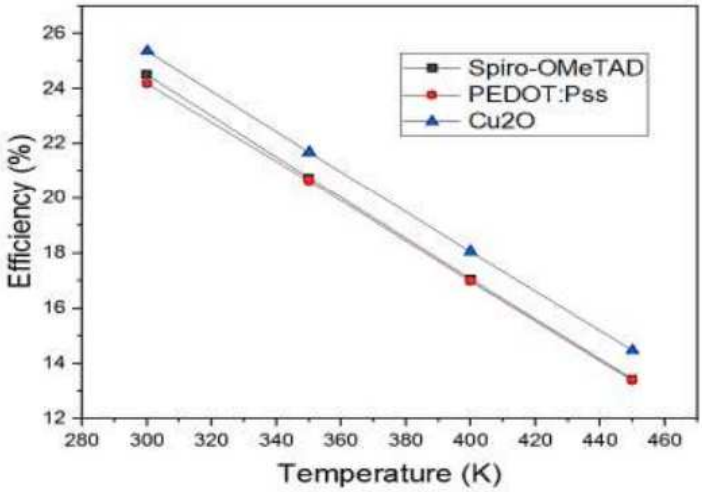

Figure 5: Effect of temperature on the efficiency

IV.CONCLUSION

In this work $CH_3NH_3SnI_3$ Perovskite solar cell with different parameters was analyzed using SCAPs-1D software device simulation. ZnO was suggested as electron transport layer (ETL). The performance of of PSC was studied with three different Hole Transport Material (HTM) layers (PEDOT:Pss/Cu_2O/spiro-OMeTAD). Thickness, doping and temperature, were varied to study the optimized performance.

Results showed that solar cell containing Cu_2O as HTM outperform all other devices. A Power conversion efficiency of 25.36% was obtained. At 300K and for a thickness of 900nm for N_A=1.5 10^{16} cm^{-3}.

In future, the results of this proposed structure need to be validated through physical fabrication and further studies.

REERENCES

[1] Burgelman, M., Nollet, P. and Degrave, S. (2000) 'Modelling polycrystalline semiconductor s olar cells', Thin Solid Films, 23rd European Photovoltaic Solar Energy Conference, Valencia, Vol. 361, pp. 527–532.

[2] Farhana Anwar and al, "Effect of Different HTM Layers and Electrical Parameters on ZnO Nanorod-Based Lead Free Perovskite Solar Cell for High-Efficiency Performance" International Journal of Photo energy Volume 2017, Article ID 9846310.

[3] Umari P, Mosconi E and De Angelis F, **"**Relativistic GW calculations on CH3NH3PbI3 and CH3NH3SnI3 Perovskites for solar cell applications", 2014 Sci. Rep. 4 4467.

[4] Chen, Q. Y, P.R. huang, T Ma, Cao C He Y, « Electronegativity explanation on the efficiency-enhancing mechanism of the hybrid inorganic-organic Perovskite ABX3 from first-principles study", Chin Phys. B, 2019, 25(2) pp. ISSN: 2313-0555

[5] A. Slami, M. Bouchaour and L. Merad, "Numerical Study of Based Perovskite Solar Cells by SCAPS-1D", International Journal of Energy and Environment Vol. 13, 2019, pp.17-21.

[6] Chong Liu, Jiandong Fan, Hongliang Li, Cuiling Zhang & Yaohua Mai, "Highly Efficient Perovskite Solar Cells with Substantial Reduction of Lead Content", Scientific Reports, 6:35705.

[7] Hossain, M.I., Alharbi, F.H., Tabet, N., 2015. "Copper oxide as inorganic hole transport material for lead halide Perovskite based solar cells". Sol. Energy 120, 370 - 380.

[8] Nogueira, A. F., Longo, C., & De Paoli, M.-A. (2004). « Polymers in dye sensitized solar cells: overview and perspectives". Coordination Chemistry Reviews, 248(13-14), 1455–1468.

[9] A. Niemegeers, M. Burgelman, K. Decock, J. Verschraegen, S. Degrave, SCAPS manual, May 2014.

INTERNATIONAL JOURNAL OF MATERIALS
DOI: 10.46300/91018.2020.7.1 Volume 7, 2020

[10] Kemp K W, Labelle A J, Thon S M, Ip A H, Kramer I J, Hoogland S and Sargent E H "Interface Recombination in Depleted Heterojunction Photovoltaics based on Colloidal Quantum Dots, 2013 Adv. Energy Mater. 3 917.
[11] Hao F Stoumpos C C Chang R P H and Kanatzidis M G, "Anomalous Band Gap Behavior in Mixed Sn and Pb Perovskites Enables Broadening of Absorption Spectrum in Solar Cells", J. Am. Chem. Soc. 2014, 136, 22, pp.8094-8099.
[12] Rutledge SA, Helmy AS. "Carrier mobility esnhancement in poly(3,4-ethylenedioxythiophene)-poly (styrenesulfonate) having undergone rapid thermal annealing", Journal of Applied Physics. 2013, 114(13):133708-1–5.
[13] Mihailetchi VD, Van Duren JK, Blom PWM, Hummelen JC, Janssen RAJ, Kroon JM, Rispens MT, Verhees WJH, Wienk MM. "Electron transport in methanofullerene", Advanced Functional Materials. 2003; 13(1), pp. 43–6.
[14] L. Huang, X. Sun, C. Li, R. Xu, J. Xu, Y. Du, Y. Wu, J. Ni, H. Cai, J. Li, Sol. Energy Mater. Sol. Cells 2016, 157, 1038.
[15] S. Bansal, P. Aryal, in 2016 IEEE 43rd Photovolt. Spec. Conf., IEEE, 2016, pp. 747–750.
[16] K. Sobayel, M. Akhtaruzzaman, K. S. Rahman, M. T. Ferdaous, Z. A. Al-Mutairi, H. F. Alharbi, N. H. Alharthi, M. R. Karim, S. Hasmady, N. Amin, "A comprehensive defect study of tungsten disulfide (WS2) as electron transport layer in Perovskite solar cells by numerical simulation", Results Phys. 2019, 12, pp. 1097-1103.
[17] A. Sahu, A. Dixit, « Inverted structure Perovskite solar cells: A theoretical study", Current Appl. Phys. 2018, 18, 1583-1591.
[18] C. Malerba, F. Biccari, C. L. A. Ricardo, M. D'Incau, P. Scardi, A. Mittiga, « Absorption coefficient of bulk and thin film Cu2O », Sol. Energy Mater. Sol. Cells 2011, 95, pp. 2848-2854.
[19] Usha Mandadapu et al "Simulation and Analysis of Lead based Perovskite Solar Cell using SCAPS-1D", Indian Journal of Science and Technology, Vol 10 (11), 2017.
[21] Hui-Jing Du and al, « Device simulation of lead-free $CH_3NH_3SnI_3$ perovskite solar cells with high efficiency", 2016 chinese Phys. B 25 108802.
[23] NREL Efficiency Chart. This Plot Is Courtesy of the National Renewable Energy Laboratory, Golden, CO.
[25] MH. Kumar, S. Dharani, WL. Leong, PP. Boix, RR. Prabhakar, T. Baikie, C. Shi, H. Ding, R. Ramesh, M. Asta, M. Graetzel, SG. Mhaisalkar, N. Mathews, "Lead-free halide Perovskite solar cells with high photocurrents", Vol.26, N°41, pp.712 2-71277.
[26] Fabregat-Santiago, F.; Garcia-Belmonte, G.; Mora-Sero, I.; Bisquert, J. Characterization of Nanostructured Hybrid and Organic Solar Cells by Impedance Spectroscopy. Phys. Chem. Chem. Phys. 2011, 13, 9083-9118.
[27] Bisquert, J.; Fabregat-Santiago, F. Impedance Spectroscopy: A General Introduction and Application to Dye-Sensitized Solar Cells. In Dye-Sensitized Solar Cells; Kalyanasundaram, K., Ed.; EPFL Press and CRC Press: Lausanne, Switzerland and Boca Raton, FL, 2010.
[28] R. Soni, R. Eva, M. Barea, and F. FabregatSantiago, "Analysis of the Origin of Open Circuit Voltage in Dye Solar Cells" Journal of Physical Chemical Letters, DOI: 10.1021/jz3005464,Vol. 3,No.12, pp 1629– 1634.

INTERNATIONAL JOURNAL OF ENERGY and ENVIRONMENT Volume 13, 2019

Numerical Study of Based Perovskite Solar Cells by SCAPS-1D

Abdelhadi SLAMI, Mama BOUCHAOUR and Laarej MERAD

***Abstract*—**This work deals with the design and analysis of lead-based Perovskite solar cells. The architecture consists of Glass/TCO/Buffer layer (TiO_2)/$CH_3NH_3PbI_3$/Spiro-MeTAD/metal back contact (Aluminium).
To study the efficiency and the performances of this solar cell, SCAPS-1D software is used in the simulation. The influence of defect density, absorber layer thickness, and working temperature on the performance of the device is presented.
The optimized PCS is obtained for the absorber layer thickness of 900 nm, the defect density of 10^{13} cm^{-3} and the 300K operating temperature. The efficiency greater than 30% is obtained.

***Keywords*:** SCAPS-1D, Perovskites solar cell, Simulation, Efficiency.

I.INTRODUCTION

In recent years, Perovskite Solar Cells (PSCs) have shown a great performance because of their low cost fabrication than traditional solar cells. It officially, entered the world of photovoltaics with a yield of 12% (2012) [1]. Since then, the yield of PSC has increased very rapidly reaching the value of 22% (2016) [2-4]. Owing the multilayer architecture of PSCs, interface not only has a main role to play in performance but influences long term stability.
By varying CH_3NH_3**X**I_3, high efficiency is predicted. Thus, several simulations are made in order to study the effect of various parameters on the efficiency of solar on CH_3NH_3**Pb**I_3 cells.
In this architecture, the effect of absorber layer properties (thickness, defect densities) and the influence of temperature on the performance of the device is studied and analyzed.

II. NUMERICAL MODELLING AND DEVICE SIMULATION

The adopted planar hetero-junction architecture is a typical CH_3 NH_3 PbI_3, based solar cell structure. The cell consists of an absorber layer and at the top p-type (Spiro-OMeTAD (HTM) and n-type (TiO_2-ETM) arranged at the bottom side as shown in figure 1.

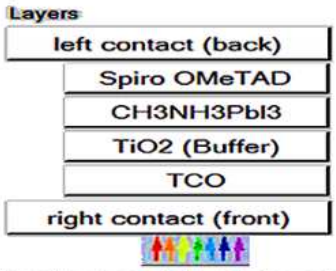

Fig. 1 Schematic representation device architecture (Glass/TCO/TiO_2-ETM/ $CH_3NH_3PbI_3$/Spiro OMeTAD/Al)

Figure 2 explains the simulation process using SCAPS. SCAPS is a one dimensional solar cell simulation program developed at the department of Electronics and Information Systems (ELIS) of the University of Gent, Belgium. It allows to simulate the behavior of photovoltaic structures. Since that, there are several modifications in this software such as the capability to work with crystalline solar cells (c-Si and GaAs, family) and amorphous cells (a-Si and micro-morphous Si) [5]. This simulator has the largest number of AC and DC electrical measurements which can be calculated in dark and light illumination and also at different temperatures. It (SCAPS) solves the Basic semiconductor equations in 1-Dimension under steady state condition.

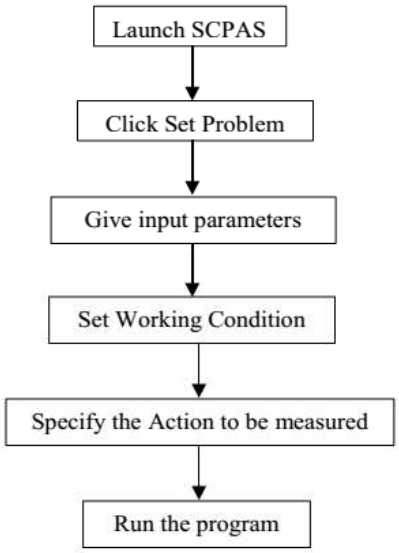

Fig. 2. SCAPS working procedure.

All simulation parameters are carefully selected from those reported in experimental data and other theoretical results [6-9]. The individual materials parameters for Spiro-OMeTAD, $CH_3NH_3PbI_3$, TiO_2 and TCO (SnO_2:F) have to be entered in terms of bandgap (Eg), electron affinity (χ), dielectric permittivity (ε), conduction band density of states (NC), valence band density of states (NV), electron mobility (μn), hole mobility (μp), donor density (NA), acceptor density (ND). Table 1 summarizes all the parameters used in the simulation.

University of Tlemcen, Faculty of Sciences, Department of Physics
Unité de Recherche « *Matériaux et Energies Renouvelables* », URMER
BP: 119, Fg Pasteur, Tlemcen, 13000, Algeria
ISSN: 2308-1007

Parameters	TCO SnO_2:F	TiO_2 (Buffer) (ETM)	$CH_3NH_3PbI_3$	Spiro-OMeTAD (HTM)
Thickness/nm	500	50	900	350
Band gap energy Eg/ev	3.5	3.2 [13]	1.55 [14]	3.17[17]
Electron affinity χ/ev	4	4 variable	3.90 [15]	2.05 variable
Relative permittivity εr	9	9	6.5 [16]	3
Effective conduction band density Nc/cm^{-3}	2.20×10^{18}	1.00×10^{19}	1.80×10^{18}	10^{20}
Effective valence band density Nv/cm^{-3}	1.80×10^{19}	1.00×10^{19}	1.80×10^{19}	10^{20}
Electron mobility µn/cm^2/V.s	20	0.02	0.5	2
Hole mobility µn/cm^2/V.s	10	2	0.5	0.01
Donor concentration N_D/cm^{-3}	2.00×10^{19}	1.00×10^{19} [13]		
Acceptor concentration N_A/cm^{-3}			1.00×10^{19}	1.00×10^{19}
Defect density N_t/cm^{-3}	1.00×10^{13}	1.00×10^{16}	1.00×10^{13}	1.00×10^{13}

Table 1. Simulation parameters of $CH_3NH_3PbI_3$ PSC [10, 11]

A. *Current – Voltage Curve*

The final model contains thickness of absorber layer as 0.9µm and the defect density as 10^{13} cm^{-3}. The doping levels of HTM and ETM are set as 10^{19} cm^{-3}. Fig 3. represents the characteristic of Perovskite solar cells of the final J-V. The open circuit voltage (Voc) is 0.67V, Short circuit current density (Jsc) is 59.78mA/cm^2, Fill factor is 74.94%, and PCE is 30.35%.

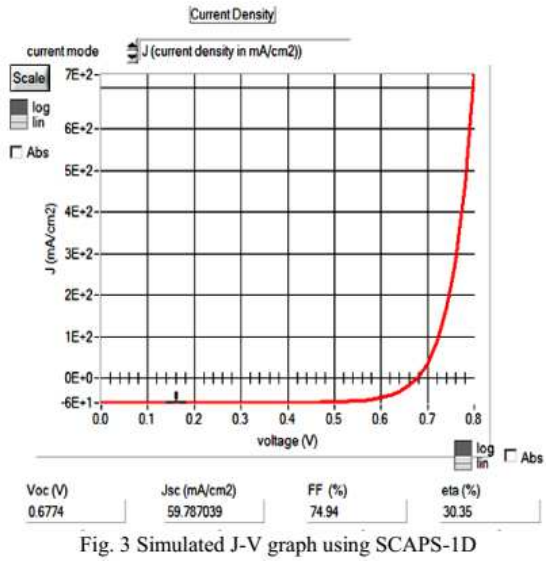

Fig. 3 Simulated J-V graph using SCAPS-1D

B. *Influence of absorber layer thickness on the I-V*

Absorber layer thickness plays a major role in determining the efficiency of the device [9]. The simulated parameters such as PCE, FF, Jsc, Voc of the $CH_3NH_3PbI_3$ solar cells, with varying Perovskite thickness is as shown in Fig 4. Maximum PCE is obtained for 30.35%. This result is achieved with J_{sc}=59.78mA/cm^2, FF=74.94%, V_{oc}=0.6774V when the thickness reaches 900 nm.

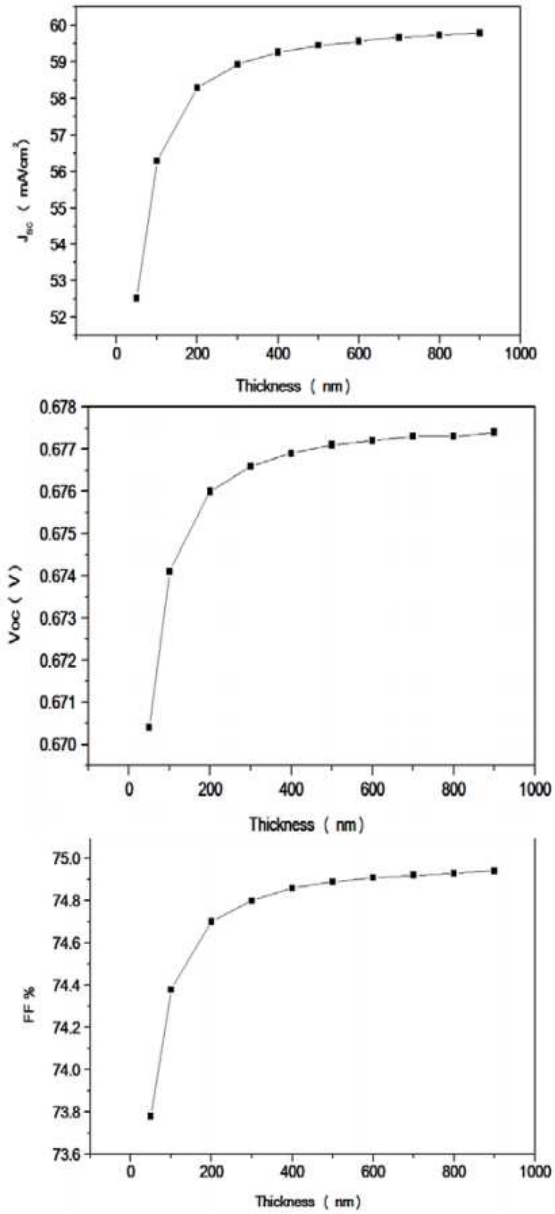

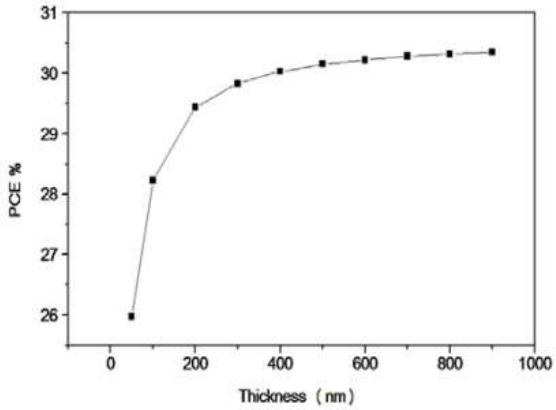

Fig. 4 Variation of solar cell parameters with thickness of absorber layer

To optimize the thickness for a good efficiency, the thickness of Perovskite layer from 50nm-900nm is varied. From the above graph (Fig.4: thickness versus efficiency), the efficiency rapidly increases from 50 nm till to 200nm up of 200nm, it slowly increases.

The increase of efficiency with increasing thickness represents the increase in the generation of the electron-hole pairs in the absorber layer.The efficiency slowly increases representing the decreases of recombination and a lot extraction rate of electron and hole pairs. The main reason for the increase of efficiency with the increase of thickness is the increase of optical density [3].

C. Influence of defect of the active layer on the I-V

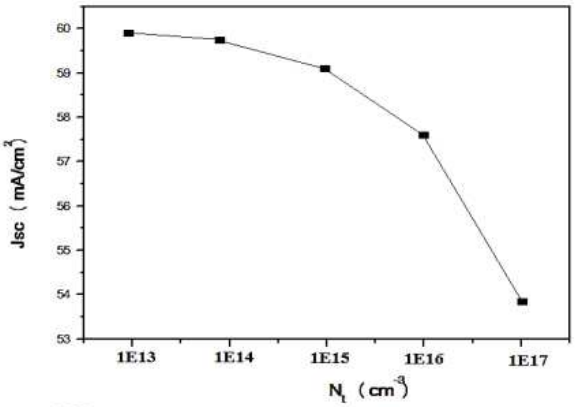

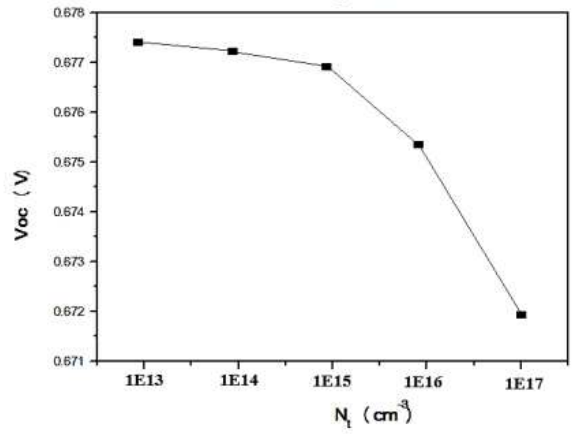

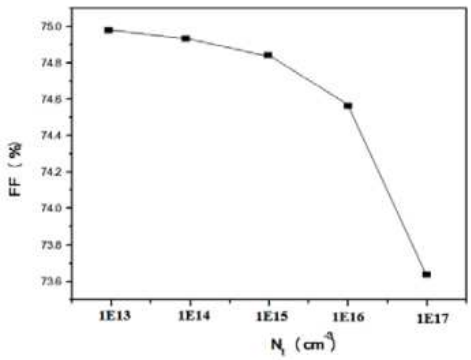

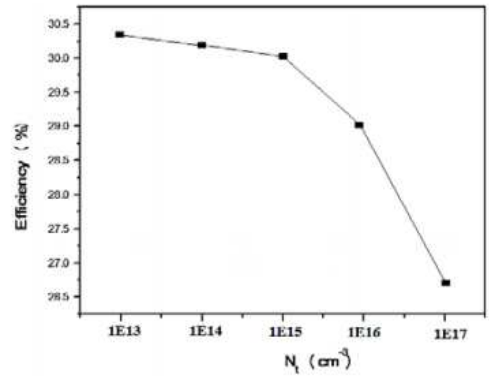

Fig.5 represents the variation of PV parameters with the defect densities (cm^{-3}). Generation, recombination, transportation process occurs inside the absorber layer, so the absorber layer quality and defect parameters greatly effect the device performance [18]. There are several defects such as vacancies, dislocation and grain boundaries which are always present in the absorber and HTM layer. These defects influence carrier recombination, reduction in lifetime and carrier mobility [11]. In the simulation model, the defect density is varied from 10^{13} cm^{-3} to 10^{17} cm^{-3}. It was observed that, if the defect density absorber layer is increasing from 10^{13} cm^{-3}, to 10^{17} cm^{-3}, the photovoltaic parameters randomly decreases and at $10^{17}cm^{-3}$ the PCE reaches to the 26.65 % and fill factor is 73.65 %, Voc=0.6715 V, Jsc=53.88 mA/cm^2. The minimum defect density of the absorber layer is predicted as 10^{13} cm^{-3} , at this condition the maximum attainable PV parameters are efficiency: 30.35%, Fill factor: 74.94%, Jsc=59.78 mA/cm^2, Voc=0.6774V.

D. Influence of temperature on the I-V

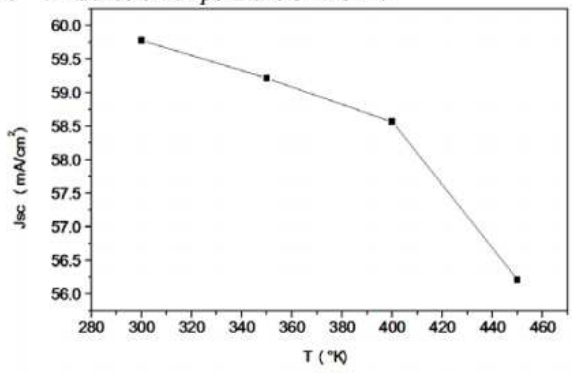

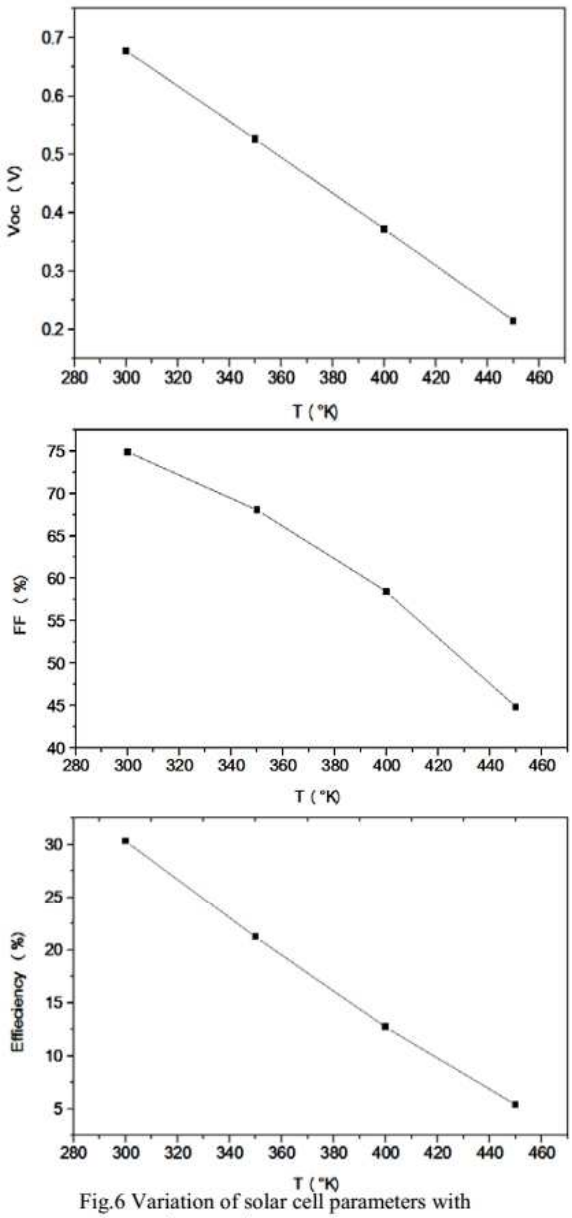

Fig.6 Variation of solar cell parameters with the operating temperature.

Temperature also influences the performance of a solar cell device. Generally, the testing temperature of a s olar cell device is 300°K, but at the installed conditions, the working temperature is more than 300°K [17]. To understand the effect of temperature on the electrical performance of a solar cell, the temperature of the simulated model varied from 300K to 450K. The changes in the characteristics are given in Fig.6. It is observed that the temperature decreases; there is a drop to 5.42%. Increasing temperature may lead to the more stress and deformation resulting in increased interconnectivity between the layers. Decrease in diffusion length increases of series resistance, by this fill factor and efficiency will be decreased [18]. To achieve good efficiency the optimum temperature of the simulated model is set to be 300K. At this temperature the maximum achievable efficiency of the model is 30.35%, fill factor is 74.94%, Jsc= 59.78 mA/cm^2 and Voc=0.6774 V.

III.CONCLUSION

The lead $CH_3NH_3PbI_3$ Perovskite solar cells with different parameters are analyzed by using one-dimensional device simulation in this work (SCAPS-1D).TiO_2 material is proposed as the Electron Transport Layer (ETL) for lead $CH_3NH_3PbI_3$ based Perovskite solar cells. The thickness and doping level of the active layer are varied to study the optimized performance. Simulated results reveal that the efficiency of this solar cell is 30.15%. In future, the results of this proposed structure need to be validated through physical fabrication and further study.

REFERENCES

[1] F. Hao, C C. Stoumpos, P. Guo, N. Zhou, T. J. Marks, R. P. H, Chang and MG, Kanatzidis, 2015 J. Am. Chem. Soc. 13711445
[2] A. Niemegeers, M. Burgelman, K. Decock, J. Verschraegen, S. Degrave SCAPS manual, January 2018.
[3] U. Mandadapu , S. V. Vedanayakam and K. Thyagarajan, "Simulation and Analysis of Lead based Perovskite Solar Cell using SCAPS-1D", *Indian Journal of Science and Technology*, vol 11, March 2017.
[4] Usha Mandadapu et al "Design and simulation of high efficiency tin halide perovskite solar cell" *International journal of renewable energy research*, vol 7, N°.4, 2017.
[5] A. Niemegeers, M. Burgelman, K. Decock, J. Verschraegen, S. Degrave, SCAPS manual, May 2014.
[6] Kemp K W, Labelle A J, Thon S M, Ip A H, Kramer I J, Hoogland S and Sargent E H *Adv. Energy Mater.* 3 917, 2013.
[7] J. Fan, Baohua B. Jia, and M. Gu,"Perovskitebased low-cost and high-efficiency hybrid halide solar cells," *Photonics Research*, vol.2, No.5, pp 111-120.
[8] F. Liu, J. Zhu, J. Wei, Y. Li, M. Lv, S. Yang, B. Zhang, J.Yao and S. Dai S Appl. Phys. Lett, 2014.
[9] Hao F Stoumpos C C Chang R P H and Kanatzidis J. *Am. Chem. Soc.* 136 8094, M G 2014.
[10] T. Minemoto and M. Murata M J. Appl. Phys, 2014.
[11] A. Toshniwal et al "Numerical simulation of Tin Based Perovskite Solar Cell: Effects of Absorber parameters and Hole Transport Materials" *Journal of Nano and Electronic Physics*, vol 9, N° 3, 2017.
[12]J.M. Ball, M.M. Lee, A. Hey, H.J. Snaith, "Low temperature processed meso-superstructure to thin film perovskite solar cells", *Energy and Environmental Science*, vol. 6, pp.1739-1743, 2013.
[13] N. K. Noel, S. D. Stranks, A. Abate, C. Wehrenfennig, S. Guarnera, A. Haghighirad, A. Sadhanala, G. E. Eperon, S. K. Pathak, M. B. Johnston, A. petrozza, L. Herz and H. Snaith,"LeadFree Organic-Inorganic Tin Halide Perovskites for Photovoltaic Applications", *Energy Environmental Science*, vol. 7, No.7, pp. 3061–3068
[14] Lee MM, Teuscher J, Miyasaka T, Murakami TN, Snaith HJ, "Efficient hybrid solar cells based on meso-super structure d'organo metal halide perovskites". *Science*, 2012.
[15]Noh JH, Im SH, Heo JH, Mandal TN, Seok SI, "Chemical management for colorful, efficient, and stable inorganic- organic hybrid nanostructured solar cells", *Nano letters* ; 13:1764-9, 2013.
[16] Hirasawa M, Ishihara T, Goto T, Uchida K, Miura N. "Magneto absorption of the lowest exciton in perovskite-type compound (CH_3NH_3)PbI_3". *Physica B: Condensed Matter*, 201:427-30, 1994.
[17] R. Soni, R. Eva, M. Barea, and F. Fabregat Santiago, "Analysis of the origin of Open Circuit Voltage in Dye Solar Cells" *Journal of Physical Chemical Letters*, Vol.3, N°12, pp 1629-1634.
[18] G. Xosrovashvili, N.E. Gorji," Numerical analysis of TiO_2/$Cu_2ZnSnS4$ nanostructured PV using SCAPS-1D", *Journal of Modern Optics*, vol,60, N°11, pp.936-940.

Abdelhadi SLAMI is currently a PhD student at Renewables Energies and Materials Unity, URMER; He received his Physics Master Degree in 2014 from Sidi Bel Abbés University.

Mama BOUCHAOUR Is a assistant Professor at the Department of Phyics at the Tlemcen, Algeria. He received his Physics from the University of Tlemcen and the Physical Energetic Magister with honours from the University of Tlemcen (Algeria) in 2001. Research at the Renewables Energies and Materials Unity, focusing on Materials for solar cells.

Laarej MERAD Is a assistant Professor at the Department of Phyics at the Tlemcen, Algeria. He received his Mechanical Energetic Engineering in 1998 from the University of Tlemcen and the Physical Energetic Magister with honours from the University of Tlemcen (Algeria) in 2002. Research at the Renewable Energies and Materials Unity, focusing on Resin formulation, synthesis, characterization and evaluation, cure behavior, interface science, elevated temperature VARTM, binders and preforms, process development, polymers performance, residual stress.

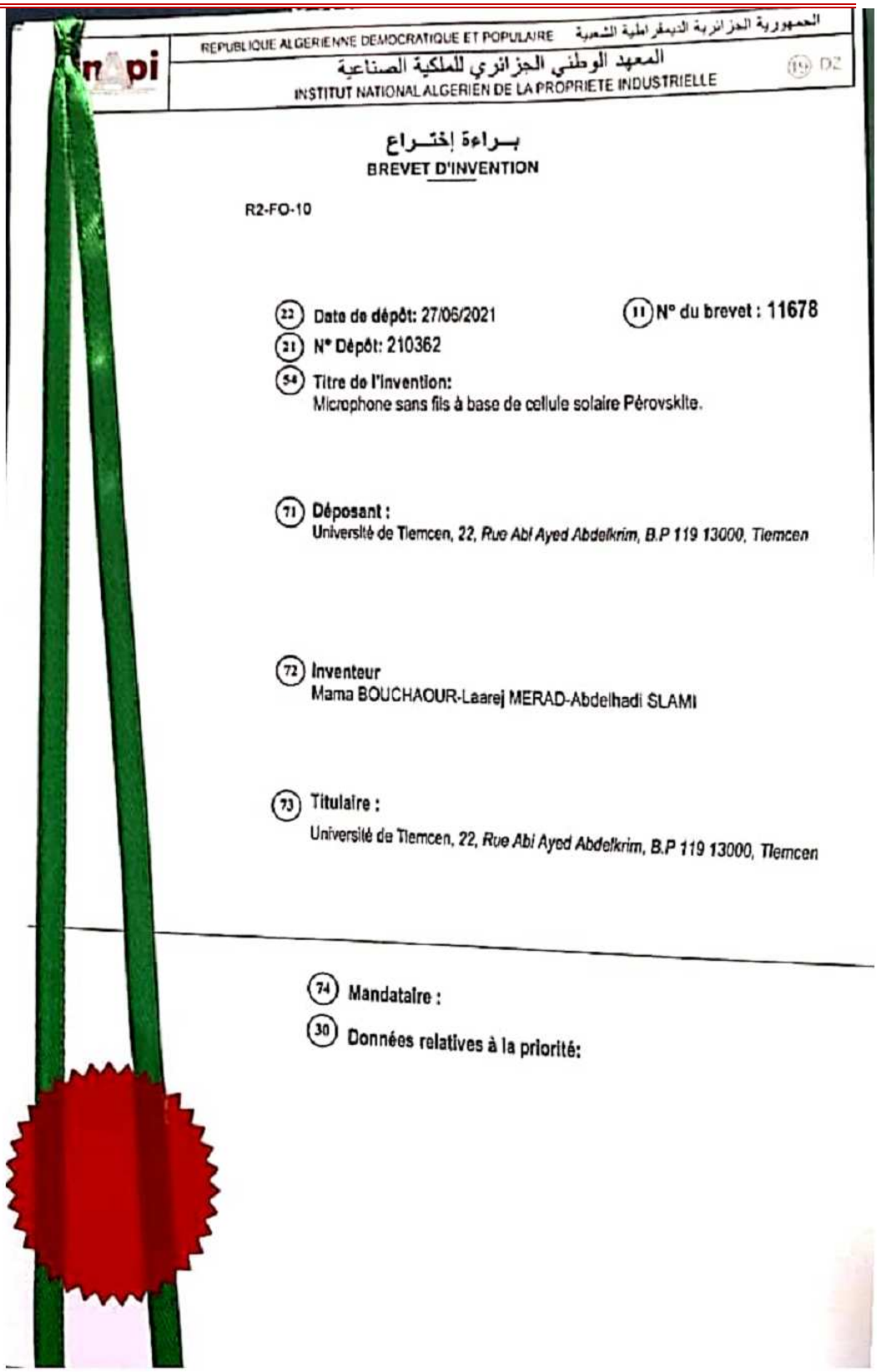

REPUBLIQUE ALGERIENNE DEMOCRATIQUE ET POPULAIRE الجمهورية الجزائرية الديمقراطية الشعبية

المعهد الوطني الجزائري للملكية الصناعية

INSTITUT NATIONAL ALGERIEN DE LA PROPRIETE INDUSTRIELLE

(19) DZ

براءة إختراع
BREVET D'INVENTION

R2-FO-10

(22) Date de dépôt: 27/06/2021 (11) N° du brevet : 11678

(21) N° Dépôt: 210362

(54) Titre de l'invention:
Microphone sans fils à base de cellule solaire Pérovskite.

(71) Déposant :
Université de Tlemcen, 22, *Rue Abi Ayed Abdelkrim, B.P 119 13000, Tlemcen*

(72) Inventeur
Mama BOUCHAOUR-Laarej MERAD-Abdelhadi SLAMI

(73) Titulaire :
Université de Tlemcen, 22, *Rue Abi Ayed Abdelkrim, B.P 119 13000, Tlemcen*

(74) Mandataire :

(30) Données relatives à la priorité:

Algerian Journal of Renewable Energy and Sustainable Development Volume: 4 | Number: 2 | 2022| December

DESIGN OF A SUSTAINABLE DISINFECTION TUNNEL OF COVID19

Abdelhadi SLAMI, Mama BOUCHAOUR and Laarej MERAD

University of Tlemcen, Faculty of Sciences, Department of Physics
Unité de Recherche "*Matériaux et Energies Renouvelables*", URMER
Fg Pasteur, BP: 119, Tlemcen, 13000, Algeria
*Corresponding author; Email: la_merad@yahoo.fr
bouchaour.m@gmail.com
slami91-hadi@hotmail.fr

Article Info

Article history:

Received May 27, 2022
Revised July 15, 2022
Accepted November 05, 2022

Keywords:

Sustainable disinfection tunnel,
PV Solar panel,
Covid19,
Disinfectant.

ABSTRACT

Cleaning and disinfection of public spaces is important and it is necessary to control the transmission of the virus. Disinfection prevents a possible other epidemic wave. In this work, we present a sustainable disinfection tunnel (SDT). Its role is to provide maximum protection to people passing through it in around 10 seconds. The model structure uses renewable energy panel and it is putted at the entrance of hotels, schools and administrations.

I. Introduction

Today, the High Council for Public Health (HCPH) insists on the importance of cleaning of outdoor and indoor public environments. In fact, it is necessary to control the transmission of the virus and thus prevent a possible other epidemic wave [1]. Especially the exceptional situation the world is going through with COVID 19 pandemic. The COVID-19 pandemic is devastating. Its spread can be slowed down by following the infection control practices and by using a sustainable system to disinfect and sterilize outgoing and incoming people in areas that must work in hygienic conditions such as: hospitals, establishments, laboratories, schools [2, 3-8]. To prevent against the propagation of this virus, authorities direct their research to prevention program against the Corona virus. One of these programs is the installation of disinfection tunnels. The first one was installed in China [9]. This was imitated by other countries [10-11]. In Algeria, the first "disinfection tunnel" of this kind was launched in April, 2020, at the entrance of the Association of Renewable Energies and Sustainable Development of Sidi Bel Abbes. Other new walk tunnels have succeeded that of Sidi Bel Abbes [12].
Nowadays, the current interest of renewable energies is due to government awareness. At the same time to fight against the CO_2 emissions and new epidemic of Corona, photovoltaic solar energy [13] is considered as an essential device in this area.
In this work, we combined the solar photovoltaic energy to the disinfection. The sustainable unit works with the principle of eliminating harmful bacteria that they transport people. Indeed, Disinfection is done by misting low pressure of the disinfectant product, flow rate and particle size, nozzle positions, and duration of disinfection. These parameters are sized to ensure even distribution of the disinfectant.

Algerian Journal of Renewable Energy and Sustainable Development 4(2) 2020: 122-125, doi: 10.46657/ajresd.2022.4.2.1

II.Design and work of Disinfection Tunnel

In this work, we combined the solar photovoltaic energy in the disinfection tunnel to use it as a source of energy for the triggering of the pump of the disinfectant liquid spraying circuit and the detector (photocells) of the passage of the persons or of equipment. The sustainable unit works with the principle of eliminating harmful bacteria that they transport people.

The structure of the unit is made of aluminum, stainless steels or other non-corrosive material. These materials allow a better stability. This unit is mobile, with four wheels equipped with a braking system, to facilitate its movement and its positioning in complete safety. These tunnels are equipped with infrared sensor which activates the pump of the disinfectant liquid spraying circuit and the detector when a person accesses [14]. Essentially spray is a mist of sodium hypochlorite solution or Sodium bicarbonate solution (distilled white vinegar; soften clothes without harsh chemicals. Vinegar is inexpensive, and it is safe. It contains no tannins "natural plant dyes" that can stain clothes [15] in order to clean, to disinfect and to neutralize odors. A temperature sensor can also be installed at the entrance to ensure the feverish state of the person passing through the disinfection unit, as shown in figure 1.

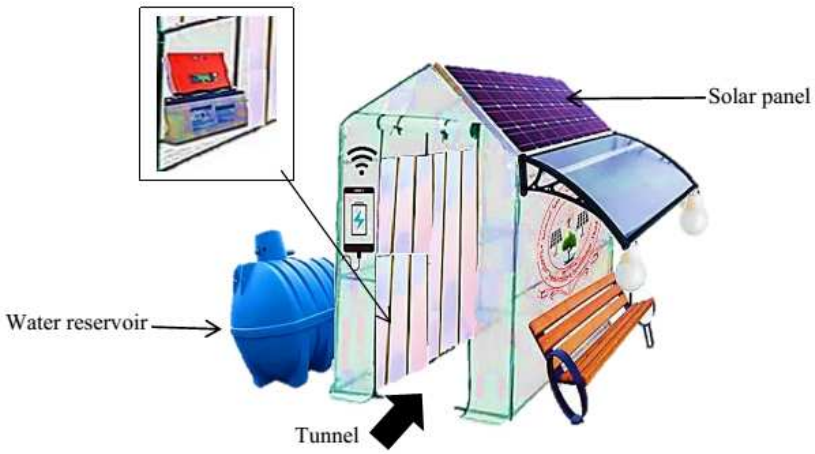

Figure 1 : Schematic representation Sustainable Disinfection Tunnel (SDT)

1. Solar system model

The aim of the autonomous solar system is to provide electrical power everywhere and at any time to secure sensitive devices when the network fails. The size of the system varies greatly depending on consumption and geographic location.

1.1. Contents of the solar kit

- Two polycrystalline solar panels 150W - 12V: A 150W solar panel is easily power most of rechargeable batteries. These draw very little power from the battery and are known to be longer-lasting.
- Specific solar cable between the panel and the regulator: The recommendation is to use standard wire. Since there are several conductors in a single run, stranded wire offers better conductivity.
- Solar regulator 30A - 12/24 V.
- Two sealed slow discharge batteries, 12 V - 110 Ah: Sealed lead acid batteries can have a design life of anywhere from 3 – 5 years.
- Inverter which converts 24 V DC (Direct Current - DC) from the battery to 220 V (Alternating Current - AC) identical to the network.
- Protection box that can accommodate up to 4 circuit breakers, 2 circuit breakers at 16A and another one at 10 A are integrated in the kit to protect the panel, the battery for 24 V_{output}. A circuit breaker can be added for an inverter.

Algerian Journal of Renewable Energy and Sustainable Development 4(2) 2020: 122-125, doi: 10.46657/ajresd.2022.4.2.1

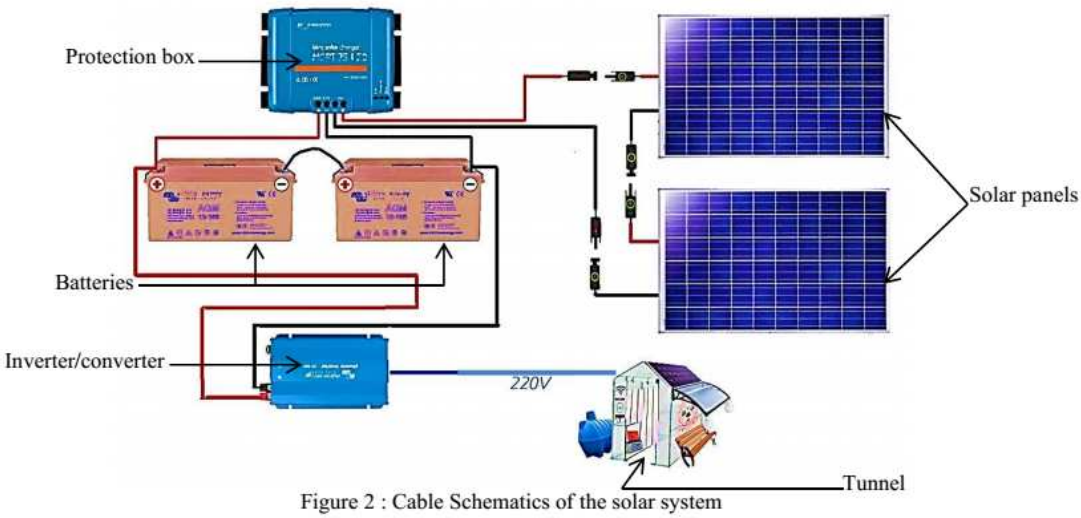

Figure 2 : Cable Schematics of the solar system

Table 1 presents the consumed energies of some components used in disinfection tunnels. This equipment does not consume a lot of energy.

Device	Energies (Wh)
Water Pump (motor)	370 w x 4 hours
2 Spots (LED)	12 w x 4 hours

The prototype is equipped with a sensor that detects the person and to launch a disinfection automatic in order to control the consumption of disinfectant product.

III. Conclusion

The COVID-19 pandemic is devastating, but by following infection control practices and instructions issued from authorities, its spread can be slowed down.
This work presents the sustainable disinfection tunnel (SDT) by using renewable energies (solar energy). It was put at the entrance of the Association of Renewable Energies and Sustainable Development of Sidi Bel Abbes.
It can try and prevent the spread of any possible epidemic crisis. The tunel can disinfect a person fully in a time span less than 15 seconds and the used solution is completely harmless. This structure will allow a total and homogeneous disinfection of people in terms of safety from the external environment. This project needs a moderate budget.

Acknowledgements

The authors would like to thank the Association of Renewable Energies and Sustainable Development of Sidi Bel Abbes for technical support.

References

[1] World Health Organization: Naming the coronavirus disease (COVID19) and the virus that causes it. Available at: https://www.who.int/
[2] Nabih, M, L., and S, Al Tabbah., "Coronavirus Disease 2019 (COVID-19): Prevention and Disinfection", *International Journal of Biology and Medicine*, pp.10-14, 2020.

DOI: 10.36811/ijbm.2020.110019
[3] Rutala, WA., Weber, DJ., "An overview of disinfection and sterilization", Disinfection, Sterilization and Antisepsis: Principles, Practices, Current Issues, New Research, and New Technologies, *Association for Professionals in Infection Control and Epidemiology*, Washington DC, pp.18-83, 2010.
[4] Recommendations on Chemical Safety for Cleaning and Disinfection Supplies, *Bulletin of Pan American Health Organization*; Communicable Diseases and Environmental Determinants of Health (CDE) (Washington, D.C., PAHO, (2020).
[5] "The use of tunnels and other technologies for disinfection of humans using chemical aspersion or UV-C LIGHT", Pan American Health Organization (2020).
[6] Algerian Ministry of Health, Population and Reform of hospitals (2020). http://www.sante.gov.dz/
[7] COVID-19 Prevention: Cleaning and Disinfection Protocol, W Environmental Health & Safety (2022).
[8] Liu J, Liao X, Qian S. "Community transmission of severe acute respiratory syndrome coronavirus 2", Shenzhen, China, *Emerg Infect Dis* (2020).
[9] Thibaud, D., and Isabelle, E., "The COVID-19 crisis and the rise of the European Centre for Disease Prevention and Control (ECDC) ". *West European Politics; Taylor & Francis Group*, vol. 44, pp. 1376–1400 (2021).
[10] Ibrahim, M., "First Virtual Fair in Science Technology & Innovation face to COVID-19 pandemic", Tunisian R&D platform, (2020). https://youtu.be/uCHvLw75dyA
[11] POSITION STATEMENT: The use of disinfection tunnels or disinfectant spraying of human, Safeguarding Africa's Health, Africa centres for disease control and prevention and the infection control Africa network (2020).
[12] Sahouane, N., Necaibia, A., "Un tunnel de désinfection intelligent dédié aux personnels de santé pour faire face à la pandémie COVID 19",
[13] Tahiri, F., Bekraoui, F., Boussaid I., Ouledali, O., Harrouz A., Direct Torque Control (DTC) SVM Predictive of a PMSM powered by a photovoltaic source. *Algerian Journal of Renewable Energy and Sustainable Development*, 2019, 1(1), 1-7. https://doi.org/10.46657/ajresd.2019.1.1.1.
[14] Manisha, B., RImjhim, K., Archana, A., Shubh, MS., Pallab, R., "Disinfection tunnels (DT): potentially counterproductive in the context of a prolonged pandemic", *JMIR Public Health and Surveillance* (2020).
[15] https://doctor.ndtv.com/living-healthy/top-5-healthiest-vinegars-you-should-stock-1787796.